

**THE EFFECTS OF MORPHOLOGY AND NEIGHBOURING SEAWEEDES
ON MACROALGAL MICROBIOTA**

by

Melissa Chen

B.Sc., Cell and Developmental Biology, University of British Columbia, Canada, 2015

A DISSERTATION SUBMITTED IN PARTIAL FULFILLMENT
OF THE REQUIREMENTS FOR THE DEGREE OF

MASTER OF SCIENCE

in

THE FACULTY OF GRADUATE AND POSTDOCTORAL STUDIES

(Botany)

THE UNIVERSITY OF BRITISH COLUMBIA

(Vancouver)

August 2017

© Melissa Chen, 2017

Abstract

Macroalgae (seaweeds) have an intimate relationship with their microbial symbionts. Microbial communities associated with macroalgal surfaces (epibiota) are generally host-specific and, historically, there has been great interest in the role of biological compounds and chemical warfare in microbial community assembly on seaweeds. However, the interaction between seaweeds and their environment may also influence community assembly of their microbiota. In my thesis, I conduct two experiments that ask how factors not related to seaweed chemistry influence microbial community assembly. First, I ask whether the interaction between flow and seaweed morphology affects the settlement and structure of microbial biofilms. In this project, I test whether three common algal morphologies select for differential biofilm communities using artificial macroalgae units (AM units) made out of latex. I find that morphology does affect initial microbial settlement and community structure, but that eventual dominance of substrate specialists (in our case a latex degrader) swamps the influence of morphology in long-term biofilms. The second chapter of my thesis asks whether macroalgae affect the microbial epibiota of each other. To test this, I co-incubate *Nereocystis leutkeana* meristem fragments with different species of mature macroalgae. I find that although water column communities change significantly when incubated with mature macroalgae, seaweed surface communities are far more resistant to change. Overall, these results support the idea that the seaweed surfaces are highly selective, and demonstrate that modulations on seaweed microbiota operate within an overarching paradigm of species specificity. With these experiments, I hope to contribute to the larger body of knowledge on seaweed-microbe associations and improve understanding of how, and why, we find the observed microbiota on seaweed surfaces.

Lay Summary

Seaweed surfaces are home to a diverse collection of microscopic organisms (microbes) that provide many benefits for their seaweed host. Seaweed surfaces are selective over which microbes can settle and grow, and my thesis investigates factors that explain why certain microbes are found on seaweeds, while others are not. First, I ask whether seaweed shape influences microbial biofilm development. I find that branched seaweed shapes develop biofilms faster than un-branched shapes, and I discuss how this relates to biofilms found on wild seaweeds. Second, I test whether seaweeds grown together influence each other's biofilms. I find that although seaweeds transmit microbes into the water, there are relatively few microbes that are transmitted from seaweed to seaweed. In general, my findings demonstrate that seaweed surfaces are highly selective. My thesis contributes knowledge about how microbes grow and settle on seaweeds, and will lead to a better understanding of microbe-seaweed relationship dynamics.

Preface

- Chapter 1: A general introduction to seaweed-associated microbes.
- Chapter 2: Matt Lemay, Laura Parfrey and Patrick Martone had the idea for the project. Project was based off results from work done by Matt Lemay, Laura Parfrey, and Patrick Martone. Melissa Chen conducted the experiments and performed the sequence analysis and statistical analysis with input from Laura W. Parfrey and Patrick Martone. Melissa Chen wrote a first draft of the manuscript. Laura Parfrey supervised the project and committee members Mary O'Connor and Patrick Martone provided feedback on analysis, results, and discussion.

This chapter is not yet published.

- Chapter 3: Melissa Chen conceived of the research question. Laura Parfrey supervised the project and committee members, Mary O'Connor and Patrick Martone provided feedback. All experimentation, statistical analysis, and writing of first drafts was done by Melissa Chen.

This chapter is not yet published.

Throughout this dissertation the word “we” refers to Melissa Chen and Laura Parfrey unless otherwise stated.

Table of Contents

| | |
|---|-------------|
| Abstract | ii |
| Lay Summary | iii |
| Preface | iv |
| Table of Contents | v |
| List of Tables | vi |
| List of Figures | vii |
| Acknowledgements | viii |
| 1 Seaweeds and their microbial symbionts | 1 |
| 1.1 Introduction | 1 |
| 1.2 Problem statement and objectives of thesis | 2 |
| 2 The effect of seaweed morphology on microbial community settlement and composition | 4 |
| 2.1 Introduction | 4 |
| 2.2 Methods | 6 |
| 2.3 Results | 12 |
| 2.4 Discussion | 20 |
| 2.5 Supplementary Figures and Tables | 24 |
| 3 Horizontal transmission of microbes between neighbouring macroalgae . | 34 |
| 3.1 Introduction | 34 |
| 3.2 Methods | 36 |
| 3.3 Results | 41 |
| 3.4 Discussion | 49 |
| 3.5 Supplementary Figures and Tables | 52 |
| Bibliography | 59 |

List of Tables

| | | |
|-----------|--|----|
| Table 2.1 | Number of replicates at each site for AM experiment. | 7 |
| Table 2.2 | Pairwise t-tests and ANOVA of richness between morphologies across time. | 14 |
| Table 2.3 | Pairwise and overall PERMANOVAs of community composition between morphologies across time. | 16 |
| Table 2.4 | S: PERMDISP of morphologies at each time point and overall. | 32 |
| Table 2.5 | S: ANOVA of richness across morphology by time point. | 32 |
| Table 2.6 | S: Welch's t-Test comparison of richness at Reed Point and Hakai by time point. | 33 |
| Table 3.1 | Comparison of community dissimilarity (PERMANOVA) and richness (Welch's t-Test) of <i>Nereocystis</i> , <i>Mastocarpus</i> , and water samples. | 43 |
| Table 3.2 | Comparison of community dissimilarity (PERMANOVA) and richness (Welch's t-Test) of water column and NMF surface communities in M-W-NMF treatments. | 46 |
| Table 3.3 | S: PERMANOVA results comparing <i>Nereocystis</i> , <i>Mastocarpus</i> , and water samples. | 57 |
| Table 3.4 | S: PERMANOVA results comparing water samples from M-W-NMF experiment. | 57 |
| Table 3.5 | S: PERMANOVA results comparing NMF surface samples from M-W-NMF experiment. | 57 |
| Table 3.6 | S: PERMANOVA results comparing water samples from the M-W experiment. | 57 |
| Table 3.7 | S: ANOVA results comparing richness of <i>Nereocystis</i> , <i>Mastocarpus</i> , and water. | 58 |
| Table 3.8 | S: ANOVA and Welch's t-Test results comparing richness of water samples from M-W-NMF experiment. | 58 |
| Table 3.9 | S: ANOVA and Welch's t-Test results comparing NMF surface samples from M-W-NMF experiment. | 58 |

List of Figures

| | | |
|-------------|--|----|
| Figure 2.1 | Artificial Macroalgae. | 6 |
| Figure 2.2 | Richness of biofilms on artificial macroalgae through time. | 13 |
| Figure 2.3 | Dispersion and community composition of AM morphologies through time. | 15 |
| Figure 2.4 | Heatmap of core OTUs across morphologies and time points. | 17 |
| Figure 2.5 | Turnover of OTUs across time points. | 18 |
| Figure 2.6 | Taxa summary of OTUs collapsed by Order. | 19 |
| Figure 2.7 | S: Richness of biofilms on AM units through time (all metrics). | 24 |
| Figure 2.8 | S: Dispersion and community composition of AM morphologies through time (un-weighted Unifrac). | 25 |
| Figure 2.9 | S: Dispersion and community composition of AM morphologies through time (weighted Unifrac). | 26 |
| Figure 2.10 | S: Overall dispersion of AM units over time (all metrics). | 27 |
| Figure 2.11 | S: Heatmap showing “core” OTUs. | 28 |
| Figure 2.12 | S: Heatmap showing presence or absence of “core” OTUs. | 28 |
| Figure 2.13 | S: Comparison of water diversity and AM biofilm diversity | 29 |
| Figure 2.14 | S: Comparison of AM biofilm diversity at Reed Point and Hakai. | 30 |
| Figure 2.15 | S: Taxa summaries plot at the OTU level. | 31 |
| Figure 2.16 | S: Dye Dip Experiment Results | 31 |
| Figure 3.1 | Experimental design for M–W and M–W–NMF experiments. | 37 |
| Figure 3.2 | Comparison of community composition and richness across macroalgal surfaces and water samples. | 42 |
| Figure 3.3 | Comparison of water column communities in M–W–NMF treatments. | 44 |
| Figure 3.4 | Comparison of NMF surface communities M–W–NMF treatments. | 45 |
| Figure 3.5 | Enrichment and reduction of NMF surface and water column communities in M–W–NMF treatments. | 47 |
| Figure 3.6 | Taxa summary plots showing enriched or reduced genera of NMF surface and water column communities. | 48 |
| Figure 3.7 | S: NMDS of <i>Nereocystis</i> , <i>Mastocarpus</i> , and water samples. | 52 |
| Figure 3.8 | S: Richness of <i>Nereocystis</i> , <i>Mastocarpus</i> , and water samples. | 52 |
| Figure 3.9 | S: NMDS of water column communities in M–W–NMF treatments. | 53 |
| Figure 3.10 | S: Richness of water column communities in M–W–NMF treatments. | 53 |
| Figure 3.11 | S: Composition and Richness of samples in the M–W experiment. | 54 |
| Figure 3.12 | NMDS of NMF surface communities from M–W–NMF treatments. | 55 |
| Figure 3.13 | S: Richness across NMF surface communities from M–W–NMF treatments. | 55 |
| Figure 3.14 | S: Taxa summary of wild and lab-incubated seaweed samples | 56 |

Acknowledgements

A thousand ‘thank you’s and gratitudes to Laura Parfrey for guiding me through my Masters. I know I am not always on time, but I am thankful you let me delve into all the rabbit holes that I do.

I would also like to thank my committee members, Mary O’Connor and Patrick Martone, for providing input and feedback on my projects through all their various stages. Your enthusiasm and interest are greatly appreciated.

Also thank you to all the undergrads, graduate students, and post-docs that have helped me along the way: Matt Lemay, Stilian Loucas, Andy Loudon, Jordan Lin, Cody Foley, Cassandra Jensen, Maryam Osmond, Gwen Griffiths, Rhea Smith, Liam Coleman, and probably many more. Additionally, thank you to the various technicians and statisticians who have helped me: Evan Morien, Marcus Campbell, Courtney Van den Elzen.

Finally, thank you to my partner, David, for providing continued support and encouragement during all the times that madness felt imminent.

Chapter 1

Seaweeds and their microbial symbionts

‘In a system where life is the universal good, but the destruction of life the well nigh universal occupation, an order has spontaneously risen which constantly tends to maintain life at the highest limit [...] Is there not, in this reflection, solid ground for a belief in the final beneficence of the laws of organic nature?’

Stephen A. Forbes, 1887

1.1 Introduction

Macroalgae (seaweeds) have an intimate relationship with their microbial symbionts. Their surfaces are rich with biological compounds that attract or deter a variety of microbes, many of which provide crucial functions for their seaweed host. Microbes promote macroalgal settlement [Joint et al., 2002, Weinberger, 2007] and are often required for normal growth and morphological development [Provasoli and Pintner, 1980, Nakanishi et al., 1996, Matsuo et al., 2005, Marshall et al., 2006]. They are known to aid in nutrient acquisition by fixing nitrogen [Rosenberg and Paerl, 1981, de Oliveira et al., 2012] or producing vitamin B12 [Croft et al., 2005] for their host, and play a role in priming immune defences against pathogenic bacteria [Küpper et al., 2002, Weinberger, 2007]. Indeed, seaweeds rely on their microbial symbionts for a wide range of functions.

Historically, there has been great interest in the role of biological compounds and chemical warfare in community assembly on seaweeds. Seaweeds produce a variety of polymers including, but not limit to, agar, carrageenan, alginate, mannose, cellulose, and pectin; all of which have associated degraders previously isolated from seaweeds [Goecke et al., 2010]. The microbes that consume these biological molecules are sometimes detrimental to their seaweed host because they cause degradation of tissue under saprotrophic conditions. However, under non-saprotrophic conditions, these microbes also provide a variety of services

that benefit the host alga.

In exchange for organic compounds, some bacteria help mineralize organic substrate and supply algae with supplemental CO₂ and minerals [Brock and Clyne, 1984, Coveney and Wetzel, 1989, Croft et al., 2005, Dromgoole and J, 1978, Rosenberg and Paerl, 1981, Carpenter and Cox, 1974]. Microbes also remove heavy metals and crude oil, which are harmful for macroalgae, from the water [Riquelme et al., 1997, Semenova et al., 2009, Yurkov and Beatty, 1998]. Finally, some microbes promote growth by supplying growth factors [Dimitrieva et al., 2006, Berland et al., 1972, Bolinches et al., 1988, Meusnier et al., 2001]. Thus, there is a fine balance between the beneficial and saprotrophic effects of symbionts that consume the polymers found on the surface of seaweeds.

Seaweeds also exude metabolites and compounds that are known to have antibiotic effects. Some seaweeds store anti-fouling compounds within their tissues [Armstrong et al., 2001], and these compounds can be released into the surrounding water column. In other cases, seaweeds like kelps produce oxidative bursts that selectively reduce the number of pathogenic bacteria on their surface [Weinberger et al., 1999, Dring, 2006, Küpper et al., 2002]. The exact mechanism by which these antifouling compounds work is highly varied, but has been described in several different seaweeds [Bhakuni and Rawat, 2006, Dubber and Harder, 2008]. Therefore, in addition to attracting potentially beneficial symbionts, seaweeds also actively deter pathogenic ones.

Microbial communities associated with macroalgal surfaces (epibionts) are generally host-specific [Egan et al., 2013, Lachnit et al., 2009, de Oliveira et al., 2012]. However, there is high variation in taxonomic community composition across individuals of the same species [Burke et al., 2011b] that may correlate to environmental conditions like seasonality [Lachnit et al., 2011] or salinity [Dittami et al., 2015]. Additionally, it has been proposed that functional traits in epibiotic communities on seaweeds are conserved, whereas taxonomic composition is not [Burke et al., 2011a]. Thus, the composition of microbial communities on seaweed surfaces is modulated by many factors in the environment, and these factors interact with the seaweed's biology to determine the final microbial community composition found on macroalgae in the environment

1.2 Problem statement and objectives of thesis

While the biological and chemical interactions between seaweeds and their microbial symbionts are obviously important drivers in determining microbial community composition on

seaweed surfaces, there are also non-biological aspects of community assembly less often addressed. For example, studies in the field of microfluidics have shown that water flow may be important in settlement rates of microbial populations [Rusconi and Stocker, 2015]. However, flow is seldom considered in studies on microbial community assembly [Rusconi and Stocker, 2015]. Additionally, studies show that the presence of some macroalgae causes faster biofilm colonization because organic exudates from the seaweed enriches certain taxa in the water column. This suggests that the richness and composition of water column communities may have important effects on the progression of biofilms. Again, knowledge about how macroalgal surface communities will change as the pool of potential colonizers shift is limited. Thus, there are many aspects of microbial settlement on seaweeds that are not yet understood.

In my thesis, I address two specific questions related to microbial community assembly on the surface of macroalgae. First, I ask whether the morphology of seaweed affects the settlement and structure of microbial biofilms. This work combines aspects of both microfluidics and community ecology to make observations about how water flow can influence microbial growth and settlement on surfaces in marine environments. My second chapter investigates the effects of nearby macroalgae on the microbial community composition of growing seaweeds. Specifically, I test whether the presence of macroalgae alters the microbial community composition of the water column and of growing *Nereocystis* meristem fragments through incubation experiments. With these experiments, I hope to contribute to the larger body of knowledge on seaweed-microbe associations and improve understanding of how, and why, we find the observed microbiota on seaweed surfaces.

Chapter 2

The effect of seaweed morphology on microbial community settlement and composition

2.1 Introduction

Seaweeds are a crucial part of coastal ecosystems and are of great ecological, cultural, and economic value. For example, they provide crucial habitat for a variety of animals ranging from juvenile fish to grazing invertebrates [Wilson et al., 2010, Bulleri et al., 2002]. They are also one of the largest groups of photosynthetic marine organisms in the ocean and they fix a significant fraction of the total carbon found in coastal marine ecosystems [Schiel and Foster, 2006, Tait and Schiel, 2011]. Finally, seaweeds are valuable to humans because of their role in traditional and modern aquaculture [McHugh, 2003]. Given their ecological and cultural significance, it is in our best interest to understand the various factors that impact seaweed biology and ecology.

Microbes influence seaweed host fitness in a variety of ways, both positive and negative. Microbial epibionts mediate seaweed settlement and growth [Marshall et al., 2006, Singh and Reddy, 2014, Matsuo et al., 2005, Joint et al., 2002], improve nutrient acquisition [Rosenberg and Paerl, 1981, Croft et al., 2005, Ilead and Carpenter, 1975, Chisholm et al., 1996], and prime the seaweed immune defence against potential pathogens [Weinberger, 2007, Küpper et al., 2002, Steinberg, 2002, Armstrong et al., 2001, Dobretsov and Qian, 2002, Maximilian et al., 1998]. However, many microbes also infect or degrade algal tissue [Küpper et al., 2002, Seyedsayamdost et al., 2011, Thomas et al., 2008]. Therefore, elucidating the processes underlying microbial community assembly on seaweed surfaces is vital to a holistic understanding of seaweed fitness.

The epibiotic (surface-associated) microbial communities associated with seaweeds are host-

specific [Lachnit et al., 2009, de Oliveira et al., 2012]. However, there can be a tremendous amount of variation in taxonomic composition across individuals of a species [Burke et al., 2011b, Tujula et al., 2010] since the microbiota of seaweed varies both seasonally [Michelou et al., 2013, Lachnit et al., 2011] and with environmental factors like salinity [Stratil et al., 2014]. Additionally, while species specificity at coarse taxonomic levels of microbial assemblages has been found in some studies [Lachnit et al., 2009], other work has shown that it is function, not membership, that correlates with host species [Burke et al., 2011a]. Thus, the variation in microbiota observed on different seaweed species is likely a result of many interacting factors; only one of which is the taxonomic identity of the seaweed itself.

A survey of more than 35 species of seaweeds by Lemay et al. 2016 at West Beach near the Hakai Research Institute revealed an unexpected correlation between microbial community structure and host morphology. That is, seaweeds with similar morphology tended to have similar microbial communities. For example, distantly related crustose seaweeds (each with an alternating upright foliose life history stage) shared more microbiota with other crusts than either crust to their corresponding foliose life stage.

We hypothesize that differences in epibiotic community structure depend partially on morphology because of the way water flows around seaweeds of various morphology. Water moving across solid surfaces form boundary layers (velocity gradients), whose thickness can affect nutrient transfer [Characklis and Marshall, 1990, Ollos et al., 2003, Lehtola et al., 2006] and particle deposition [Abelson and Denny, 1997]. For example, water velocity increases as it flows around obstacles, which may promote the deposition of particles denser than water [Abelson and Denny, 1997]. Additionally, the behaviour of flexible objects in flow can alter the thickness and steepness of the velocity gradients found on the surfaces of seaweeds. Obstacles in flow (like branches) produce wakes, which can reduce overall water speed at downstream branches [Johnson et al., 2001] and reduce shearing forces experienced by microbes.

Although flow is known to affect microbial settlement in a variety of ways [Characklis and Marshall, 1990, Ollos et al., 2003, Lehtola et al., 2006], quantifying and describing the interaction between seaweeds and the flow of water is complex and difficult. Further, seaweed morphology is confounded by a variety of factors that are known to influence composition of surface microbiota, such as chemical composition, making it difficult to determine whether the correlation between morphology and microbial community structure observed in Lemay et al. 2016 (unpublished) was truly due to morphology or not. Thus, in order to tease apart the relative effects of morphology from other biological traits, we conducted a microbial

settlement experiment using artificial seaweeds.

Our goal for this project is to test whether morphology, in the absence of biological factors, affects settlement rate or community composition of microbial communities.

2.2 Methods

Artificial Macroalgae Experiment



Figure 2.1: **Artificial Macroalgae.** Finely branched (left), bladed (centre) and crustose (right) representative morphologies were cut from 0.4mm latex sheeting. AM units had surface areas of approximately 44cm^2 (per side). Finely branched and bladed morphologies were $7.5 \times 9\text{cm}$ (width x length) and crustose morphologies were $7.5 \times 7.5\text{cm}$. Finely branched morphologies were created by cutting bladed morphologies into fine strips. Finely branched and bladed morphologies were glued to $7.5 \times 7.5\text{cm}$ laminate tiles by their “stipe”, whereas crustose morphologies were glued flat against the tile. Replicates at each site can be found in Table 2.1

Artificial macroalgae (AM) were cut out of 0.4mm latex sheeting (Radical Rubber olive-grn40, Elastica Engineering) into three morphologies: crustose, bladed, and finely branched (Fig. 2.1). The AM were glued to $7.5 \times 7.5\text{cm}$ laminate tiles with silicon glue. The bladed and finely branched morphologies were glued by the base of the “stipe”, whereas the crustose morphologies were glued flat against the tiles. The surface area for each of the three morphologies was approximately equal at 44cm^2 : the finely branched morphology was simply the bladed morphology cut into filaments, whereas the crustose morphology was created by rounding off the pointed tip of the bladed morphology.

| Site | Morphology | Replicates at each time point | | | | | | | |
|------------|------------|-------------------------------|---------|-------|---------|--------|---------|-----------|--|
| | | 20 m | 1 h | 3 h | 6 h | 12 h | 1 d | 4 d | |
| Reed Point | FB | 3 (3) W | 3 (3) | 3 (3) | 2 (3) | 3 (3) | 3 (3) W | - | |
| | BL | 3 (3) W | 3 (3) | 3 (3) | 3 (3) | 3 (3) | 3 (3) W | - | |
| | CR | 3 (3) W | 3 (3) | 3 (3) | 3 (3) | 2 (3) | 3 (3) W | - | |
| Hakai | FB | 10 (10) | 10 (10) | - W | 10 (10) | 9 (10) | - | 10 (10) W | |
| | BL | 10 (10) | 8 (10) | - W | 10 (10) | 9 (10) | - | 11 (10) W | |
| | CR | 10 (10) | 9 (10) | - W | 9 (10) | 6 (10) | - | 8 (10) W | |

Table 2.1: **Number of replicates at each site for AM experiment.** Replicates for finely branched (FB), bladed (BL), and crustose (CR) morphologies are shown in the table below. Numbers in brackets are number of replicates originally deployed. Some replicates were lost at the sampling stage, while others at the sequence quality filtering stage. The BL morphology on day 4 has 11 replicates because one blade from time point "1 hour" was mislabelled as "4 days". "W" indicates time points when water samples were taken.

The first experiment was conducted at Reed Point Marina in the Burrard Inlet near Vancouver, BC while a larger second experiment was done in the Central Coast of BC on Calvert Island, BC at the Hakai Research Institute. The two sites differed in a number of characteristics including salinity, season, and geographic location. At Reed Point, salinity was between 12-15ppt throughout the course of the experiment and sampling was done in March 2016. The Burrard Inlet is influenced by several rivers, most notably the Fraser River, and the salinity is highly variable over the course of the year. The second experiment was done on Calvert Island at the Hakai Research Institute dock in mid-summer (August 2016) and the salinity was 32ppt for the entire experiment and is largely consistent seasonally.

In both experiments, tiles attached to the artificial macroalgae were suspended off the docks at approximately 1m below the water surface and positions of morphologies, replicates, and time points along the docks were randomized. Sampling was destructive. The first experiment was conducted in March 2016 at Reed Point Marina and three replicates of each morphology were sampled destructively at each of five time points: 20 minutes, 3 hours, 6 hours, 12 hours, and 24 hours. Three water samples were taken concurrently at 20 minutes and 24 hours, each. We chose these time points to capture initial colonization and community dynamics. Results from experiment one at Reed Point were intriguing, but sample size was small. Thus, we conducted experiment two at Hakai with more replicates and with time points adjusted according to initial results to capture initial colonization while also capturing a more mature community (20 minutes, 1 hour, 6 hours, 12 hours, 4 days, water samples at 3 hours and 4 days). The different location also allowed us to assess the

robustness and generality of these findings. A table of sampling times and replicates can be found in Table 2.1.

AM units were sampled at each time point by rinsing each unit for 10 seconds with filter-sterilized seawater, and then swabbing one side of the surface for 10 seconds using sterile cotton swabs (Puritan- Item#: CA10805-154). The swab heads were then snapped off into 2mL cryotubes (VWR- Item#: 10018-760) and frozen at -20°C until extraction. Salinity was measured using a refractometer.

At Hakai, water flow was estimated by suspending pre-weighed Lifesaver brand “Pep-o-mints” on a cotton string 1 m below the water surface for one minute. The mints were then oven dried for at least one hour, or until dry to the touch. The dry weight before and after submersion was calculated and compared to the standard curve in Anderson and Martone (2014). According to their standard, the water flow at Hakai was less than 0.5 m/s and close to 0m/s, although we observed movement in the water visually. Water flow at Reed Point Marina was quantified visually: flow was also minimal.

Water samples were taken on day 1 and day 4 at Hakai, and at 20 minutes and 24 hours at Port Moody. Three separate 500mL samples of water at each time point were pre-filtered through 150 μm sieves to minimize sampling plant-debris and large animals, and then filtered through 0.22 μm membranes (Durapore- Item#: GVWP04700) using a peristaltic pump (Cole-Parmer- Item#: RK-77913-70) at approximately 180rpm (level 30). Filters were transferred to 2mL cryotubes and either frozen immediately at -20°C (Hakai) or kept on dry ice until return to the lab (Reed Point). All samples were transported frozen back to UBC for further processing.

Library prep

The 96-well MoBio PowerSoil DNA extraction kit was used to extract DNA from both the water filters and AM swabs. Filters and swabs were transferred to the extraction kit using tweezers sterilized with 2% HCl, then ethanol and flame. Extractions followed the MoBio Powersoil DNA extraction protocol with the following modifications based on recommendations in the Earth Microbiome protocol (<http://www.earthmicrobiome.org/>). First, a 10-minute incubation at 65°C in a water bath was added after the addition of C1 and before shaking in the shaker, next, the plates were shaken at 20 shakes per second for 20 minutes total instead of using the recommended shaker in the manual, and lastly filters were allowed to soak in C6 at room temperature for 10 minutes prior to elution into the final elution plate. The DNA elution was stored at -20°C .

The V4 region of the 16S small subunit ribosomal RNA marker gene was sequenced to profile bacteria and archaea. The amplicon library prep was done in-lab using the following primers: barcoded 515 forward primers (5'-GTGYCAGCMGCCGCGGTAA-3') and 806 reverse primers (5'-GGACTACHVGGGTWTCTAAT-3'). Forward primers were tagged with 12bp Golay barcodes, which were unique to each sample. Primers were used at final concentrations of 0.5uM with 4-5uL of DNA extract. DNA extracts were amplified in 20uL reactions using Phusion High-fidelity proofreading Mastermix (Thermofisher- Item#: F548L). Reactions underwent the following thermocycler settings: 98⁰C for 10 seconds, 25 cycles of 98⁰C (1s), 50⁰C (5s), 72⁰C (24s), and a final extension phase of 72⁰C for 1 minute. Samples that were not amplified adequately with 4uL of DNA at 25 cycles were re-amplified with 5uL DNA at 30 cycles. Lastly, the successful PCR products were quantified using Pico-green (Thermofisher- Item#: P11496) and pooled at 45ng/sample. The pooled samples were then sent to the Centre for Comparative Genomics and Evolution Bioinformatics (CGEB) at Dalhousie University for sequencing on the Illumina MiSeq platform with 2x300bp chemistry.

Processing of sequence data

Raw sequences were demultiplexed using `split_libraries_fastq.py` in QIIME version 1.9 (Quantitative Insights into Microbial Ecology, (QIIME), [Caporaso et al., 2010]) and then combined with the entire West Beach data set from Lemay (2016). All sequences were trimmed (`fastx_trimmer`) and clipped (`fastx_clipper`) to 250 bp and filtered with a quality threshold of Q19 (`fastq_quality_filter`) with the Fastx Toolkit (Hannon Lab), yielding 22,648,504 raw sequences. The remaining reads were processed into operational taxonomic units (OTUs) using Minimum Entropy Decomposition (MED, [Eren et al., 2014]) with the minimum substantive abundance (-m) parameter set to 150, yielding 5,820 unique OTUs and 15,840,802 reads. The resulting OTU matrix was transcribed into a QIIME-compatible format. Taxonomy was then assigned to the representative sequence for each MED node, hereafter referred to as OTUs, by matching it to the SILVA 128 database clustered at 99% with `assign_taxonomy.py` in QIIME using `uclust` [Edgar, 2010]. Chloroplast, mitochondrial, and eukaryotic DNA were filtered out. Thirty-eight OTUs suspected of being contaminants (abundance in PCR controls at least 50% of the maximum abundance found in any other sample) were also removed. Twenty-five contaminants were from the genus *Pseudomonas* and eight from the genus *Achromobacter*, which are both common lab contaminants. The remaining contaminants were an uncultured Alphaproteobacterium, a *Lactobacillus* (Firmicutes), a *Dokdonia* (Flavobacteriia), an uncultured member of Cellvibrionaceae (Gammaproteobacteria), and a member of Clostridiales (Firmicutes). PCR controls samples had between 1 and 9,417 reads per sample. Finally, samples with less than 1000 reads per sample were removed.

The final OTU table consisted of 5,820 unique sequences and 15,840,802 reads, with a mean of 25,508 reads per sample. For alpha and beta diversity analysis, samples were rarefied to 4,000 reads per sample. Representative sequences were aligned with PyNAST in QIIME and a phylogenetic tree was created using FastTree [Price et al., 2009] in QIIME with the `make_phylogeny.py` script.

Microbial richness across time and morphologies

Alpha diversity was calculated in QIIME with the metrics Chao1, PD_whole_tree, and Observed_otus. Chao1 is a metric that incorporates estimates of unobserved diversity into their richness calculations, which is valuable in microbial datasets because samples generally have many rare taxa [Chao, 1984]; PD_whole_tree calculates diversity given phylogenetic distance [Faith and Baker, 2006]; and observed_otus is simply the richness of the sample. These three metrics were chosen because they differed in the way diversity is quantified, and thus would provide meaningful comparisons. Alpha diversity values were imported into R [R Core Team, 2016] for statistical analysis. Overall differences in diversity between time and morphology (ANOVA: Morph + Time + Morph*Time, non-sequential (Type III)) were assessed using “lm” and “Anova” in the “car” package [Fox and Weisberg, 2011]. Differences between morphologies were also assessed at each time point using a one-way ANOVA (“anova”: chao1 Morph “stats” package [R Core Team, 2016]) for overall comparisons and pairwise t.tests (“pairwise.t.test” : “stats” package [R Core Team, 2016]) for pairwise comparisons. For pairwise comparisons, p -values were corrected for multiple comparisons using the Benjamini-Hochberg procedure (also known as the “False Discovery Rate” method), which controls for the proportion of expected type I errors [Benjamini et al., 1995].

Community composition across time and morphologies

In order to compare community composition across morphologies and time, distance matrices were created in `beta_diversity.py` (QIIME) with a rarefied OTU table using three metrics: unweighted Unifrac, weighted Unifrac [Lozupone and Knight, 2005], and Bray-Curtis [Bray and Curtis, 1957]. The Unifrac metric assesses community distance by comparing the number of shared to unshared branches in a phylogenetic tree of two communities (unweighted unifrac does not account for abundance and weighted Unifrac does), while Bray-Curtis incorporates only membership and relative abundance into its distance calculations. Distance matrices were imported into R and the “isomds” command from the “MASS” package [Venables and Ripley, 2002] was used to create 2-dimensional NMDS plots. Polygons were drawn around treatments by using “chull” in the “grDevices” package [R Core Team, 2016]. First,

we tested for overall differences in community composition by running a permutational anova (“adonis”) from the “vegan” package [Oksanen et al., 2017] with the factors time and morphology plus interactions (Time + Morph + Time:Morph). Then, we ran individual pairwise comparisons between the three morphologies at each time point (“adonis”: Morph). Pairwise comparisons were corrected for multiple comparisons using the Benjamini-Hochberg procedure.

Taxa summary plots were generated by combining taxa summaries outputs from `summarize_taxa.py` (QIIME) at the L4 level and the OTU level in base R.

To create the OTU heat map, the OTU table was filtered to only include core OTUs from morphologies and water samples at each site using a custom python script. This was done to reduce the overall number of OTUs in the table. A “core OTU” was defined as an OTU found in $\geq 90\%$ of samples in any given treatment (a single morphology at a single time point), whose maximum relative abundance in the entire data set is over 0.1%. The OTU table was imported into R and reordered using “cor” (Pearson correlation coefficient) to maximize clustering of abundant OTUs based on treatment. Finally, OTU abundances for the filtered table were visualized using “heatmap2” in “gplots” [Warnes et al., 2016]. OTUs are scaled by row, which means that the intensity of colour shows the abundance of that OTU relative to the average abundance of that OTU in all samples.

Dispersion of morphologies across time

Dispersion of AM units through time was quantified two ways. First, the mean distance (from the distance matrix) between all combinations of two morphologies at each time point was calculated. This yielded three pairwise comparisons (FB:CR, CR:BL, BL:FB). Additionally, overall dispersion of each time point (PERMDISP) was calculated using “betadisper” from the “vegan” package [Oksanen et al., 2017]. Differences in dispersion between time points and morphologies was also assessed separately using “betadisper” (“vegan” package) and “anova” (“stats” package [R Core Team, 2016]).

Turnover across time

Turnover was defined as the number of “new” OTUs at each time point (relative to the previous time point) divided by the total number of OTUs. This was calculated for all time points (except the first time point) and plotted using `plot()` in base R.

Test to quantify shear force on morphologies

We conducted a dye-dipping experiment to determine whether dye on different morphologies of AM was sheared off the surface at different rates. The experiment modified a method from Hoegh-Guldberg (1988) [Hoegh-Guldberg, 1988], which used a solution of methylene blue and Triton-X (a detergent) to estimate the surface area of coralline seaweeds. A viscous dye solution was made by dissolving approximately 0.8g of methylene blue (Michrome) and 1mL of Triton X (BDH- Item#: R06433) into 1L of tap water. The solution was then filtered through fiber-glass GF/F filters (Whatman- Item#: 28497-958) to remove solid particles and impurities.

Ten replicates of finely branched and bladed AM morphologies were subjected to three treatments. In the first treatment the AM units were dipped in dye, shaken 10 times and then put directly in 50mL falcon tubes with 25mL of tap water to measure how much dye is initially adhered to the surface. For the second treatment, AM units were dipped, shaken 10 times, and then submerged in a 1L beaker of still tap water for 5 seconds before transferring AM units into 50mL falcon tubes with 25mL of water. In the third treatment, AM units were dipped, shaken 10 times, and submerged in a 1L beaker full of tap water that was stirred by a magnetic spinner at maximum speed before transferring AM units into 50mL falcon tubes with 25mL of water. In all three treatments, the 50mL falcon tubes were shaken vigorously for 5 seconds and allowed to soak for 1 hour, then AM units were removed from the falcon tube, rinsed, and dried. Subsequently, the dye concentration in the water of the 50 mL falcon tubes were measured by taking absorbance measurements at a wavelength of 668 nm with the Jaz Spectrometer using the Spectrasuite software. Readings were done over integration times of 100ms each, and final measurements were averaged over 100 scans. The same 10 AM units were used for each of three treatments to allow for direct comparisons between the three treatments on a single AM unit.

2.3 Results

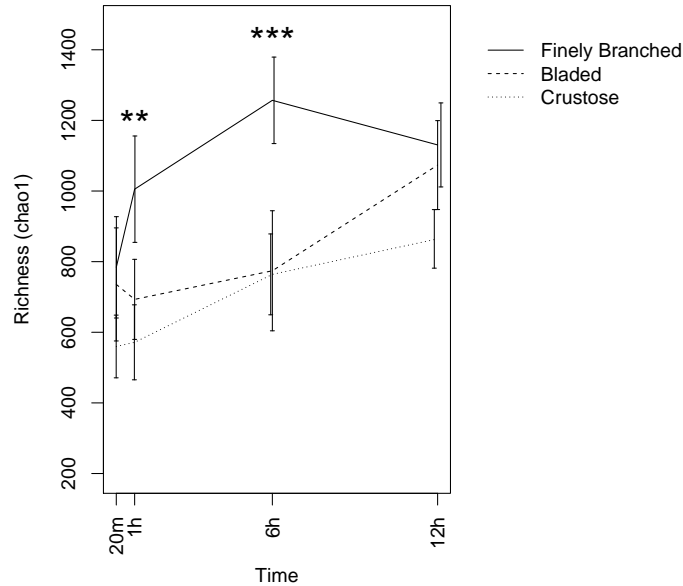
Sequencing yielded 1,123-106,093 sequences per sample after quality filtering; the final number of replicates and water samples included in the analysis after quality filtering can be found in Table 2.1.

Results were consistent between richness and community distance metrics. Since all alpha diversity metrics yielded similar conclusions, only Chao1 results are shown and described below. Additionally, only results from Bray-Curtis are shown because it incorporates both membership and abundance into its calculations- both of which appear to be important in

defining community structure across treatment groups.

Community composition across morphologies through time

A. Reed Point



B. Hakai

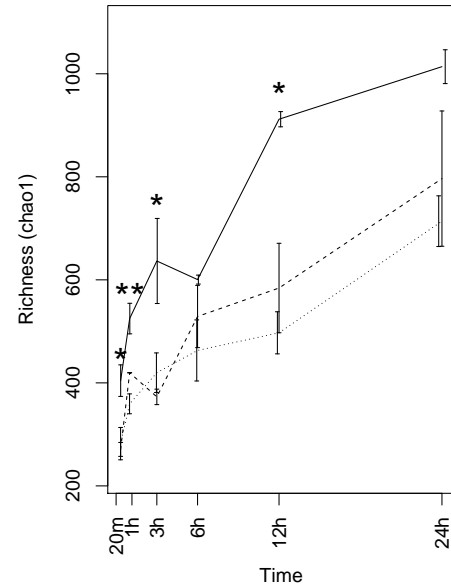


Figure 2.2: **Richness of biofilms on artificial macroalgae through time.** Richness (Chao1 metric) of AM biofilms through time at (A) Reed Point and (B) Hakai. Significance is indicated by stars: * = $p < 0.05$; ** = $p < 0.01$; *** = $p < 0.001$. Error bars are ± 1 SD. Richness increases with time and finely branched morphologies are more diverse than bladed or crustose morphologies at intermediate time points (See Table 2.2 for pairwise comparisons). The interaction term between Time and Morphology was not significant, but there is a trend where finely branched morphologies are more diverse at intermediate time points.

Finely branched morphologies initially accumulated diversity faster than bladed and crustose morphologies (Fig. 2.2). Although the interaction between morphology and time is not significant (which would imply that the rate of diversity increase differed between morphologies) (Hakai: ANOVA MorphxTime $p = 0.0575$, $F_{2,133} = 2.918$; Reed Point: ANOVA MorphxTime $p = 0.202$, $F_{2,46} = 1.655$), finely branched AM units are significantly more diverse than bladed or crustose AM units at early (and most) time points (Table 2.2, Hakai: ANOVA Morph $p < 0.001$, $F_{1,133} = 26.653$; Reed Point: ANOVA Morph $p < 0.001$, $F_{1,46} = 38.451$). At later time points, however, similar richness of microbial taxa is found on all three morphologies.

The composition of microbial communities also became more distinct across morphologies over the first part of the time series in both the Hakai and Reed Point data sets (Fig. 2.3). In

| Sites | Test type | Factors | <i>p</i> -Values: between morphologies | | | | | | | Overall |
|------------|------------------|---------|--|--------------------------------------|------------------------------------|--|------------------------------------|---------------------------|----------------------------|---|
| | | | 20 minutes | 1 hour | 3 hours | 6 hours | 12 hours | 1 day | 4 days | |
| Reed Point | ANOVA | Morph | 0.039 ($F_{2,6}=5.86$) | 0.0071 ($F_{2,6}=12.59$) | 0.048 ($F_{2,6}=5.23$) | 0.43 ($F_{2,5}=0.99$) | 0.021 ($F_{2,5}=9.29$) | 0.15 ($F_{2,6}=2.6$) | - | 0.0033 ($F_{2,46}=6.48$) |
| | | FB:BL | 0.045 | 0.03 | 0.069 | 0.5 | 0.028 | 0.24 | - | 0.012 |
| | Pairwise t-tests | FB:CR | 0.045 | 0.0077 | 0.071 | 0.5 | 0.028 | 0.21 | - | 0.0049 |
| | | BL:CR | 0.8 | 0.12 | 0.61 | 0.5 | 0.45 | 0.56 | - | 0.55 |
| Hakai | ANOVA | Morph | 0.16 ($F_{2,27}=1.93$) | 0.003 ($F_{2,24}=7.45$) | - | < 0.001 ($F_{2,26}=10.12$) | 0.1 ($F_{2,21}=2.57$) | - | 0.67 ($F_{2,26}=0.4$) | < 0.001 ($F_{2,133}=16.86$) |
| | | FB:BL | 0.69 | 0.024 | - | < 0.001 | 0.6 | - | 0.91 | 0.013 |
| | Pairwise t-tests | FB:CR | 0.22 | 0.0031 | - | < 0.001 | 0.12 | - | 0.69 | < 0.001 |
| | | BL:CR | 0.23 | 0.33 | - | 0.94 | 0.15 | - | 0.69 | 0.16 |

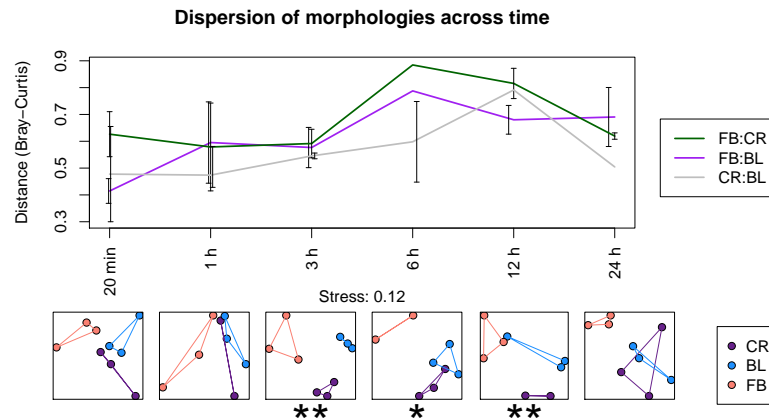
Table 2.2: **Pairwise t-tests and ANOVA of richness between morphologies across time.** Two tests were done to quantify richness over time. First, an ANOVA was done overall (Morph, Time, MorphxTime) and at each time point (Morph). Results show *p* values of the ‘Morph’ factor only. Additionally, pairwise t-tests were done at each time point to determine which morphology (if any) was driving significant results in the ANOVA. All pairwise *p*-values are adjusted using the Benjamini-Hochberg procedure (False Discovery Rate). Results show that the finely branched (FB) morphology drives the significant effect for ‘Morph’ in the ANOVA results. Bladed (BL) and crustose (CR) morphologies do not differ in richness at any time point. At the final time point for Reed Point and Hakai (1 day and 4 days, respectively), there are no significant differences in richness between morphologies.

both experiments, compositional differences between morphologies are most pronounced at intermediate time points (3-12 hours, depending on the data set), but communities converge at later time points (Fig. 2.3).

Plotting the core OTUs associated with each morphology over time reveals that OTUs are differentially abundant on finely branched morphologies relative to crustose or bladed morphologies (Fig. 2.4). The enrichment of OTUs on finely branched morphologies correlates well with a map of core OTUs (Fig. 2.4, Fig. S2.11), but poorly with a presence/absence map (Fig. S2.12). This suggests that finely branched morphologies accumulate biofilms that are structurally different from crustose or bladed biofilms, not necessarily in terms of membership, but rather in terms of differential abundance.

The pattern of overall community turnover over time differed between the two experiments. At Hakai, microbial communities across all morphologies became less dispersed over time (Fig. 2.3b, Fig. S2.10b, PERMDISP $p < 0.001$, $F_{4,131}=97.403$), suggesting that microbial communities on all AM units became more similar as settlement progressed. Additionally, core OTU turnover was low at Hakai (Fig. 2.5), which means core members of the community were not changing. Conversely, at Reed Point, dispersion does not change over time (Fig. 2.3a, Fig. S2.10a, PERMDISP $p = 0.131$, $F_{5,45}=1.807$), suggesting that biofilms on AM units are just as different from each other at the beginning of the experiment as they are at the

A. Reed Point



B. Hakai

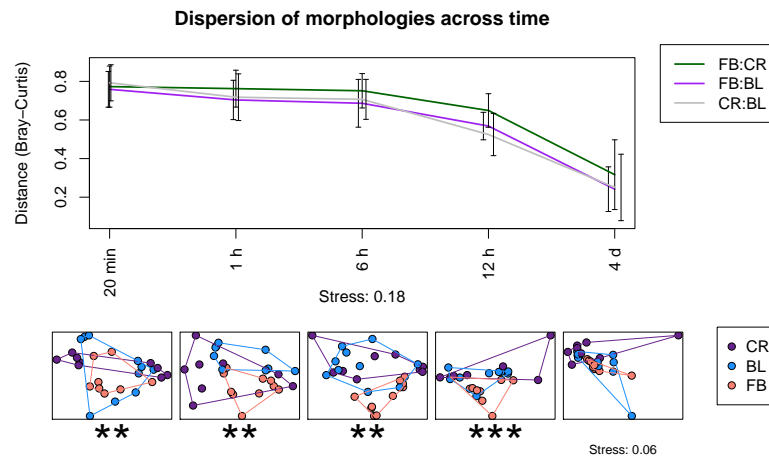


Figure 2.3: **Dispersion and community composition of AM morphologies through time.** Pairwise dispersions were calculated by averaging distances from a Bray-Curtis distance matrix for each pair of morphologies. Error bars show ± 1 SD. Below each time point is a corresponding NMDS plot of samples from that time point, coloured by morphology. Significant differences between morphologies (PERMANOVA Morph) are listed below each plot and shown with stars: * = $p < 0.05$; ** = $p < 0.01$; *** = $p < 0.001$. Complete statistics are shown in Table 2.3. At Reed Point (A), dispersion of morphologies (shown above) and overall dispersion (Fig. S2.10a) does not differ significantly with time. At Hakai (B), dispersion of morphologies (shown above) and overall dispersion (Fig. S2.10b) decreases significantly with time. However, in both experiments, communities initially become more distinct with time. The 4-day time point of Hakai was plotted from a separate NMDS calculation (and thus has a different stress value) to better capture within-time-point variation between morphologies.

end. There was also higher turnover of core OTUs through time at Reed Point (Fig. 2.5).

| Sites | Test type | Factors | p-Values: between morphologies | | | | | | | Overall |
|------------|--------------------|---------|---|---|--|---|---|---------------------------------|---------------------------------|---|
| | | | 20 minutes | 1 hour | 3 hours | 6 hours | 12 hours | 1 day | 4 days | |
| Reed Point | PERMANOVA | Morph | 0.078 ($R^2=0.36, df=2.8$) | 0.54 ($R^2=0.28, df=2.7$) | 0.007 ($R^2=0.42, df=2.8$) | 0.011 ($R^2=0.42, df=2.7$) | 0.003 ($R^2=0.48, df=2.7$) | 0.059 ($R^2=0.39, df=2.8$) | - | 0.001 ($R^2=0.11, df=2.33$) |
| | | FB:BL | 1 ($R^2=0.16, df=1.5$) | 1 ($R^2=0.22, df=1.5$) | 0.6 ($R^2=0.27, df=1.5$) | 0.3 ($R^2=0.34, df=1.4$) | 0.3 ($R^2=0.28, df=1.5$) | 0.3 ($R^2=0.4, df=1.5$) | - | 0.057 ($R^2=0.07, df=1.34$) |
| | Pairwise PERMANOVA | FB:CR | 0.3 ($R^2=0.39, df=1.5$) | 1 ($R^2=0.23, df=1.4$) | 0.3 ($R^2=0.36, df=1.5$) | 0.3 ($R^2=0.45, df=1.4$) | 0.3 ($R^2=0.52, df=1.4$) | 0.3 ($R^2=0.41, df=1.5$) | - | 0.003 ($R^2=0.12, df=1.32$) |
| | | BL:CR | 0.3 ($R^2=0.28, df=1.5$) | 1 ($R^2=0.21, df=1.4$) | 0.3 ($R^2=0.42, df=1.5$) | 0.6 ($R^2=0.26, df=1.5$) | 0.3 ($R^2=0.43, df=1.4$) | 1 ($R^2=0.15, df=1.5$) | - | 0.063 ($R^2=0.07, df=1.33$) |
| | | | | | | | | | | |
| Hakai | PERMANOVA | Morph | 0.009 ($R^2=0.14, df=2.26$) | 0.006 ($R^2=0.14, df=2.26$) | - | 0.002 ($R^2=0.2, df=2.28$) | 0.001 ($R^2=0.17, df=2.23$) | - | 0.1 ($R^2=0.12, df=2.28$) | 0.001 ($R^2=0.09, df=2.95$) |
| | | FB:BL | 0.13 ($R^2=0.1, df=1.17$) | 0.033 ($R^2=0.13, df=1.17$) | - | 0.006 ($R^2=0.2, df=1.19$) | 0.006 ($R^2=0.16, df=1.17$) | - | 0.99 ($R^2=0.05, df=1.20$) | 0.012 ($R^2=0.04, df=1.94$) |
| | Pairwise PERMANOVA | FB:CR | 0.075 ($R^2=0.13, df=1.16$) | 0.015 ($R^2=0.12, df=1.18$) | - | 0.003 ($R^2=0.19, df=1.18$) | 0.012 ($R^2=0.17, df=1.14$) | - | 0.12 ($R^2=0.15, df=1.17$) | 0.003 ($R^2=0.05, df=1.87$) |
| | | BL:CR | 0.13 ($R^2=0.09, df=1.18$) | 0.59 ($R^2=0.08, df=1.16$) | - | 0.4 ($R^2=0.08, df=1.18$) | 1 ($R^2=0.07, df=1.14$) | - | 0.52 ($R^2=0.09, df=1.18$) | 0.46 ($R^2=0.02, df=1.88$) |
| | | | | | | | | | | |

Table 2.3: **Pairwise and overall PERMANOVAs of community composition between morphologies across time.** Two tests were done to quantify community dissimilarity over time. First, a PERMANOVA was done overall (Morph, Time, MorphxTime) and at each time point (Morph). Results show p -values of the ‘Morph’ factor only. Additionally, pairwise PERMANOVAs were done at each time point to determine which morphology (if any) was driving significant results in the overall PERMANOVA. P -values for pairwise comparisons were adjusted using the Benjamini-Hochberg method (False Discovery Rate). Results show that the finely branched (FB) morphology drives the significance behind the overall PERMANOVA results. Bladed (BL) and crustose (CR) morphologies do not differ significantly in composition at any time point in either Hakai or Reed Point samples. At the final time point, differences between morphologies are not significantly different at either site.

However, despite differences in community turnover trends, both experiments saw microbial communities on differing morphologies become more distinct (Fig. 2.3). This suggests that distinctiveness of communities on AM morphologies (whether FB, CR, and BL morphologies are different or not) is decoupled from gamma diversity (heterogeneity between samples and treatments) at these two sites.

Shared core OTUs between morphologies and time points

Common inhabitants of biofilms found on AM units at both Hakai and Port Moody included those from the Order Pseudomonadales, Alteromonadales, Burkholderiales, Flavobacteriales, and an unidentified representative of Alphaproteobacteria (Fig. 2.6). Flavobacteriales and the unidentified Alphaproteobacteria are also found at significant abundances in the water. Members of Pseudomonadales appear to decrease as microbial communities progress, whereas Flavobacteriales increase. AM surface communities begin less taxonomically diverse than the water column, but are significantly more diverse than the water at later time points (Fig. S2.13). Hakai AM surface communities are more diverse than ones at Reed Point (Welch’s t -Test $p = <0.001$, $t_{150.6} = 4.316$; Fig. S2.14, Table S2.6), but water column diversity does not differ between Hakai and Reed Point (PERMANOVA $p = 0.334$, $F_{1,8} = 1.057$). Thus, through some mechanism, diversity of microbial biofilms on AM surfaces is greater at Hakai

than Reed Point despite no apparent difference in diversity of the water column.

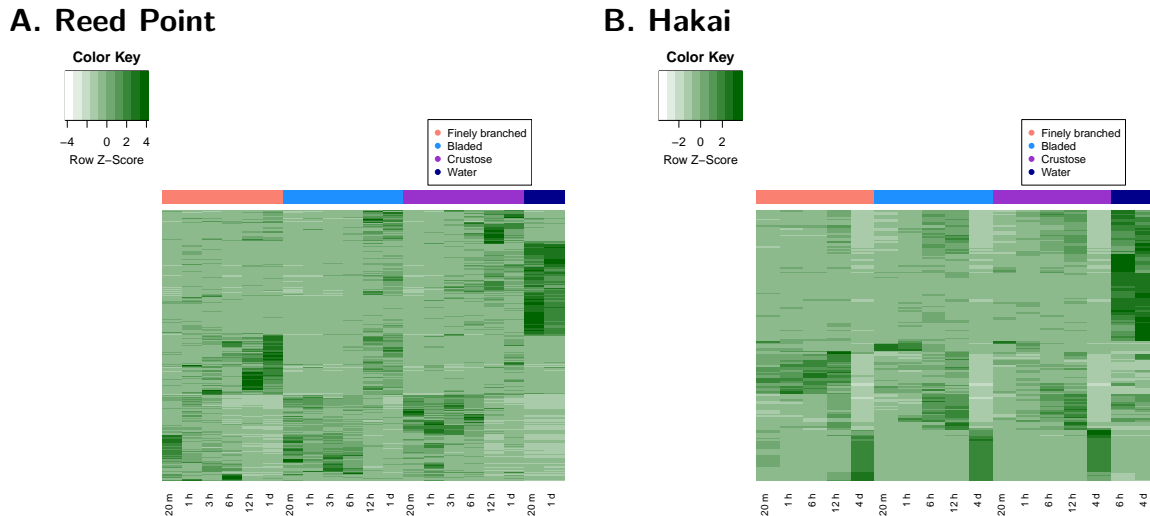


Figure 2.4: **Heatmap of core OTUs across morphologies and time points.** The heatmap shows core OTUs only. Core OTUs are defined as being present in >90% of samples in each treatment (morphology per time point) and observed at >0.1% relative abundance at least once in entire dataset. Colouring is scaled by rows, meaning that each OTU is coloured based on how abundant it is compared to other samples. At both Reed Point (A) and Hakai B, there is differential enrichment of OTUs between finely branched and bladed or crustose morphologies.

At early time points, there are many shared dominant taxa between sites at the Order level (Fig. 2.6), but few shared OTUs (Fig. S2.15). However, a few shared OTUs emerge late in colonization, including *Oleispira*, which dominates biofilm communities on day 4 at Hakai.

Selection for latex-degrading bacteria is important at later time points

Communities sampled on day 4 are drastically different to all other time points, and are dominated by a single OTU from the genus *Oleispira* (Fig. 2.6). Bacteria from the genus *Oleispira* are known to be hydrocarbon degraders [Yakimov et al., 2003, Mason et al., 2003], and we believe this OTU is degrading the latex from our AM units. There were 87 OTUs in both data sets assigned to *Oleispira*, and 44 OTUs with the exact same taxonomic description as the OTU described above, but only one OTU was ever observed at relative abundances over 2% (with most at abundances below 0.1%).

Oleispira was found in all Hakai water samples and on all morphologies across all time points, but always at abundances less than 0.07% in the water and less than 5.1% on AM

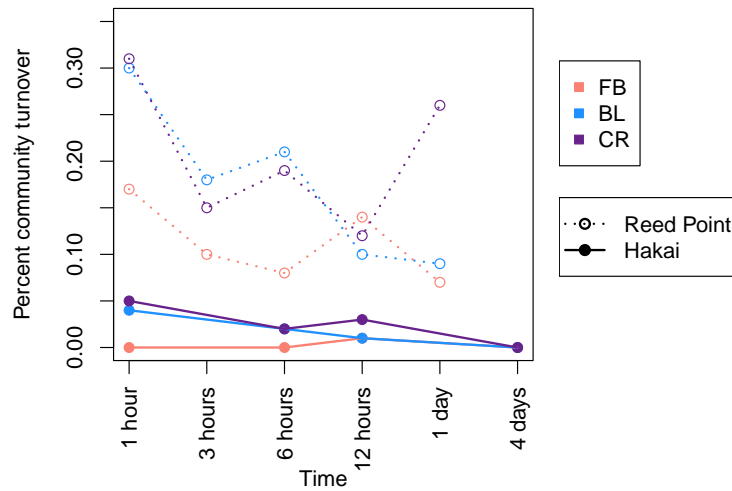


Figure 2.5: **Turnover of OTUs across time points.** Percent of OTUs at each time point that were not found in previous time point are plotted against time— in other words, this represents the percent turnover of communities on each morphology through time. There are consistently higher rates of turn over on AM units at Reed Point compared to Hakai. There is almost no turnover at most points at Hakai.

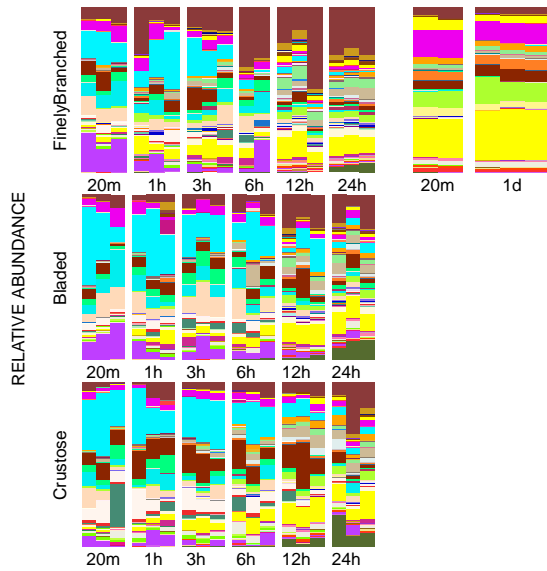
units (average 0.7%, excluding 4 outliers with 30%+ abundances) in time points 20min-12h. *Oleispira* was also found in the Reed Point data set in both the AM samples and the water column. Like the Hakai data set, *Oleispira* from Reed Point are abundant in all water column samples at abundances less than 0.07%. Also, AM unit samples in time points 20min-12h at Reed Point are composed of less than 5% (average 0.6%) *Oleispira*, while its abundance in the 24hour Reed Point time point is 4-20% (average 9%). Thus, we predict that *Oleispira* would have dominated the communities at Reed Point like they did at Hakai if the experiment had continued past 24 hours.

We observed *Oleispira* in similar abundances in the water column at both sites at all time points, which suggests that *Oleispira* is found natively in the water column. However, since we did not sample AM units prior to either experiment (although we did dip AM units in ethanol in the Hakai experiment) we cannot be certain that *Oleispira* was not introduced to the AM units in the lab.

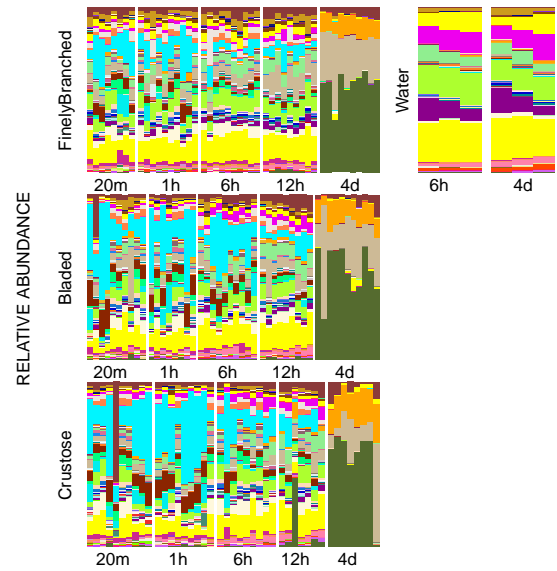
Dye experiment results

The results from the dye-dipping experiment to test whether shear forces differed on the surface of AM units yielded insignificant results (Fig. S2.16). Although there were trends

A. Reed Point



B. Hakai



Legend



Figure 2.6: **Taxa summary of OTUs collapsed by Order.** Taxa summaries show all replicates from all time points at the Order level, except for *Oleispira*, which is shown at the genus level. *Oleispira* is observed at very low abundances ($<0.7\%$, excluding outliers) until the 12 hour time point in both experiments. At Hakai, it is the most abundant OTU on all morphologies by day 4. Hakai samples are more diverse than Reed Point samples (Fig. S2.14).

where the bladed morphology lost more dye, these trends were not supported statistically (Welch's t-Test "Moving water" $p = 0.39$, $t_{11,x} = 0.89$; "Still water" $p = 0.51$, $t_{9.9,x} = 0.68$). There was a great amount of noise in all treatment groups, so if there were any real effects

of morphology it was likely swamped by the natural variation found in our data. Thus, although the results yielded insignificant results across morphology, we do not believe it means shear forces on the surface of AM morphologies are necessarily the same. Rather, the precision of our methods was likely insufficient to detect any differences.

2.4 Discussion

Flow and morphology interact to influence microbial settlement

The direction and speed of water flow across solid surfaces is known to influence microbial settlement and biofilm development. For example, biofilm formation increases when water speeds are high [Rusconi et al., 2014, Rusconi and Stocker, 2015] and when environments are physically heterogenous [Abelson and Denny, 1997, Singer et al., 2010]. Additionally, flow speed [Stewart and Carpenter, 2003] and spatial heterogeneity [Singer et al., 2010] of surfaces can affect the rate of mass transfer of nutrients to biofilms, which can further influence biofilm development. However, despite the acknowledgement that water flow is potentially crucial to understanding how and when microbes colonize surfaces [Rusconi et al., 2014, Rusconi and Stocker, 2015], there has been little experimental work that tests the interaction between flow and seaweed morphology *in situ*. Therefore, we wanted to experimentally test whether seaweed morphology effects overall biofilm community development.

Our results show that macroalgal morphology affects both microbial settlement and community composition. In both replicate experiments, finely branched morphologies experience faster microbial settlement rates than bladed or crustose morphologies (Fig. 2.2, Table 2.2). This supports our hypothesis that the narrow tendrils on finely branched morphologies cause greater microbial deposition, since particles denser than water will separate from the main stream of flow as it moves around protrusions (a phenomenon called ‘inertial impaction’) [Abelson and Denny, 1997]. The behaviour of finely branched tendrils in flow may also produce slower-flowing ‘wakes’ [Johnson et al., 2001]. Slower water velocity at downstream tendrils may additionally facilitate settlement by reducing shear forces experienced by microbes [Rutter and Vincent, 1988].

Finely branched morphologies also hosted structurally different microbial communities compared to bladed and crustose morphologies. We find that it is differential enrichment of core OTUs, and not differences in membership, that drives the divergence of finely branched morphologies (Fig. 2.4). These trends are consistent with observations made in other systems: biofilms found in stream beds with varying levels of physical heterogeneity also differ in rel-

ative abundance of core members rather than membership [Singer et al., 2010]. Streamline and turbulent flow regimes can also produce a variety of biofilm structures (chain-like versus colony-like growth patterns, respectively) [Singer et al., 2010], and influence the mass transfer rates of nutrients [Stewart and Carpenter, 2003]. Therefore, we hypothesize that shifts in community structure found between our AM morphologies are likely due to a combination of differential mass transfer of nutrients [Singer et al., 2010, Stewart and Carpenter, 2003] and physical biofilm structure [Singer et al., 2010] induced by differential flow regimes around AM unit morphologies.

*Dominant OTU *Oleispira* masks signal of morphology over time*

Differences in community structure between morphologies became insignificant in the last time points of both experiments. This correlates to the sudden growth (and eventual dominance) of a few taxa, including a latex-degrader, *Oleispira*. There are small differences in community composition between AM morphologies at the 4 day time point at Hakai (see in Fig. 2.5), but the signal of morphology is seemingly overwhelmed by the signal of a few substrate specialists (*Oleispira* and a few others).

In contrast to our AM morphologies, whose biofilms were highly uneven, real seaweeds are generally host to a diverse collection of coexisting microbial lineages [Egan et al., 2013]. Theories in ecology predict that habitat heterogeneity and disturbance both increase biodiversity in local communities [Huston, 1979]. Therefore, seaweed biofilms are likely more even than latex biofilms because they possess greater physical surface heterogeneity (many seaweeds are textured or ruffled), and also exude a variety of antimicrobial compounds, which can be considered a source of ‘press’ disturbance and are known to increase evenness in microbial communities associated with seaweeds [Persson et al., 2011].

Relevance for real seaweeds

Lemay et al. (2016) observed a strong correlation between seaweed morphology and microbial community composition in the species *Mastocarpus spp.*. Our experiment shows that morphology alone is sufficient to drive differences in microbial community structure between artificial seaweeds. On real seaweeds, however, other factors like polysaccharide chemistry [Dininno and McCandless, 1978, Eveleigh et al., 1979, Falshaw et al., 2003] and tissue age [Bengtsson et al., 2012] correlate with morphology. These factors potentially contribute to the differences in microbial community structure observed on *Mastocarpus spp.* in Lemay et al. (2016). Therefore, although morphology drives differences in community structure on artificial seaweeds, it is not necessarily the single driver of differential community

structure between real seaweed morphologies.

On real seaweeds, initial settlement of microbes may influence final community structure through downstream settlement effects. It is known that many different microbes are capable of performing similar metabolic tasks within the seaweed microbiome and it was previously hypothesized that neutral mechanisms like the competitive lottery model may explain the high taxonomic variation observed between individual macroalga microbiota [Burke et al., 2011a]. However, differences in initial biofilm members driven by morphology may also help explain the variation found in final (or climax) communities of macroalgal biofilms. Microbes are known to produce a range of antimicrobial compounds that prevent invasion from other bacteria [Matz et al., 2008, Egan et al., 2008], and pre-established biofilms are known to resist invasion from several laboratory strains of bacteria [Rao et al., 2010]. Conversely, many types of bacteria are described as having facilitative effects on the growth and attachment of invertebrates, algal spores, and diatoms [Huggett et al., 2006]. Thus, initial colonization differences among morphologies and seaweeds may result in drastically different downstream microbial and epiphytic communities.

Our results also open many questions about the interaction between seaweed morphology and its epibionts. Microbial density on seaweed surfaces can vary by as much as five orders of magnitude [Armstrong et al., 2001, Bengtsson and Øvreås, 2010], and one might ask whether morphological complexity correlates with microbial density. Microbial density can influence both the direct and indirect effects of seaweed biofilms on their host. For example, some bacteria are known to increase settlement of macro-epiphyte spores and larvae (such as other seaweeds and invertebrates) [Huggett et al., 2006] and epiphytes increase drag experienced by their macroalgal hosts [Anderson and Martone, 2014]. Thus, future experiments may be done to test, for example, whether highly branched seaweeds are at greater risk for epiphyte colonization due to higher recruitment of spores and larvae by microbial epibionts. This is but one example of how morphology and microbial settlement may interact to affect larger ecological relationships.

Conclusion

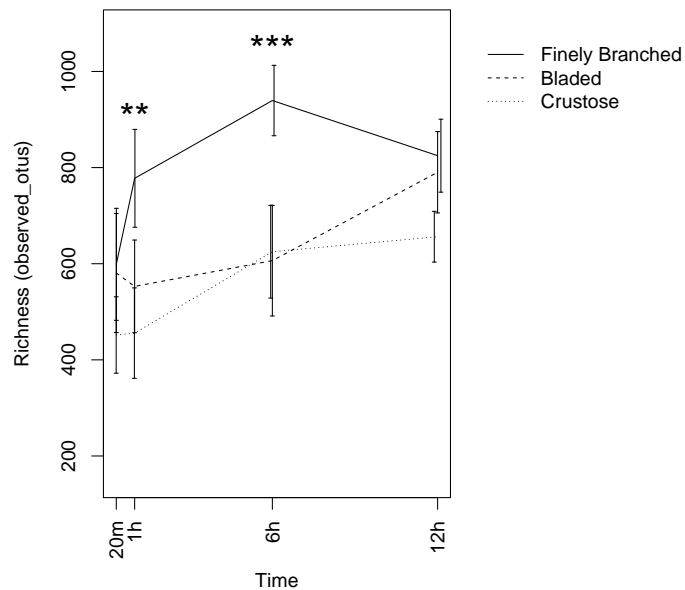
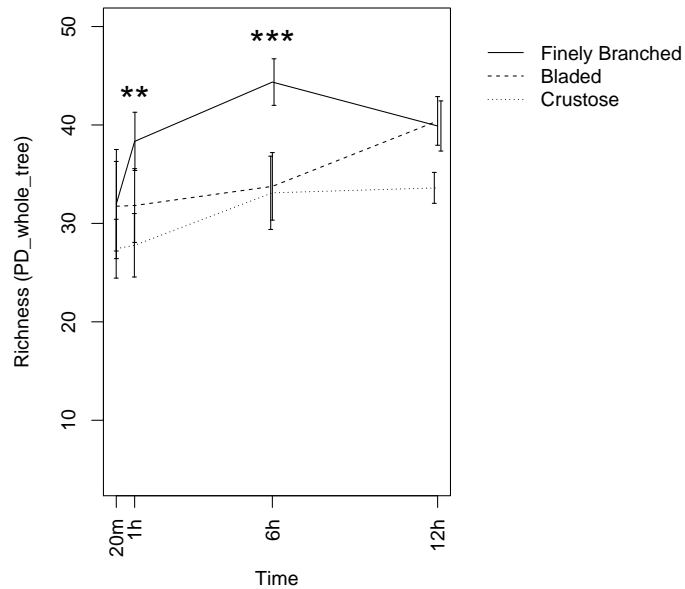
We propose that morphology of seaweed may modulate, limit, or encourage the assembly of certain members of the seaweed microbiota due to the interaction between morphology and water flow. Our findings suggest that initial settlement differs between finely branched and bladed or crustose morphologies, and we hypothesize that these differences are a result of differential rates of settlement, shear forces, and transfer of nutrients to the seaweed surface

. At latter time points however, other factors (like the presence of a substrate specialist) tend to swamp any signal from morphology. Thus, morphology is likely one of many factors involved in determining final microbial community composition on real seaweeds.

There are many organisms, microbial and macrobial, that live epiphytically on seaweeds. Most of these organisms rely on a spore dispersal stage at some point in their reproductive cycle, and the dispersal of these spores usually operate at the microbial scale. Since microbial and non-microbial epiphytes have the potential to be both symbiotic and detrimental to seaweeds [Egan et al., 2013], knowledge about how flow, settlement, and morphology change interactions with potential epiphytes will be crucial to understanding community-level dynamics on seaweeds.

2.5 Supplementary Figures and Tables

A. Reed Point



B. Hakai

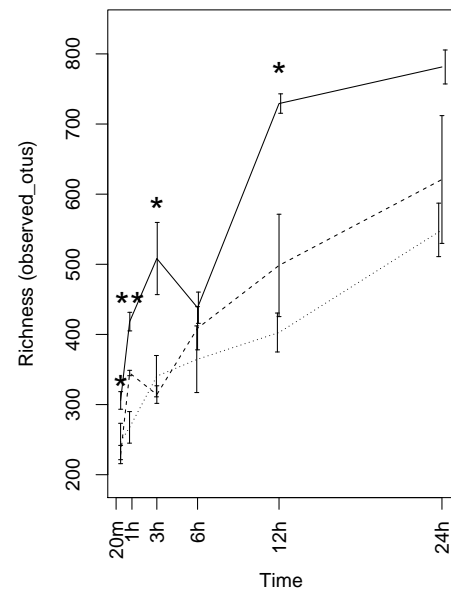
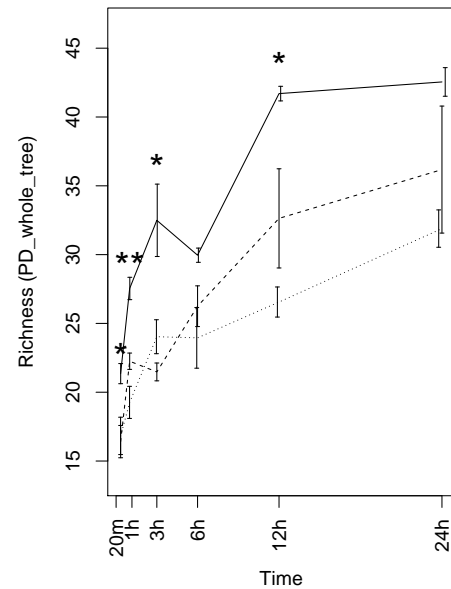
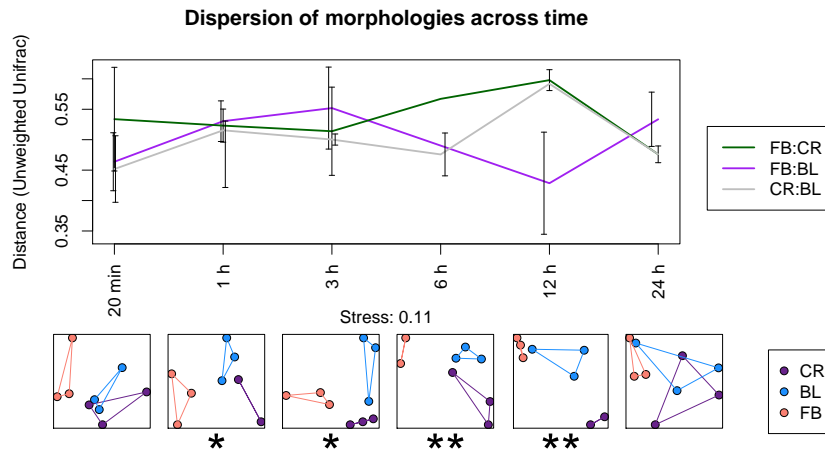


Figure 2.7: **S: Richness of biofilms on AM units through time.** Richness (PD_whole_tree and observed_otus metrics) of AM biofilms through time at (A) Reed Point and (B) Hakai. Significance is indicated by stars: * = $p < 0.05$; ** = $p < 0.01$; *** = $p < 0.001$. Error bars are +/-1SD.

A. Reed Point



B. Hakai

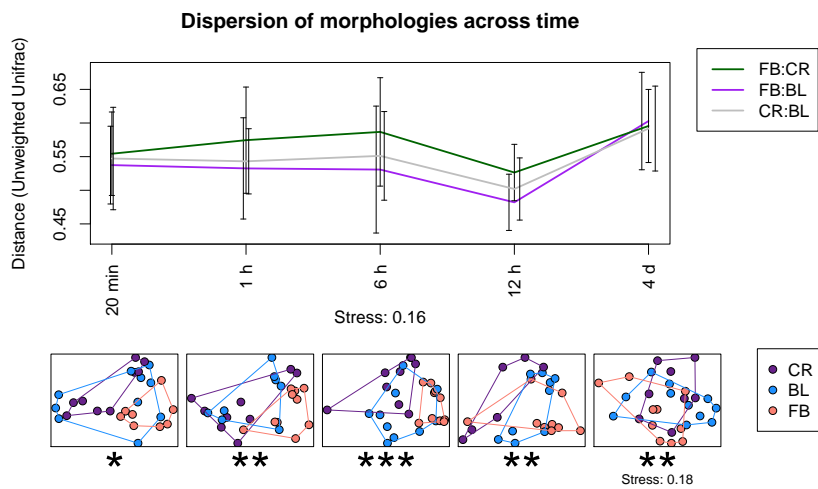
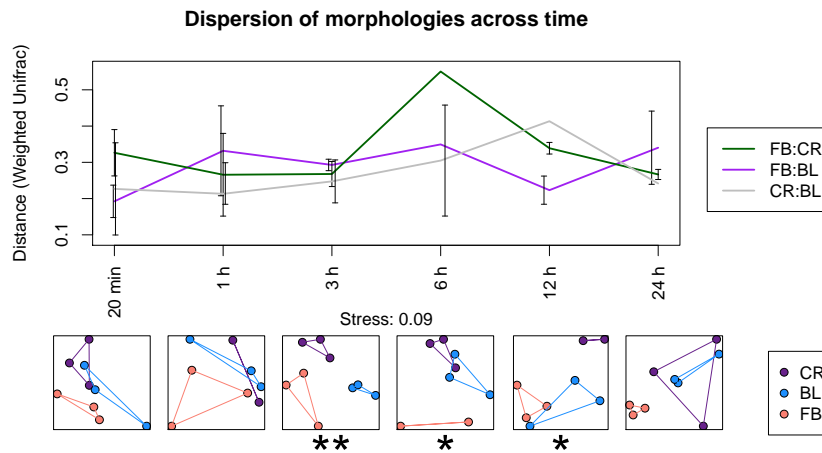


Figure 2.8: **S: Dispersion and community composition of AM morphologies through time.** Pairwise dispersions were calculated by averaging distances from a un-weighted Unifrac distance matrix for each pair of morphologies. Error bars show ± 1 SD. Below each time point is a corresponding NMDS plot of samples from that time point, coloured by morphology.

A. Reed Point



B. Hakai

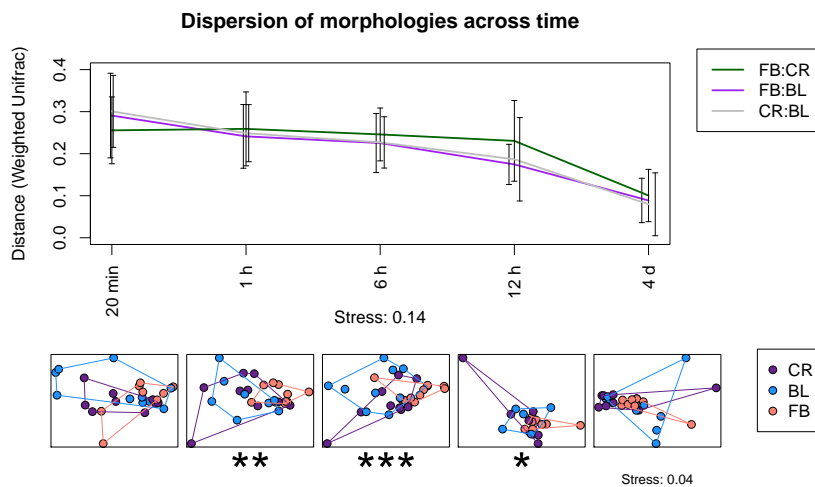
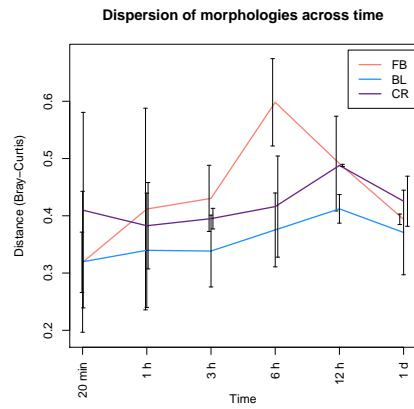


Figure 2.9: **S: Dispersion and community composition of AM morphologies through time.** Pairwise dispersions were calculated by averaging distances from a weighted Unifrac distance matrix for each pair of morphologies. Error bars show ± 1 SD. Below each time point is a corresponding NMDS plot of samples from that time point, coloured by morphology.

A. Reed Point



B. Hakai

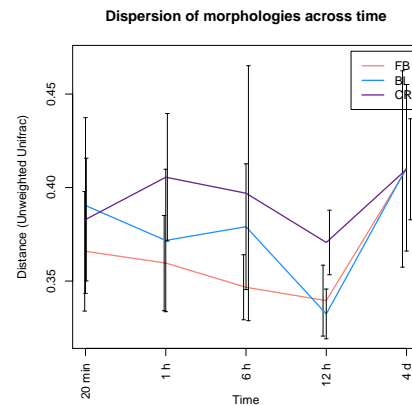
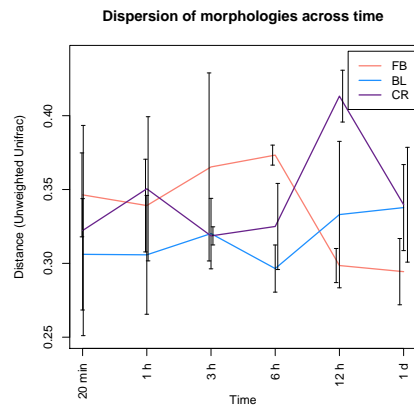
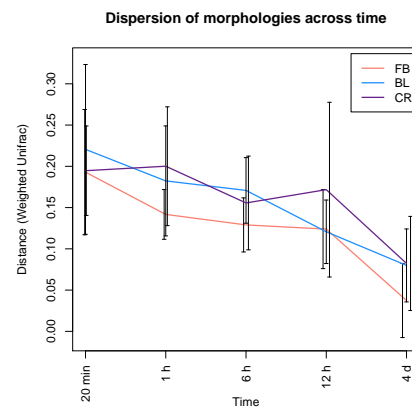
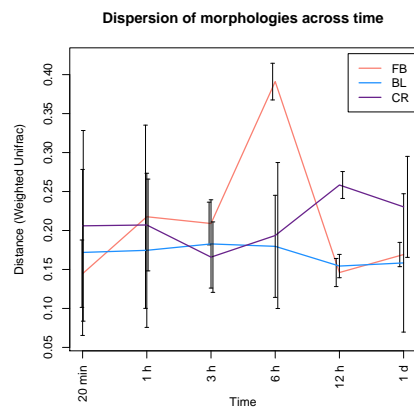
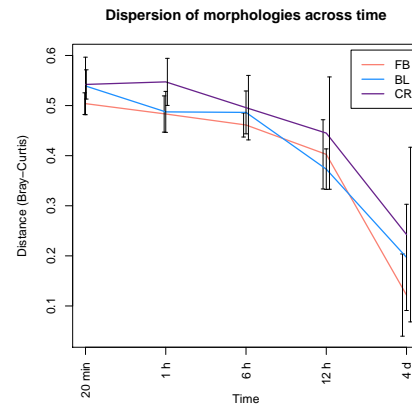


Figure 2.10: **S: Overall dispersion of AM units over time.** Dispersion was calculated using “betadisper” in the “vegan” package in R. Overall and time-separated PERMDISP calculations can be found in Table S2.4. Row (A) shows Reed Point; row (B) shows Hakai. Metrics used were Bray-Curtis (top), unweighted Unifrac (middle), and weighted Unifrac (bottom).

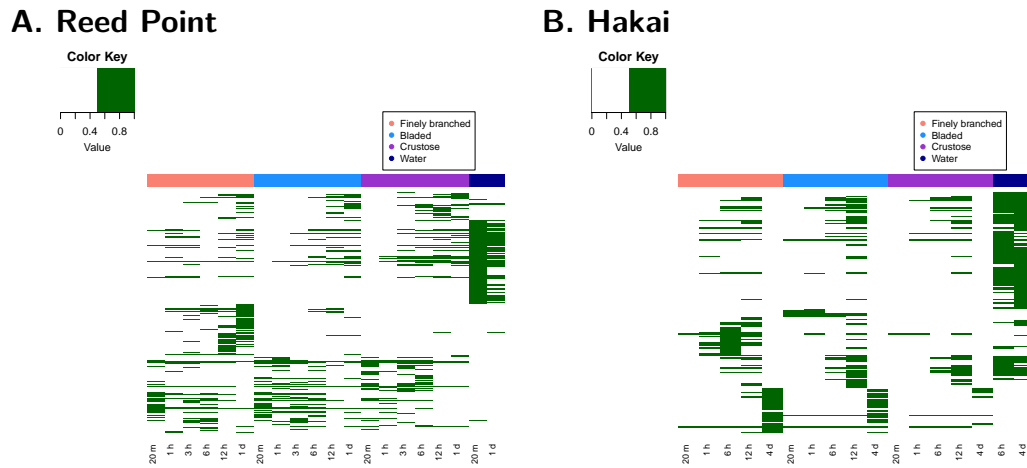


Figure 2.11: **S: Heatmap showing “core” OTUs.** A core OTU must be present in $>90\%$ of samples in treatment and also observed at least once above 0.1% relative abundance. Core OTUs correspond with OTUs that are enriched in each morphology and time point. (Fig. 2.4).

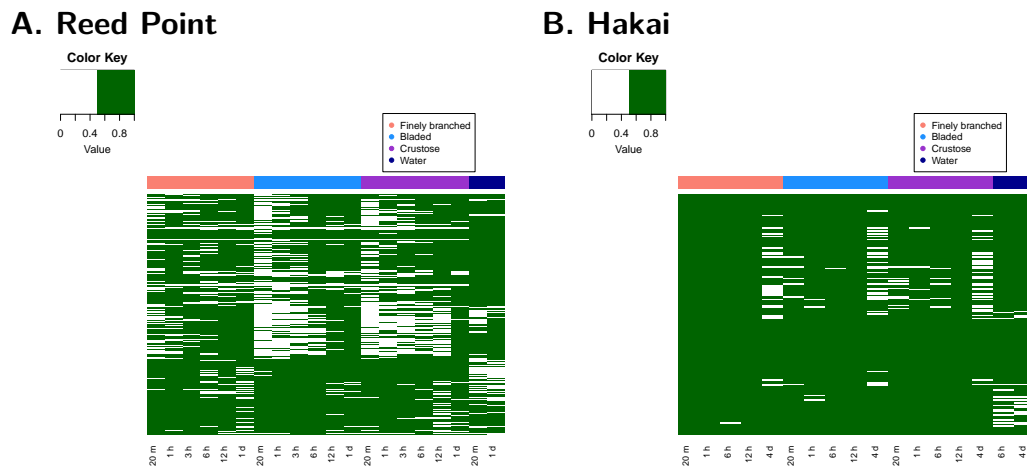


Figure 2.12: **S: Heatmap showing presence or absence of “core” OTUs.** At Hakai (B), nearly all OTUs are present across all time points. Conversely, we see that core OTUs turn over through time at Reed Point (A).

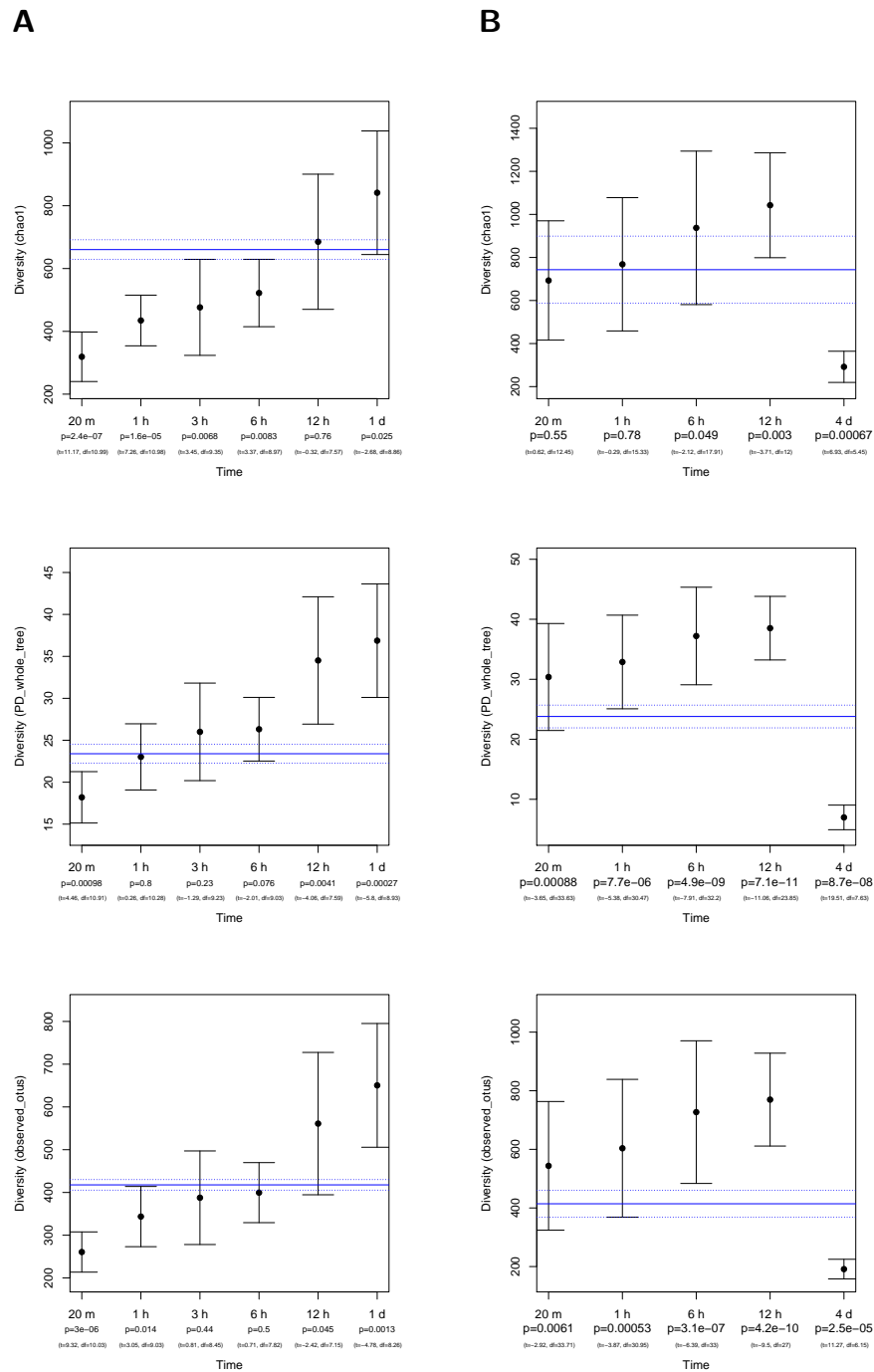


Figure 2.13: **S: Comparison of water diversity and AM biofilm diversity** Blue line represents average richness of water across both sampling time points. Black points with +/-1SD error bars represent richness of all AM biofilms at that time point. Significance values and parameters (Welch's t-Test) are listed below each time point.

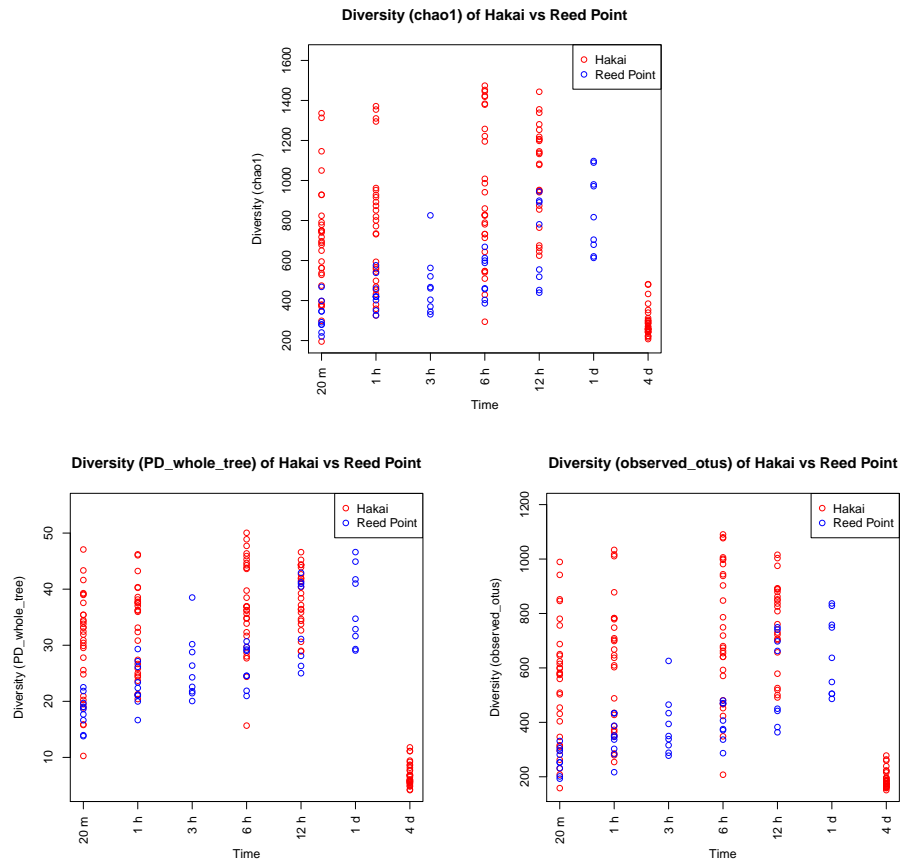


Figure 2.14: **S: Comparison of AM biofilm diversity at Reed Point and Hakai.** Blue dots represent Reed Point, whereas red dots represent Hakai. Diversity is significantly different between the sites at all time points (Refer to Table 2.6).

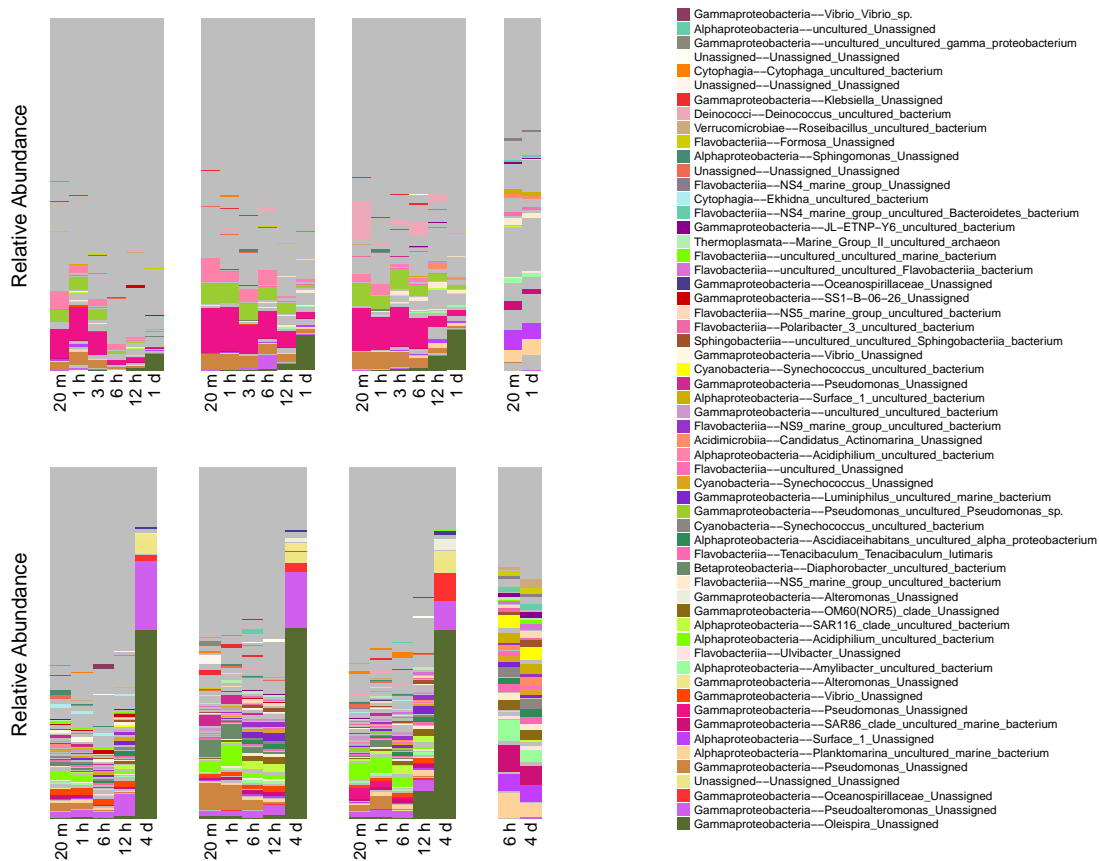


Figure 2.15: **S: Taxa summaries plot at the OTU level.** OTUs observed above 3% relative abundance in at least one sample are coloured; the rest are blocked grey.

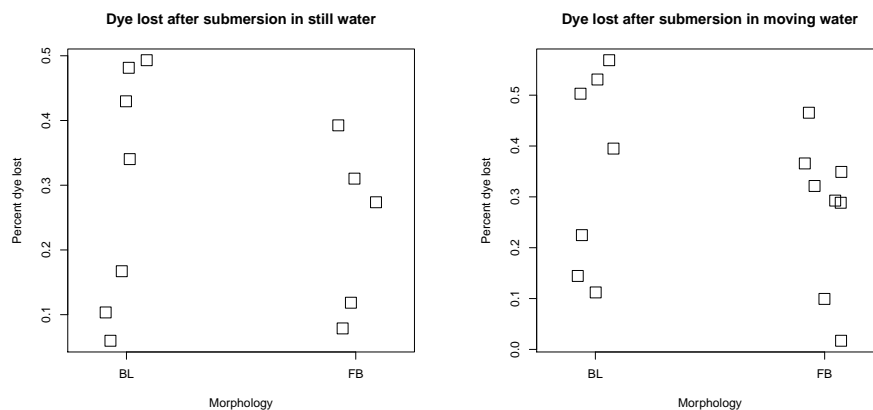


Figure 2.16: **S: Dye Dip Experiment Results** There were no significant differences between the amount of dye lost between morphologies in either still (“Still water” $p = 0.51$, $t_{9,9,x} = 0.68$) or moving water (Welch’s t-Test “Moving water” $p = 0.39$, $t_{11,x} = 0.89$).

| | | <i>p</i> -Values for PERMDISP | | | | | | | |
|------------|---------------------|-------------------------------|-----------------------|---------------------|----------------------|---------------------|---------------------|---------------------|--------------------------|
| | Site | 20 minutes | 1 hour | 3 hours | 6 hours | 12 hours | 1 day | 4 days | Overall |
| Reed Point | Bray-Curtis | 0.77 (f=0.27, df=2) | 0.61 (f=0.56, df=2) | 0.31 (f=1.45, df=2) | 0.74 (f=0.32, df=2) | 0.18 (f=2.46, df=2) | 0.17 (f=2.37, df=2) | - | 0.27 (f=1.34, df=2) |
| | Weighted Unifrac | 0.59 (f=0.58, df=2) | 0.77 (f=0.28, df=2) | 0.63 (f=0.5, df=2) | 0.74 (f=0.32, df=2) | 0.26 (f=1.81, df=2) | 0.13 (f=2.95, df=2) | - | 0.21 (f=1.61, df=2) |
| | Un-weighted Unifrac | 0.9 (f=0.11, df=2) | 0.76 (f=0.3, df=2) | 0.84 (f=0.18, df=2) | 0.86 (f=0.15, df=2) | 0.11 (f=3.49, df=2) | 0.1 (f=3.42, df=2) | - | 1 (f=0, df=2) |
| Hakai | Bray-Curtis | 0.092 (f=2.64, df=2) | 0.0012 (f=8.97, df=2) | - | 0.037 (f=3.74, df=2) | 0.52 (f=0.68, df=2) | - | 0.43 (f=0.86, df=2) | 0.045 (f=3.18, df=2,133) |
| | Weighted Unifrac | 0.39 (f=0.99, df=2) | 0.02 (f=4.61, df=2) | - | 0.95 (f=0.05, df=2) | 0.46 (f=0.81, df=2) | - | 0.34 (f=1.13, df=2) | 0.44 (f=0.83, df=2) |
| | Un-weighted Unifrac | 0.015 (f=5.01, df=2) | 0.0029 (f=7.5, df=2) | - | 0.1 (f=2.48, df=2) | 0.22 (f=1.64, df=2) | - | 0.74 (f=0.31, df=2) | 0.37 (f=1, df=2) |

Table 2.4: **S: PERMDISP of morphologies at each time point and overall.** PERMDISP was calculated at each time point to confirm PERMANOVA results. Reed Point AM unit morphologies do not have different dispersions at any time point, but Hakai samples have different dispersions at the 1 hour and 6 hour time points.

| | | <i>p</i> -Values for ANOVA | | | | | | | |
|------------|---------------|----------------------------|--------------------------|------------------------|----------------------------|------------------------|-----------------------|------------------------|-----------------------------|
| | Site | 20 minutes | 1 hour | 3 hours | 6 hours | 12 hours | 1 day | 4 days | Overall |
| Reed Point | Chao1 | 0.039 (f=5.86, df=2,6) | 0.0071 (f=12.59, df=2,6) | 0.048 (f=5.23, df=2,6) | 0.43 (f=0.99, df=2,5) | 0.021 (f=9.29, df=2,5) | 0.15 (f=2.6, df=2,6) | - | 0.0033 (f=6.48, df=2,46) |
| | PD_whole_tree | 0.064 (f=4.5, df=2,6) | 0.0035 (f=16.68, df=2,6) | 0.018 (f=8.45, df=2,6) | 0.25 (f=1.88, df=2,5) | 0.04 (f=6.59, df=2,5) | 0.15 (f=2.67, df=2,6) | - | 0.0016 (f=7.39, df=2,46) |
| | Observed_OTUs | - | - | - | - | - | - | - | 1.6e-05 (f=11.99, df=2,133) |
| Hakai | Chao1 | 0.16 (f=1.93, df=2,27) | 0.003 (f=7.45, df=2,24) | - | 0.00056 (f=10.12, df=2,26) | 0.1 (f=2.57, df=2,21) | - | 0.67 (f=0.4, df=2,26) | 3e-07 (f=16.86, df=2,133) |
| | PD_whole_tree | 0.45 (f=0.81, df=2,27) | 0.0066 (f=6.23, df=2,24) | - | 8e-04 (f=9.51, df=2,26) | 0.024 (f=4.5, df=2,21) | - | 0.85 (f=0.16, df=2,26) | 1.6e-05 (f=11.99, df=2,133) |
| | Observed_OTUs | - | - | - | - | - | - | - | 1.6e-05 (f=11.99, df=2,133) |

Table 2.5: **S: ANOVA of richness across morphology by time point.**

| Metric | | 20 min | 1 hour | 6 hours | 12 hours | Overall |
|---------------|-------------|--------|--------|---------|----------|---------|
| Chao1 | p-value | <0.001 | <0.001 | <0.001 | 0.002 | <0.001 |
| | t-statistic | 6.562 | 5.103 | 5.445 | 3.931 | 4.316 |
| | Df | 36.997 | 33.196 | 34.521 | 13.516 | 150.616 |
| PD_whole_tree | p-value | <0.001 | <0.001 | <0.001 | 0.198 | 0.376 |
| | t-statistic | 6.342 | 4.944 | 5.396 | 1.384 | 0.888 |
| | Df | 36.065 | 27.887 | 25.663 | 9.386 | 148.219 |
| Observed_otus | p-value | <0.001 | <0.001 | <0.001 | 0.009 | <0.001 |
| | t-statistic | 6.577 | 5.102 | 6.35 | 3.107 | 3.785 |
| | Df | 35.543 | 33.899 | 34.781 | 11.547 | 150.96 |

Table 2.6: **S: Welch's t-Test comparison of richness at Reed Point and Hakai by time point.**

Chapter 3

Horizontal transmission of microbes between neighbouring macroalgae

3.1 Introduction

Macroalgae (seaweeds) have an intimate relationship with their microbial symbionts. Some microbes provide benefits for their seaweed hosts by improving nutrient acquisition [Rosenberg and Paerl, 1981, Croft et al., 2005, Ilead and Carpenter, 1975, Chisholm et al., 1996], promoting settlement and growth [Joint et al., 2002], and priming immune responses against potential pathogens [Küpper et al., 2002, Maximilian et al., 1998, Steinberg et al., 1997, Weinberger, 2007, Armstrong et al., 2001, Dobretsov and Qian, 2002]. Other microbes, however, cause tissue bleaching [Case et al., 2011, Zozaya-Valdes et al., 2015] and initiate or exasperate tissue degradation [Küpper et al., 2002, Egan et al., 2013]. Since microbes influence many aspects of seaweed biology, it is important to understand how the assembly of the macroalgal microbiota occurs.

Macroalgae live in a rich microbial “soup” within the ocean and constantly contact a variety of microbes. A subset of these microbes are capable of colonizing macroalgal surfaces, and seeds the assembly of seaweed microbiota. Composition of the seaweed microbiota are generally species specific [Bondoso et al., 2014, Hollants et al., 2011, Lachnit et al., 2011, Staufenberger et al., 2008] because they are modulated and regulated, both specifically and generally, through a variety of macroalgal exudates. Polysaccharides (alginate, carageenan, cellulose, etc), which compose the bulk of macroalgae biomass, are a rich source of energy and carbon, and can promote epibiont settlement and growth [Steinberg, 2002, Lachnit et al., 2011]. Conversely, some metabolites, such as hydrogen peroxide [Küpper et al., 2002] and antibacterial furanones [Maximilian et al., 1998], are inhibitory toward microbial settlement and growth. The combination and proportion of exudates found on seaweed surfaces impose selection on colonizing microbes, and result in diverse microbial assemblages across seaweed species.

Macroalgae modify the surrounding water column and nearby biofilms as a result of their exudates. Organic exudates from macroalgae increase microbial biomass and alter both microbial functional profiles and community structure in the surrounding water column [Clasen and Shurin, 2014, Krumhansl and Scheibling, 2012, Miller and Page, 2012, Newell et al., 1980, Wada and Hama, 2013] and on nearby biofilms [Fischer et al., 2014, Vega Thurber et al., 2012, Zaneveld et al., 2016]. Macroalgal exudates can also alter microbial community composition by inhibiting growth of bacterial lineages [Lam and Harder, 2007, Lam et al., 2008]. Therefore, we know that macroalgae alter the microbial water column community and nearby biofilm composition in at least two ways: by contributing to the organic carbon pool in the water column, and by inhibiting microbial growth through chemical exudates.

We hypothesize that macroalgae affect the composition of microbial communities on the surfaces of other macroalgae. In dense communities of seaweeds, individuals may collectively contribute to a shared “plume” of exudates that both reduces potential pathogens and enriches helpful symbionts. This may in turn alter composition of epibiotic communities. For example, biofilms contain higher proportions of common seaweed-associated bacteria when in close proximity to seaweeds [Fischer et al., 2014]. Therefore, the prevalence of microbes consistently found in association with seaweeds (the ‘core’ microbiota) may be greater in dense communities of macroalgae, and reinforcement of these microbes may positively influence host health as the core often consists of beneficial symbionts [Shade and Handelsman, 2011]. In contrast, potential pathogens may be more effectively eliminated from the water column in dense communities of seaweeds. Although population density is hypothesized to correlate with disease transmittance at the population level, it can simultaneously increase immunity at the individual level [Hawley and Altizer, 2011]. Therefore, net rate of infection decreases if the benefits of improved immunity outweigh the increased exposure risk. Increasing canopy cover is known to correlate with greater shifts in nearby microbiota [Zaneveld et al., 2016], and many seaweeds are known to release a variety of antimicrobial compounds into the water [Lam et al., 2008, Egan et al., 2013]. Thus, we hypothesize that individual macroalgae living in large communities of seaweeds may experience lower rates of colonization by potentially pathogenic microbes.

We test the hypothesis that the microbiota of macroalgae changes when living in close proximity to other macroalgae and assess whether shifts in microbial communities on macroalgae are associated with changes in growth rate. Our study investigates the influence of macro-ecological communities on micro-ecological assemblages, and emphasizes the connection between host and symbiont ecology. The factors that govern patterns in macro- and micro-ecology are linked, we hope to improve our understanding of ecosystem dynamics by

applying ecological principles at a broader scale.

3.2 Methods

Sampling methods

Samples of macroalgae were collected on September 6th 2016 from Brockton Point, Vancouver, British Columbia from the intertidal at low tide. Blades from individual *Nereocystis leutkeana* and *Mastocarpus sp.* thalli were brought back to UBC in a cooler lined with wet paper towels (species were separated), and then transferred to overnight holding tanks with salinities of 30ppt and temperatures maintained at 16⁰C. The *Nereocystis* and *Mastocarpus* were kept in separate tanks. The next day, all samples were distributed into experimental tanks.

Environmental samples were taken a few days later, on September 13th. Again, several samples of *Nereocystis* and *Mastocarpus* were gathered from the intertidal; all from separate plants. Five *Nereocystis* blades, all from separate plants, were swabbed at two locations each: meristem (10cm from blade base) and mature blade (50cm from blade base). The blade surface was rinsed with sterile artificial seawater (ASW, always 30ppt unless noted otherwise) for 10 seconds, and then swabbed with a sterile cotton swab (Puritan- Item#: CA10805-154) for 10 seconds. The cotton swab tip was then snapped off into 2mL cryotubes (VWR- Item#: 10018-760) and kept on ice until return to the lab. Five *Mastocarpus* blades were also swabbed using the same method. Environmental (wild) samples were compared to swabs from experimental seaweeds to test whether lab incubation significantly affected microbial community composition and diversity on seaweed surfaces.

Macroalgae–Water Experiment

In the first experiment, referred to hereafter as the “Macroalgae–Water (M–W) experiment”, we assessed the degree to which microbes are transferred from seaweed to the surrounding water column by incubating *Nereocystis* and *Mastocarpus* alone in seawater for 6 days (see Fig. 3.1A for experimental design). Ten 10L tanks were placed in a 2-layer water table. The temperature of all tanks was regulated by the water table and kept at 16⁰C. Lights were kept on for 24h a day. Additionally, a bubbler was placed in each of the tanks and set to the maximum setting. Five tanks contained only *Nereocystis* and the other five tanks only *Mastocarpus* (Fig. 3.1A). Seaweeds were incubated in tanks for six days. On the sixth day, we sampled one random seaweed individual and took one 500mL water sample from each

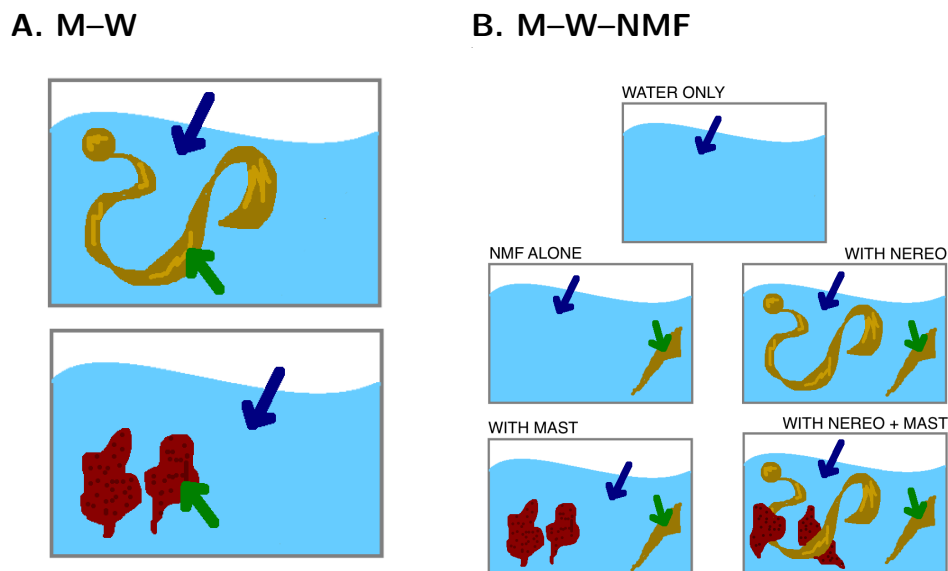


Figure 3.1: **Experimental design for M–W and M–W–NMF experiments.** (A) In the M–W experiment, either *Mastocarpus* ($n = 5$) or *Nereocystis* ($n = 5$) was incubated alone in 10L tanks for 6 days. Water was incubated at 16°C and lights were kept on 24h a day. Each tank had one bubbler on at the maximum setting. Both water (dark blue arrows) and macroalgal surfaces (green arrows) were sampled. (B) In the M–W–NMF experiment, NMF fragments were incubated with either *Nereocystis* ($n = 5$, middle right), *Mastocarpus* ($n = 5$, bottom left), or both ($n = 5$, bottom right). A NMF alone control ($n = 5$, middle left) and a water only control ($n = 5$, top) were also included. The experiment lasted 5 days. Water temperature was maintained at 16°C and light was on 24h a day. Water was sampled from every tank (dark blue arrows), and NMF surfaces were sampled where applicable (green arrows).

tank. Individuals were rinsed with ASW for 10 seconds and then swabbed for 10 seconds with a sterile cotton swab (Puritan- Item#: CA10805-154). Swabs were immediately frozen at -20°C in 2mL cryotubes (VWR- Item#: 10018-760). Water samples were collected in sterile 500mL PPE bottles, pre-filtered with an acid-sterilized 150 μm sieve, and then pumped through sterile 0.22 membranes (Durapore- Item#: GVWP04700) with a peristaltic pump (Cole-Parmer- Item#: RK-77913-70) at approximately 180rpm (level 30) to collect microbial biomass. The tubing was rinsed with 500mL of 2% HCl, followed by a rinse with 1500mL deionized water between replicates.

Macroalgae–Water–NMF experiment

We conducted a second experiment (the Macroalgae–Water–NMF (M–W–NMF) experiment) to determine how the presence of seaweed influences the surface microbial community of neighbouring seaweeds (see Fig. 3.1 for experimental design). Specifically, our goal was

to test whether *Nereocystis* meristem fragments (NMFs) co-incubated with other seaweed had different epibiotic microbial communities than meristem fragments incubated alone. Additionally, we wanted to test whether shifts in the epibiotic community structure of NMFs corresponded to any changes in growth rate. We chose to use meristematic *Nereocystis* fragments for two reasons. First, *Nereocystis* can grow up to 14cm per day [Kain, 1987], which maximizes the potential effect size for differential growth rates between treatments. Additionally, *Nereocystis* growth is concentrated in the meristematic region (the first 10cm of the blade or so), and areas of new growth tend to have less microbial diversity [Bengtsson et al., 2012]. Thus, the surfaces of *Nereocystis* meristems are optimal areas to test for meaningful shifts in epibiotic community structure because they are highly selective.

In the second experiment, twenty-five tanks with 5L of 30ppt water each were incubated in a water table held at 16°C. A bubbler was placed in each tank and lights were left on 24h a day. Salinity and temperature were monitored through the experiment to ensure they were constant and uniform. Each tank contained either: (1) water only, (2) water with one NMF fragment, (3) water with one NMF fragment and approximately 50g (wet weight) of *Nereocystis* blades, (4) water with one NMF fragment and approximately 50g (wet weight) of *Mastocarpus* blades, or (5) water with one NMF fragment and approximately 50g (wet weight) combined of *Nereocystis* and *Mastocarpus* blades. All treatments were incubated for five days. Dissolved oxygen, pH, temperature, and salinity were also all measured at the beginning and end of the experiment using the Orion STAR A329 (ThermoScientific, Item#-STARA3295) and a standard refractometer.

NMFs were prepared by cutting 10-cm fragments of *Nereocystis* meristem from the base of each blade with scissors. Each fragment's length and width were measured using a measuring tape to the nearest half millimetre, and its wet weight determined by blotting twice on a paper towel and weighing it on a scale to 2 decimal places. NMFs and other algal tissue were kept physically separated by coarse plastic mesh.

At the end of the incubation period, all NMFs were sampled and 500mL of water from each tank filtered using the same methods as described for the M-W experiment.

Library prep

The 96-well MoBio PowerSoil DNA extraction kit was used to extract DNA from both the water filters and AM swabs. Filters and swabs were transferred to the extraction kit using tweezers sterilized with 2% HCl, then ethanol and flame. Extractions followed the MoBio Powersoil DNA extraction protocol with the following modifications based on recommen-

dations in the Earth Microbiome protocol (<http://www.earthmicrobiome.org/>). First, a 10-minute incubation at 65°C in a water bath was added after the addition of C1 and before shaking in the shaker; next, the plates were shaken at 20 shakes per second for 20 minutes total instead of using the recommended shaker in the manual; and lastly filters were allowed to soak in C6 at room temperature for 10 minutes prior to elution into the final elution plate. The DNA elution was stored at -20°C.

The 16S small subunit ribosomal RNA marker gene was sequenced to profile bacteria and archaea. The amplicon library prep was done in-lab using the following 16s primers: barcoded 515 forward primers (5'-GTGYCAGCMGCCGCGGTAA-3') and 806 reverse primers (5'-GGACTACHVGGGTWTCTAAT-3'). Primers were used at final concentrations of 0.5uM with 4uL of DNA extract. DNA extracts were amplified in 20uL reactions using Phusion Flash High-fidelity proofreading Mastermix (Thermofisher- Item#: F548L). Reactions underwent the following thermocycler settings: 98°C for 10 seconds; 25 cycles of 98°C (1s), 50°C (5s), 72°C (24s); and a final extension phase of 72°C for 1 minute. Lastly, the successful PCR products were quantified using Pico-green (Thermofisher- Item#: P11496) and pooled at 45ng/sample. The pooled samples were then sent to the Centre for Comparative Genomics and Evolution Bioinformatics (CGEB) at Dalhousie University for sequencing on the Illumina MiSeq platform with 2x300bp chemistry.

Sequence Processing

Raw samples were demultiplexed with `split_libraries_fastq.py` in QIIME version 1.9 (Quantitative Insights into Microbial Ecology; (QIIME) [Caporaso et al., 2010]), yielding 3,688,981 reads. Sequences were trimmed (`fastx_trimmer`), clipped (`fastx_clipper`), and filtered (`fastq_quality_filter`) using the Fastx Toolkit (Hannon Lab) to 250bp with a minimum quality threshold of Q19. The remaining 3,661,707 raw sequences were processed into operational taxonomic units (OTUs) using Minimum Entropy Decomposition (MED; [Eren et al., 2014]) with the minimum substantive abundance (-m) parameter set to 100, yielding 1,363 unique OTUs and 3,050,864 reads. The resulting OTU matrix was transcribed into a QIIME-compatible format. Taxonomy was then assigned to the representative sequence for each MED node, hereafter referred to as OTUs, by matching it to the SILVA 128 database clustered at 99% similarity with `assign_taxonomy.py` in QIIME using `uclust V1.2.22q` [Edgar, 2010]. Chloroplast, mitochondrial, and eukaryotic DNA were filtered out and five reads suspected of being contaminants were removed. The identity of those five reads were one uncultured *Rubritalea* (Verrumicrobia), one *Marivita* (Alphaproteobacteria), a *Sulfitobacter* (Alphaproteobacteria), one *Pseudomonas* (Gammaproteobacteria), and an uncultured *Plantomycete*. Lastly, sam-

ples with less than 1000 reads per sample were removed. The final OTU table consisted of 1,314 unique sequences and 2,302,993 reads, with a mean of 26,471 reads per sample. For alpha and beta diversity analysis, samples were rarefied to 1000 reads per sample. Representative sequences were aligned with PyNAST in QIIME and a phylogenetic tree was created using FastTree [Price et al., 2009] in QIIME with the `make_phylogeny.py` script.

Community dissimilarity

To compare community composition across treatments, distance matrices were created in `beta_diversity.py` (QIIME) with the rarefied OTU table using three metrics: weighted Unifrac, unweighted Unifrac [Lozupone and Knight, 2005], and Bray-Curtis [Bray and Curtis, 1957]. Matrices were imported into R and the “`isomds`” command from the “`MASS`” package [Venables and Ripley, 2002] was used to create 2-dimensional NMDS plots. Polygons were drawn around treatments using “`chull`” in the “`grDevices`” package [R Core Team, 2016]. Pairwise permutational anovas were calculated across treatments using “`adonis`” from the “`vegan`” package [Oksanen et al., 2017] and p-values were adjusted for multiple comparisons using the Benjamini-Hochberg method (also known as the “False Discovery Rate (FDR)” method) [Benjamini et al., 1995] with “`p.adjust`” in the “`stats`” package [R Core Team, 2016]. We also tested for differences in dispersion between groups using “`betadisper`” in the “`vegan`” package [Oksanen et al., 2017]. We chose to show only Bray-Curtis results because the metric accounted for both abundance and membership in microbial communities, but results were consistent across all three metrics.

Alpha diversity

Alpha diversity for each treatment was calculated in QIIME using the `alpha_diversity` pipeline. The metrics `Chao1` [Chao, 1984], `PD_whole_tree` [Faith and Baker, 2006], and `Observed_otus` were used, but since results were similar between the three, only `Chao1` is shown in the results. `Chao1` was chosen because it estimates community richness while correcting for rare taxa. In contrast, `PD_whole_tree` calculates diversity based on phylogenetic distance of the sample. Pairwise comparisons between treatments was calculated using “`t.test`” in the “`stats`” package [R Core Team, 2016] with the method “`Welch’s t-Test`” and p-value adjustments for multiple comparisons was done using the Benjamini-Hochberg (aka “False Discovery Rate”) method [Benjamini et al., 1995] with the “`p.adjust`” command in the “`stats`” package [R Core Team, 2016]. Tables were initially created using “`xtable`” in the package “`xtable`” [Dahl, 2016] and then edited manually in LaTeX.

OTU enrichment and Taxa summaries

Fold-change enrichment and reduction of genera were calculated using “DESeq2” in the R package “DESeq2” [Love et al., 2014] with the “Wald” test. First, the OTU table (unrarefied) was collapsed at level 6 (Genera) using `summarize_taxa_through_plots.py` (QIIME). Then, genera with less than 100 counts per sample were removed. For water samples, all treatments (NMF only, *Nereocystis* alone, *Mastocarpus* alone, and *Nereocystis* + *Mastocarpus*) were compared to the NMF alone control separately. Additionally, all treatments for NMF-surface samples were compared to the NMF-alone control separately. All genera that were significantly enriched or reduced ($p < 0.05$, after p-value adjustment (Benjamini-Hochberg method (FDR)) and were observed at abundances greater than 3% at least twice in each experiment were kept. Enrichment/reduction results were plotted using “heatmap.2” in the “gplots” package [Warnes et al., 2016].

To plot taxa summary plots, OTU tables collapsed by genera were separated into four experimental groups: M–W–NMF water samples, M–W–NMF NMF surface samples, M–W samples, and environmental samples. Within each experimental group, genera at less than 3% relative abundance and with no significant enrichment in the NMF-incubation experiment are depicted as grey bars. The remaining genera are plotted in colour in Figure 3.6.

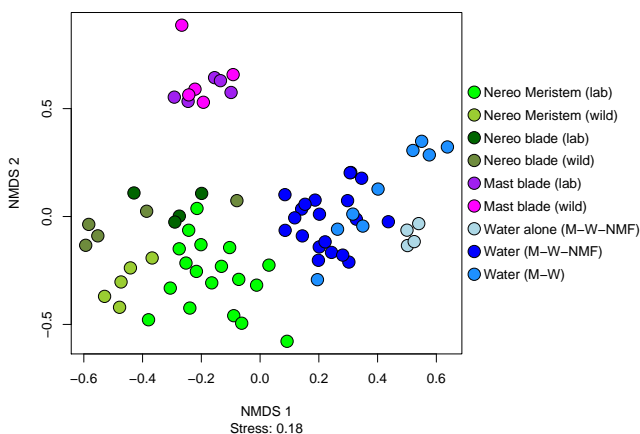
3.3 Results

Sequence processing yielded a total of 2,302,993 reads between 1,314 OTUs. There were a total of 18 samples from the M-W experiment retained (9 water samples and 9 seaweed swabs); 42 samples from the M-W-NMF experiment retained (24 water samples and 18 NMF swabs); and 15 wild seaweed swabs (5 *Mastocarpus* and 10 *Nereocystis* swabs) retained. Reads per sample ranged from 1,007 to 72,849 (with an average of 26,471).

Comparison of experimental and in situ seaweeds

First, we compared surface communities from lab-incubated seaweeds with wild seaweeds sampled *in situ* to determine whether lab incubation of samples significantly impacted their microbial community composition. We found that seaweed surface communities cluster by seaweed identity (species) across all *in situ* and laboratory samples (Fig. 3.2a), regardless of treatment type (PERMANOVA Nereo vs Mast vs Water $p = 0.001$, $R^2 = 0.248$, $df = 2,74$; PERMDISP $p < 0.001$, $F_{2,74} = 16.30$). Additionally, richness of microbial communities was similar between all seaweed of the same species (Fig. 3.2b). *Mastocarpus* surface communities were consistently and significantly more diverse than *Nereocystis* surface communities (Fig. 3.2b, Table 3.1). Thus, it appears that community structure and diversity is highly conserved

A. NMDS of all samples



B. Richness of all samples

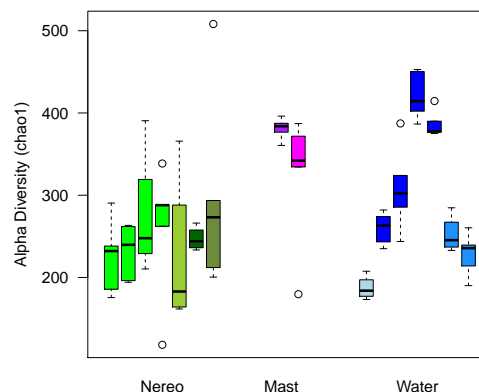


Figure 3.2: **Comparison of community composition and richness across macroalgal surfaces and water samples.** For statistical results, refer to Table 3.1. (A) NMDS of *Nereocystis* (green shades, $n = 32$), *Mastocarpus* (purple shades, $n = 10$), and water samples (blue shades, $n = 33$) (created from a Bray-Curtis distance matrix). For pairwise comparisons, see 3.1. *Nereocystis* samples are always more similar to each other than to *Mastocarpus*, regardless of treatment type. (B) Diversity (Chao1 metric) of *Nereocystis* (green shades), *Mastocarpus* (purple shades), and water samples (blue shades). *Mastocarpus* surfaces are richer than *Nereocystis* surfaces. For pair wise comparisons, see Table 3.1.

within algal species. This provides a framework for interpreting our results in a broader ecological context, and emphasizes that the effects of treatments on microbial community structure are subtle modulations on a more general pattern of species specificity.

Water column communities across treatments

Incubation of seaweeds significantly altered both the composition and diversity of microbes in the water column in a species specific manner. Tanks with seaweed (*Nereocystis*, *Mastocarpus*, and both) had water column communities that were significantly different in composition from the control (NMF alone) (Fig. 3.3A, Table 3.2; PERMDISP $p = 0.593$, $F_{2,12} = 0.546$). Further, the richness of water column communities increased in treatments where seaweed was added (Fig. 3.3B, Table 3.2). Water column communities from *Nereocystis* and *Mastocarpus* treatments differed significantly from each other in both the M-W (PERMANOVA $p = 0.049$, $R^2 = 0.266$, $df = 1,8$, Fig. S3.11) and M-W-NMF experiments (Table 3.2). Additionally, microbial richness was higher in water incubated with *Mastocarpus* (*Mastocarpus* and *Nereocystis* + *Mastocarpus* treatments) than without *Mastocarpus* (*Nereocystis*, NMF alone, and water only treatments) (Welch's t-Test $p < 0.001$, $t_{19,862} = 8.034$. Refer to

| Group 1 | Group 2 | PERMANOVA (Community Dissimilarity) | | Welch's <i>t</i> -Test (Richness) | |
|-------------------|-------------------|--|---|--------------------------------------|-----------------------|
| | | <i>p</i> | | <i>p</i> | |
| Nereo (n = 32) | Mast (n = 10) | 0.001 | ($R^2=0.191$, $F.model_{1,41}=9.466$) | 0.00192 | ($t_{17.58}=-4.14$) |
| Nereo (n = 32) | Water (n = 33) | 0.001 | ($R^2=0.168$, $F.model_{1,64}=12.765$) | 0.0375 | ($t_{62.58}=-2.24$) |
| Mast (n = 10) | Water (n = 33) | 0.001 | ($R^2=0.242$, $F.model_{1,42}=13.06$) | 0.0375 | ($t_{19.52}=2.23$) |

Table 3.1: **Comparison of community dissimilarity (PERMANOVA) and richness (Welch's t-Test) of *Nereocystis*, *Mastocarpus*, and water samples.** PERMANOVA (with a Bray-Curtis distance matrix) and Welch's t-Test (Chao1 richness) with Benjamini-Hochberg (FDR) adjusted *p*-values of *Nereocystis* surfaces, *Mastocarpus* surfaces, and water samples. All three groups are significantly different from each other. *Mastocarpus* surfaces are richer than *Nereocystis* surfaces. Water samples are more diverse than *Nereocystis* surfaces, but less diverse than *Mastocarpus* surfaces.

Table 3.2 for all pairwise comparisons). This trend is consistent with the higher richness observed on *Mastocarpus* surfaces compared to *Nereocystis* surfaces (Fig. 3.2B). Interestingly, although richness of water column communities correlated with whether or not *Mastocarpus* was present, overall community composition clustered by presence or absence of *Nereocystis* (see pairwise comparisons in Table 3.2). Thus, shifts in water column community composition and richness with the addition of macroalgae differed depending on which species was used.

NMF surface communities across treatments

Microbial communities from NMF surfaces incubated alone were different than communities from NMFs incubated with any other macroalgae (Table 3.2), but treatments with different combinations of macroalgal co-incubates were not different from each other (Fig. 3.4A, see Table 3.2 for PERMANOVA results, PERMDISP $p = 0.04$, $F_{1,6} = 6.824$). Since the *p*-values observed in the treatment comparisons (treatments with *Nereocystis* and treatments without *Nereocystis*) was almost significant, we also examined the results from weighted and unweighted Unifrac PERMANOVA analyses: all other metrics also yielded insignificant results ($p < 0.1$ for all pairwise tests). Therefore, it appears the while there was a shift in community composition on NMFs when a seaweed co-incubate is added, we did not detect differences between *Nereocystis*, *Mastocarpus*, and *Nereocystis* + *Mastocarpus* treatments.

Growth of NMFs

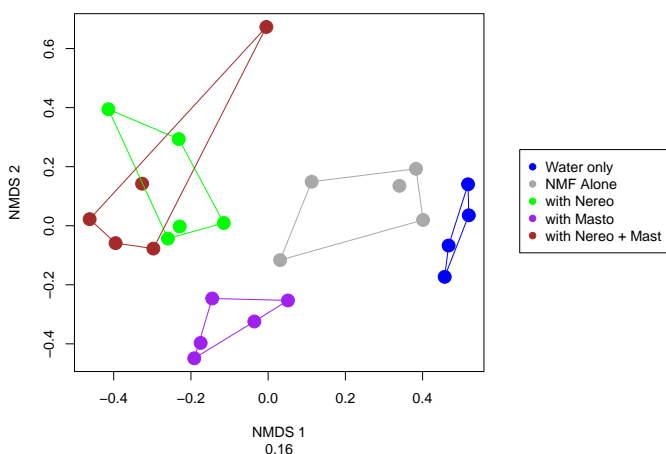
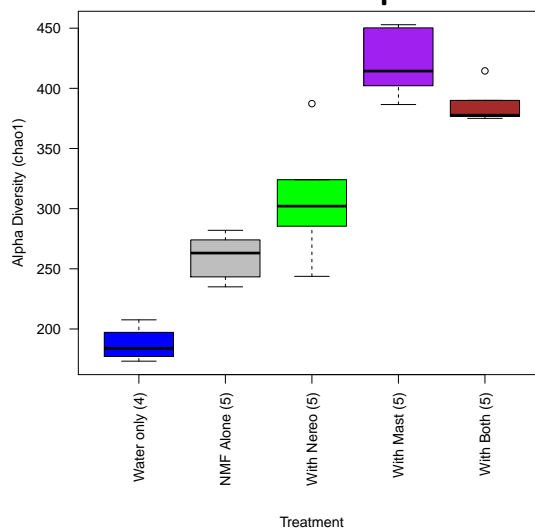
A. NMDS of water samples**B. Richness of water samples**

Figure 3.3: **Comparison of water column communities in M–W–NMF treatments.** For statistical results, refer to Table 3.2. (A) NMDS of water community composition (created from a Bray-Curtis distance matrix) from the M–W–NMF experiment. The water only control is not significantly different from the NMF alone treatment, indicating the addition of an NMF does not significantly alter the water column community. Water column communities are significantly different between treatments (with *Nereocystis*, *Mastocarpus* and both) and the control (NMF alone). Furthermore, water column communities with *Nereocystis* added are different than water column communities with *Mastocarpus* added. (B) Richness (Chao1 metric) of water column communities across treatments in the M–W–NMF experiment. Water column communities are richer in NMF alone treatments than water only treatments. Additionally, all treatments with macroalgae (*Nereocystis*, *Mastocarpus*, and both) are richer than the NMF alone treatment. Finally, treatments with *Mastocarpus* are richer than treatments with *Nereocystis*. This follows the trend observed in Figure 3.2, where *Mastocarpus* surfaces were richer than *Nereocystis* surfaces.

We found no significant difference in growth rates of NMFs between treatments, but all NMFs grew. NMFs grew proportionally to their original surface area: growth in length ranged from 0.7-3.8cm and growth in width ranged from 0-1.7cm. Growth in NMFs indicates that meristem fragments were alive and productive.

In summary, the addition of seaweed to tanks in the lab significantly altered the microbial community composition of the water column, and these shifts were different depending on which macroalgal species was added. Conversely, communities on NMF surfaces were only sensitive to the presence or absence of a macroalgal co-incubate: there were no detectable differences in community structure between treatments with different species of macroalgal co-incubates.

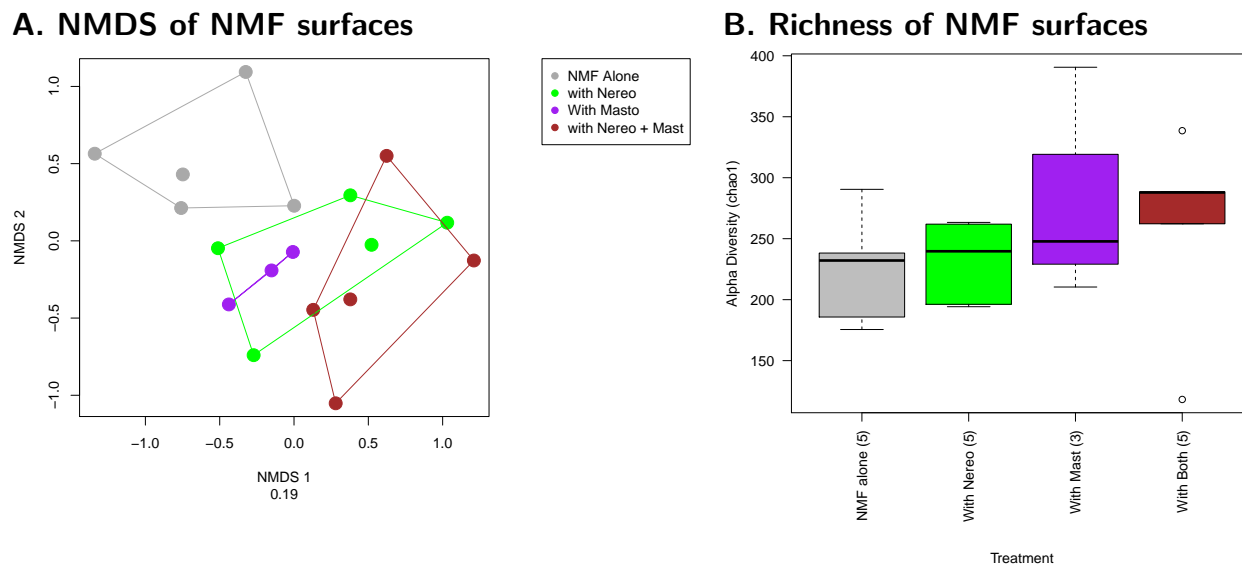


Figure 3.4: **Comparison of NMF surface communities M–W–NMF treatments.** For statistical results, refer to Table 3.2. (A) NMDS of NMF surface communities (created from a Bray-Curtis distance matrix) from the M–W–NMF experiment. NMF surface communities are significantly different when co-incubated with macroalgae (*Nereocystis*, *Mastocarpus* and both) than incubated alone (NMF alone). NMF surface communities are not significantly different between treatments with different macroalgae. (B) Richness (Chao1 metric) of NMF surface communities in the M–W–NMF experiment. We found no statistical difference in richness between treatments, but there is a trend where treatments with *Mastocarpus* are richer than treatments without *Mastocarpus*. This is consistent with trends observed in the water column (Fig. 3.3) and on algae surfaces (Fig. 3.2).

Taxonomic composition of communities and enrichment of select genera

We compared the taxonomic composition of communities from the water column and associated with NMF surfaces (Fig. 3.6). Additionally, we used “DESeq2” [Love et al., 2014] to identify genera enriched in each treatment relative to the control. In our comparison of enriched genera, we only consider groups that are both significantly enriched (corrected $p < 0.05$) and greater than 3% relative abundance in two or more samples per treatment group.

Some genera were found consistently in all water samples. These genera included *NS3a* and *Wenyinzhuangia* (Flavobacteriia); *Hyphonomas*, *Roseibacterium*, and *Sulfitobacter* (Alphaproteobacteria), and *Pseudohongiella* (Gammoproteobacteria) (representation shown in grey in Fig. 3.6).

We also found twenty differentially enriched taxa in water column samples that were simultaneously greater than 3% relative abundance: five genera were enriched across all treatments

| Group 1 | Group 2 | PERMANOVA (Community Dissimilarity) | | Welch's <i>t</i> -test (Richness) | |
|-------------|-------------------------------|--|--|--------------------------------------|----------------------------------|
| | | Water samples | NMF surface | Water samples | NMF surface |
| ●Water Only | ●NMF Alone | 0.09 ($R^2=0.162$, $F.model_{1,8}=1.35$) | | <0.001 ($t_{6.98}=6.26$) | |
| ●NMF Alone | ●Nereo ●Mast ●NereoMast | 0.001 ($R^2=0$, $F.model_{1,19}=3.062$) | 0.003 ($R^2=0$, $F.model_{1,17}=2.278$) | <0.001 ($t_{26.441}=-5.664$) | 0.685 ($t_{38.636}=-0.409$) |
| ●Nereo | ●Mast | 0.012 ($R^2=0.293$, $F.model_{1,9}=3.31$) | 0.06 ($R^2=0.216$, $F.model_{1,7}=1.655$) | <0.001 ($t_{7.74}=-10.96$) | 0.854 ($t_{10.85}=-0.69$) |
| ●Nereo | ●NereoMast | 0.018 ($R^2=0.336$, $F.model_{1,9}=4.046$) | 0.293 ($R^2=0.124$, $F.model_{1,9}=1.133$) | <0.001 ($t_{31.07}=-4.25$) | 0.854 ($t_{5.33}=-0.33$) |
| ●Mast | ●NereoMast | 0.078 ($R^2=0.154$, $F.model_{1,9}=1.458$) | 0.06 ($R^2=0.206$, $F.model_{1,7}=1.559$) | 0.00232 ($t_{27}=-3.52$) | 0.854 ($t_{8.51}=0.19$) |

Table 3.2: Comparison of community dissimilarity (PERMANOVA) and richness (Welch's *t*-Test) of water column and NMF surface communities in M–W–NMF treatments. PERMANOVA (with a Bray-Curtis distance matrix) and Welch's *t*-Test (Chao1 richness) with Benjamini-Hochberg (FDR) adjusted (in pairwise comparisons only) p-values of water sample comparisons. Water column communities are different between the control and treatments, as well as between different treatments. Conversely, NMF surface communities only different between control and treatments, and not between different treatments. Richness of water column communities are different in all comparisons, whereas NMF surface communities are all similar in richness.

and two genera were reduced in all treatments. Enriched genera included *Winogradskyella* and *Polaribacter_4* (Flavobacteriia); *Glaciecola* and *Pseudoalteromonas* (Gammaproteobacteria) and an uncultured genera of Saprospiraceae (Sphingobacteriia), whereas reduced genera included *Pseudophaeobacter* and an uncultured Rhodospirillaceae (both from Alphaproteobacteria). There were also taxa that were only enriched when water was co-incubated with each species of seaweed. For example, *Algibacter*, a Flavobacteriia isolated from green algae [Nedashkovskaya, 2004], was found enriched in water co-incubated with *Nereocystis*, but not *Mastocarpus*. Treatments with *Nereocystis* also saw a reduction in the genera *OM43* (Betaproteobacteria), *Marivita* (Alphaproteobacteria), and *Alcanivorax* (Gammaproteobacteria). There were no genera enriched or reduced in both treatments with *Mastocarpus*, but treatments with *Mastocarpus* alone showed a decrease in an uncultured Simkaniaceae (Chlamydiae), *Colwellia* (Gammaproteobacteria), and *Rubritalea* (Verrucomicrobiae).

Communities on NMF surfaces, in contrast to the water samples, show less differential enrichment across treatments (Fig. 3.6, 3.5). Although not shown, there is high variability in the relative abundance of dominant taxa. Thus, NMF surfaces are also more variable than water column communities. Across all treatments, only five genera were significantly enriched or reduced from the control (while at >3% relative abundance). One of these genera

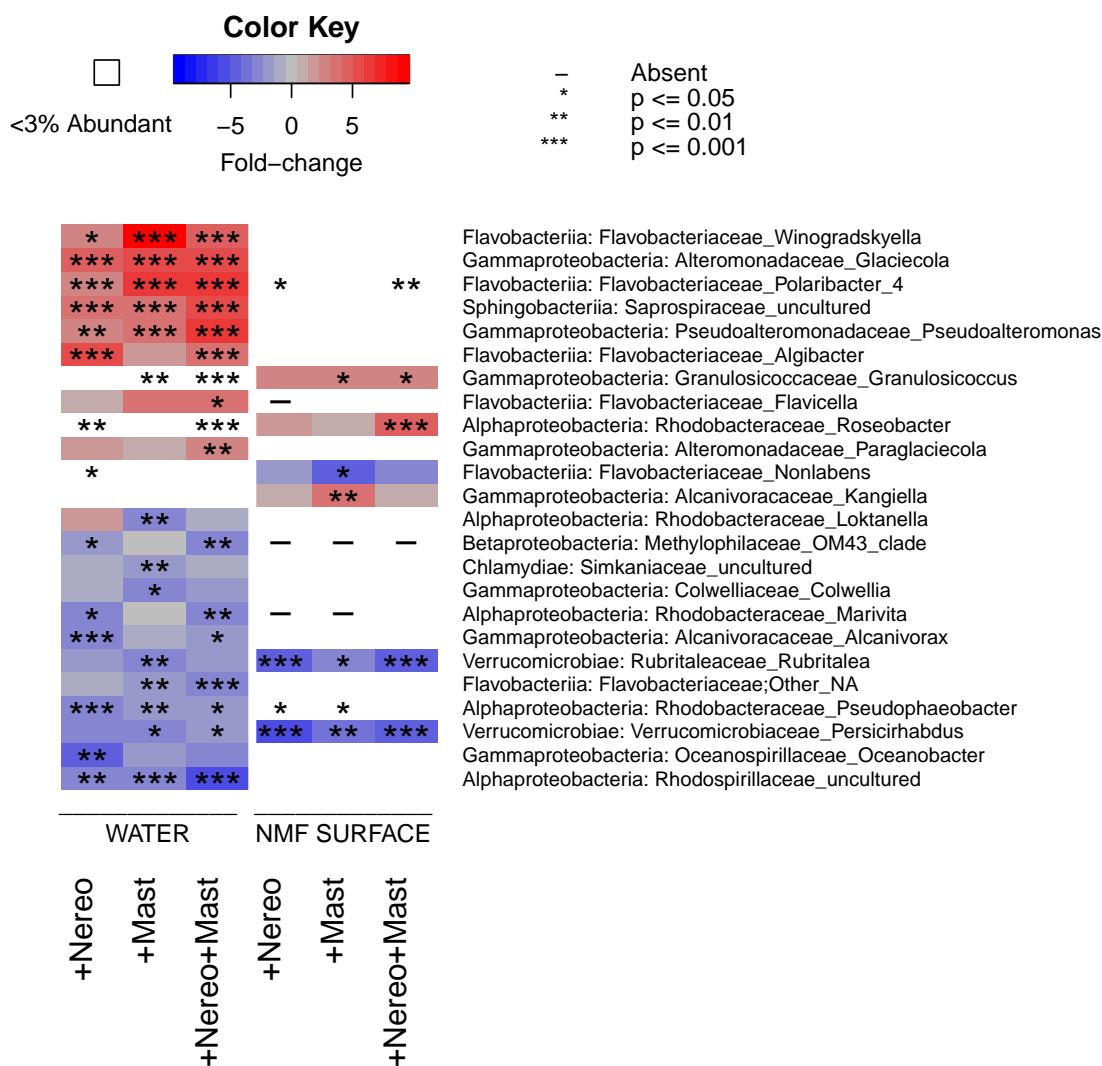


Figure 3.5: **Enrichment and reduction of NMF surface and water column communities in M–W–NMF treatments.** Fold-change enrichment or reduction of microbial genera was calculated using “DESeq2” in the “DESeq2” package in R. Both water sample treatments and NMF surface treatments were compared to the NMF Alone control in order to calculate fold-change of taxa. For a genera to be retained, fold-change p -values must be < 0.05 . Additionally, each genera must occur at $< 3\%$ relative abundance at least twice in the data set. Stars indicate the level of significance for each taxa, whereas colours indicate fold-change. Taxa with dashes represent taxa that are not found in those samples, whereas white spaces mean they were not found in at least 3% relative abundance in any two samples. There are more differentially enriched genera in the water column (twenty at $> 3\%$ abundance) than on NMF surfaces (six at $> 3\%$ abundance). Additionally, taxa that are enriched and abundant in the water column do not correlate well with those on NMF surfaces.

(*Rubritalea*) was reduced across all treatments.

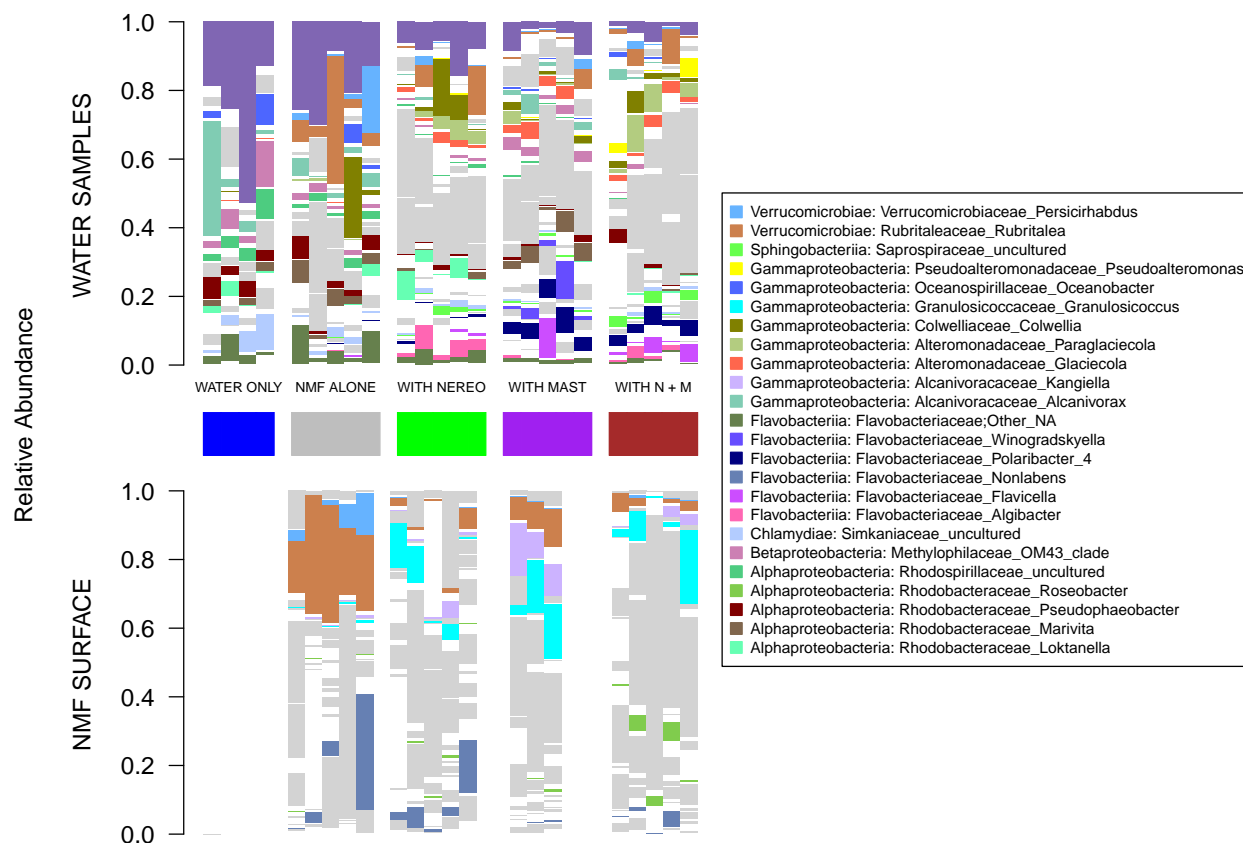


Figure 3.6: **Taxa summary plots showing enriched or reduced genera of NMF surface and water column communities.** Taxa summary plots show all genera that are >3% abundant in at least 2 samples. The legend lists the class, family, and genus of each taxa. Colored genera are those that are also significantly enriched or reduced compared to controls (See Figure 3.5 or the “Methods” section for details on how this was calculated). Genera that were >3% abundant in water samples but not enriched (shown as grey bars) include: *NS3a* and *Wenyingshuangia* (Flavobacteriia); *Hyphomonas*, *Roseibacterium*, and *Sulfitobacter* (Alphaproteobacteria); and *Pseudohongiella* (Gamaproteobacteria). Genera that were >3% abundant in NMF surface samples but not enriched (shown as grey bars) include: *Dokdonia* (Flavobacteriia); an uncultured Saprospiraceae (Sphingobacteriia); *Litorimonas*, an uncultured Rhodobacteraceae, and *Erythrobaacter* (Alphaproteobacteria); *Glaciecola*, *Paraglaciecola*, an uncultured Alteromonadaceae, *Colwellia*, *Thalassotalea*, *Arenicella*, and *Alcanivorax* (Gammaproteobacteria). Taxa that were differentially enriched represent less of the overall community on NMF surfaces than in the water column.

There is a striking decline in abundance of the genus *Rubritalea* on NMF surfaces when any macroalgae is added (*Nereocystis*, *Mastocarpus*, and *Nereocystis* + *Mastocarpus* treatments) (Fig. 3.6, 3.5). Bacteria from this genus are highly abundant on NMF surfaces when they are incubated alone, and are also highest in abundance in the water of NMF-alone tanks. It is not abundant in the water-only control, suggesting it is NMF-surface associated. *Rubritalea*

is also found in significant abundances on wild *Nereocystis*: although abundant in both swab locations, it is more abundant in the 10cm swabs than 50cm swabs (Fig. S3.14).

Changes in Water Quality During Experiment

We measured temperature, salinity, dissolved oxygen, and pH of the water in both the M-W and M-W-NMF experiments. Temperature and salinity were not significantly different between treatments. Dissolved oxygen and pH in treatments with macroalgae co-incubates were higher in treatments without macroalgae. In the M-W-NMF experiment, these differences are significant (One-way ANOVA: Dissolved oxygen $p < 0.001$, $F_{4,58}=15.429$; pH $p < 0.001$, $F_{4,58}=11.556$) but in the M-W experiment, they are not (One-way ANOVA: Dissolved oxygen $p = 0.316$, $F_{1,18}=1.0621$; pH $p = 0.058$, $F_{1,18}=4.115$).

3.4 Discussion

Different species of macroalga induce different community shifts in the water column

The goal of our project was to determine the extent to which neighbouring macroalgae alter the microbiota of each other. Our hypothesis was based on previous observations that significant microbial community shifts occur in the water column [Lam and Harder, 2007, Lam et al., 2008, Clasen and Shurin, 2014, Miller and Page, 2012] and on nearby biofilms [Vega Thurber et al., 2012, Fischer et al., 2014, Zaneveld et al., 2016] when co-incubated with macroalgae. Additionally, experiments done by Lam *et al.* 2008 show that different species of macroalgae cause differential shifts in microbial community composition in the water. Therefore our first goal was to verify that *Nereocystis* and *Mastocarpus* induced microbial community shifts in the surrounding water column, and that these shifts were different between species.

Our results confirm that the effect of macroalga on water column communities is species-specific. In general, treatments with *Nereocystis* experienced more enrichments and reductions in individual microbial genera than treatments with *Mastocarpus*. The richness of microbiota found on *Nereocystis* is also consistently lower than on *Mastocarpus*. This suggests that *Nereocystis* exudates may be more selective than *Mastocarpus* exudates.

Interestingly, *Nereocystis* + *Mastocarpus* treatments produce water column communities that are more similar in composition to *Nereocystis* only treatments, but more similar in richness to *Mastocarpus* treatments. Additionally, treatments with both macroalgae are less

rich than treatments with *Mastocarpus* alone, which suggests that the effect of different macroalgae on the water column community is not additive. Although the *Nereocystis* + *Mastocarpus* treatment is significantly less diverse than the treatment with *Mastocarpus* only, it is unclear whether this trend is due to potential antagonistic effects between *Mastocarpus* and *Nereocystis* exudates, or if it is because there was less total *Mastocarpus* tissue in the combined treatment.

Microbial communities associated with macroalgal surfaces are more resistant to change than water column

Horizontal transmission of microbes between neighbouring macroalgae may affect enrichment of certain members of the macroalgal epibiotic community, but we find that macroalgal surface communities are, in general, highly resistant to change. Our data shows that, unlike in water column communities, NMF surface communities do not differ when co-incubated with different species of seaweed. Instead, we only detected differences between control (NMF alone) and treatment samples, which were largely driven by the reduction of a single genera, *Rubritalea*.

Identification of NMF-specific genera

The genus *Rubritalea* (Verrucomicrobia) was found on all NMF surfaces, while other genera were highly variable across samples. *Rubritalea* also appears to drive the shift in community composition when NMF are grown with other macroalgae (Fig. 3.6, Fig. 3.5). Representatives of the genus *Rubritalea* produce pink-orange pigments and squalene [Scheuermayer et al., 2006, Kasai et al., 2007, Yoon et al., 2008, Yoon et al., 2007], the latter of which is a precursor to steroids and D-vitamins [Bloch, 1983]. Interestingly, both steroids and D-vitamins are known to promote growth in some species of macroalgae [Fries, 1983]. *Rubritalea* was previously isolated from sponges [Scheuermayer et al., 2006] and is a close relative to *Akkermansia*, which is commensal to humans. This suggests *Rubritalea* is a generally host-associated genus. The mechanism behind why *Rubritalea* is reduced in co-incubation treatments is unknown. It is possible that *Rubritalea* are reduced because they are proportionally less represented in co-incubation treatments, which generally have higher microbial richness. Alternatively, *Rubritalea* may be outcompeted by other members of the microbiota when near mature blades of macroalgae.

Rubritalea is also found (at >3% relative abundance) on wild seaweeds. It is more abundant in regions closer to the meristem (10cm versus 50cm from blade base, Fig. S3.14), which further supports the hypothesis that it is a *Nereocystis* meristem-specific microbe.

There is high host specificity across samples

We found a strong signal of host specificity in our data. Comparisons between all samples (including wild and lab-incubated seaweed) show that the strongest driving factor of microbial community composition is macroalgal species (*Nereocystis* vs *Mastocarpus*), and not sampling location (*in situ* or in-lab) (Fig. 3.2). While previous studies show high variation in microbial community membership within a single species of macroalgae [Burke et al., 2011b, Burke et al., 2011a], our data suggests that the variation in microbial taxa between different species of macroalgae may be even greater. Other studies that compare within-species with between-species variation in microbiota structure have also found that species is a stronger predictor of microbial community composition than location [Lachnit et al., 2009]. Therefore, the high variation in microbial community composition observed in studies of individual species of macroalgae may be misleading because the variation is not compared to the variation that exists between species.

Conclusion

In conclusion, we found that the influence of neighbouring macroalgae on NMF epibiotic communities is limited. We identified only six genera that were differentially enriched across any treatment group, and there were no significant differences between community structures of NMF communities incubated with different species of macroalgae. This suggests that macroalgal surfaces are more resistant to change than the surrounding water column. We also place our findings in a larger context: although there is high variation between NMF and *Nereocystis* mature blade samples, it is clear that macroalgal species is a stronger driver in microbial community assembly than environment or treatment. Whether the subtle changes in microbiota observed on NMFs translate to biologically important functional differences are unknown, but future work may be done to elucidate the effects of these microbes on overall community function.

3.5 Supplementary Figures and Tables

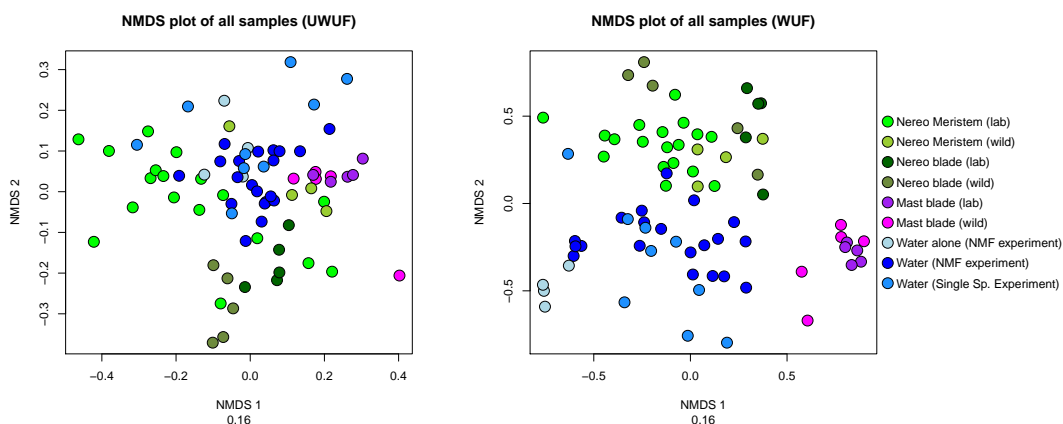


Figure 3.7: **S:** NMDS of *Nereocystis*, *Mastocarpus*, and water samples. Un-weighted (left) and weighted (right) unifracs metrics. *Nereocystis*, *Mastocarpus*, and water samples cluster separately. For statistical results, refer to Table 3.3.

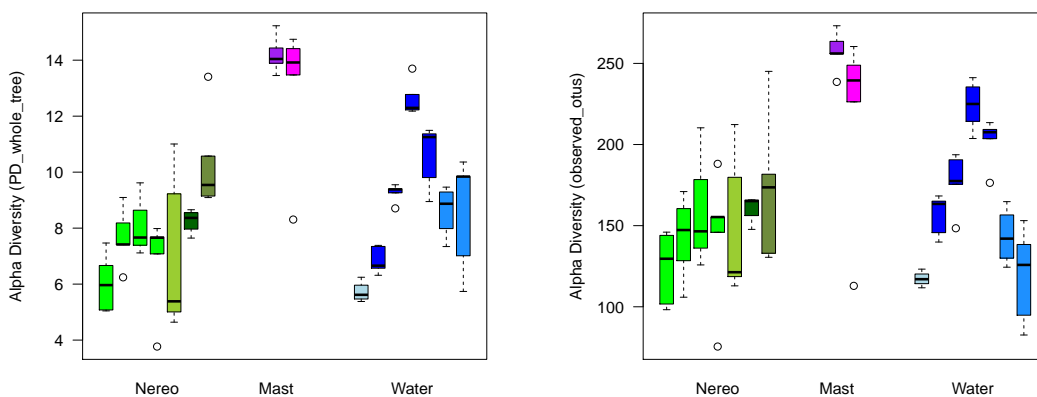


Figure 3.8: **S:** Richness of *Nereocystis*, *Mastocarpus*, and water samples. PD_whole_tree metric (left) and observed_otus (right) metric. *Mastocarpus* surfaces are consistently richer than *Nereocystis* surfaces. For statistical results, refer to Table 3.7

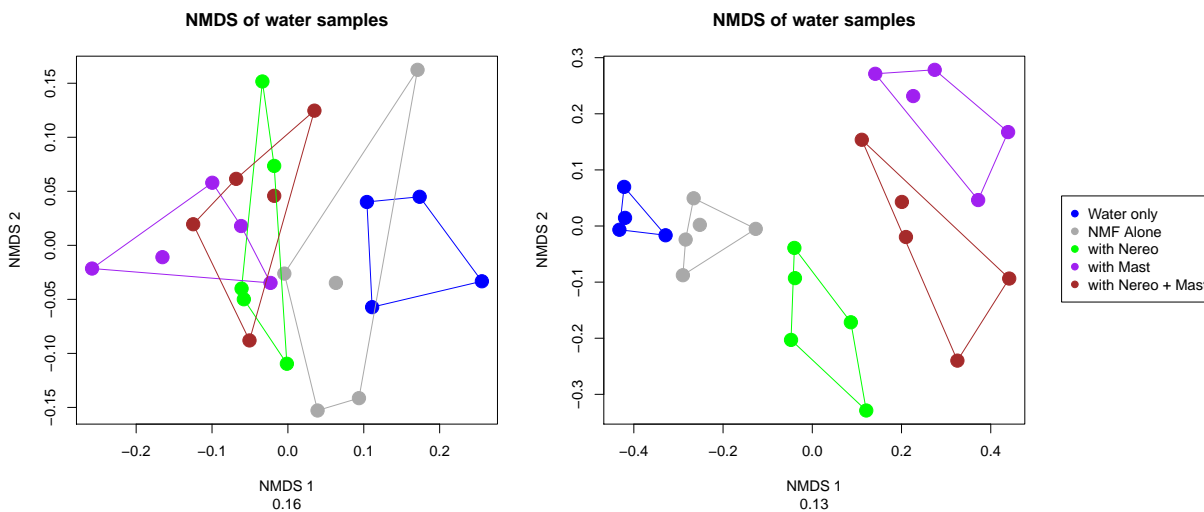


Figure 3.9: **S: NMDS of water column communities in M–W–NMF treatments.** NMDS of water community composition (created from an un-weighted (left) and weighted (right) Unifrac distance matrix) from the M–W–NMF experiment. NMF alone treatments are different from all three treatments (with *Nereocystis*, *Mastocarpus*, or both). Treatments are also significantly different from each other. For statistical results, refer to Table S3.5.

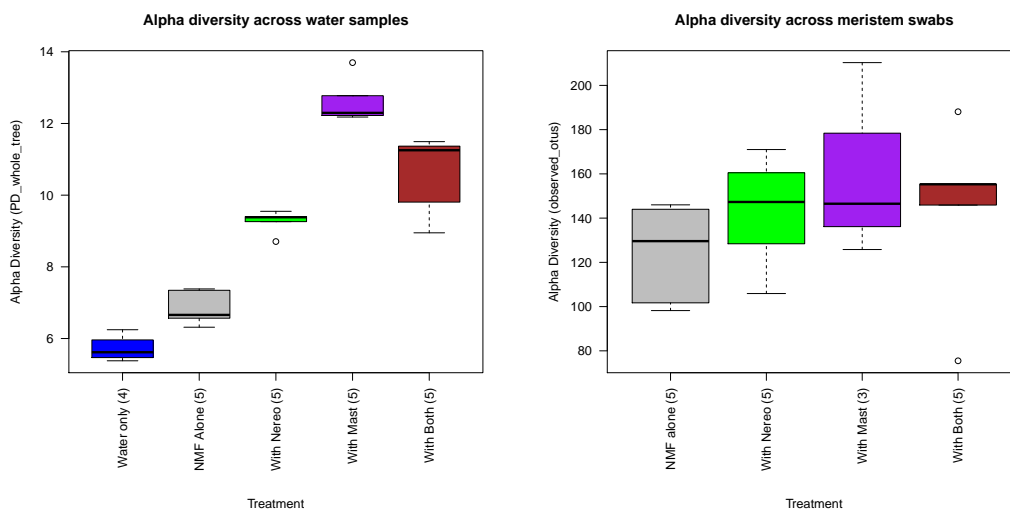


Figure 3.10: **S: Richness of water column communities in M–W–NMF treatments.** Richness (PD_whole_tree metric on the left and observed_otus on the right) of water column communities across treatments in the M–W–NMF experiment. Richness in treatments with *Mastocarpus* is higher than treatments with *Nereocystis* only. Richness in treatments with macroalgae co-incubates is higher than treatments without. For statistical results, refer to Table 3.9.

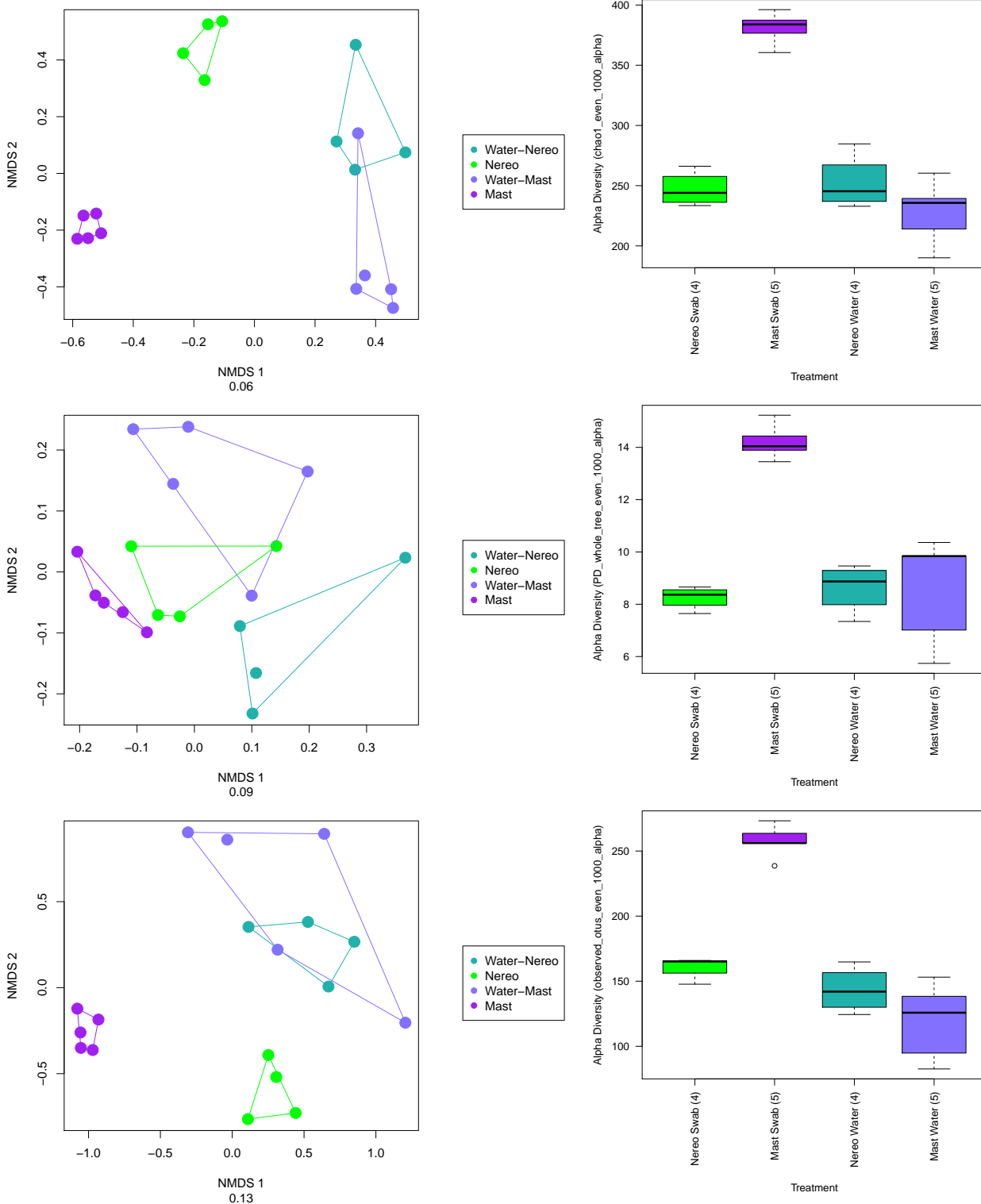


Figure 3.11: **S: Composition and Richness of samples in the M-W experiment.** NMDS plots of community dissimilarity (left) and box plots of richness (right) in all metrics used. NMDS metrics are Bray-Curtis (top left), un-weighted Unifrac (centre left), weighted Unifrac (bottom left); richness metrics used are Chao1 (top right), PD_whole_tree (middle right), and observed_otus (bottom right). For statistics, refer to Table S3.6

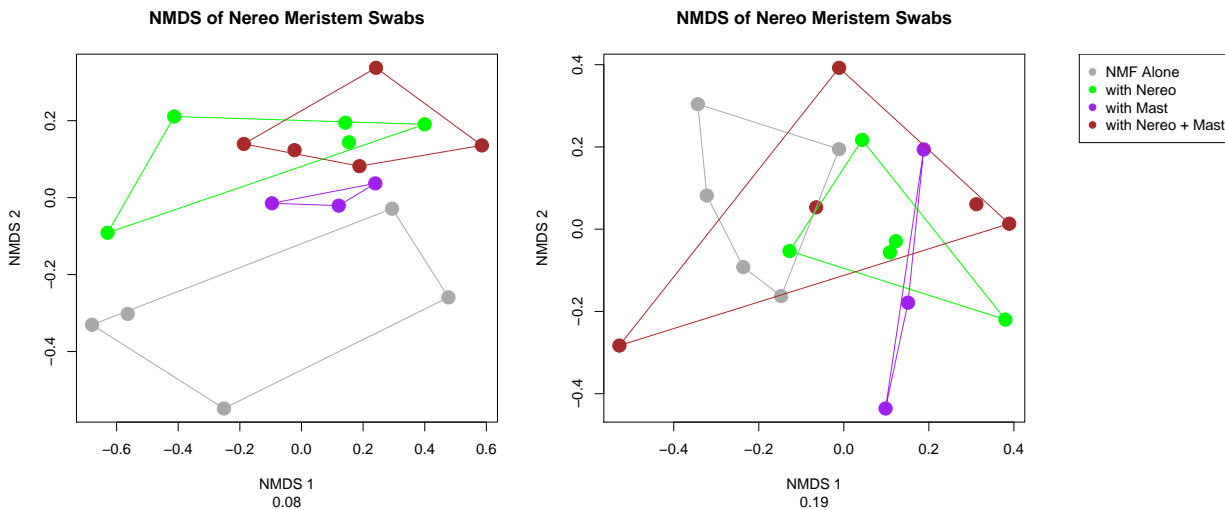


Figure 3.12: **S: Comparison of NMF surface communities from M–W–NMF treatments.** NMDS of NMF surface communities (created from an un-weighted (left) and weighted (right) Unifrac distance matrix) from the M–W–NMF experiment. NMF communities do not show significant differences between treatments, but NMF Alone treatments are different from NMF with (any) macroalgae treatments. For statistical results, refer to Table 3.5.

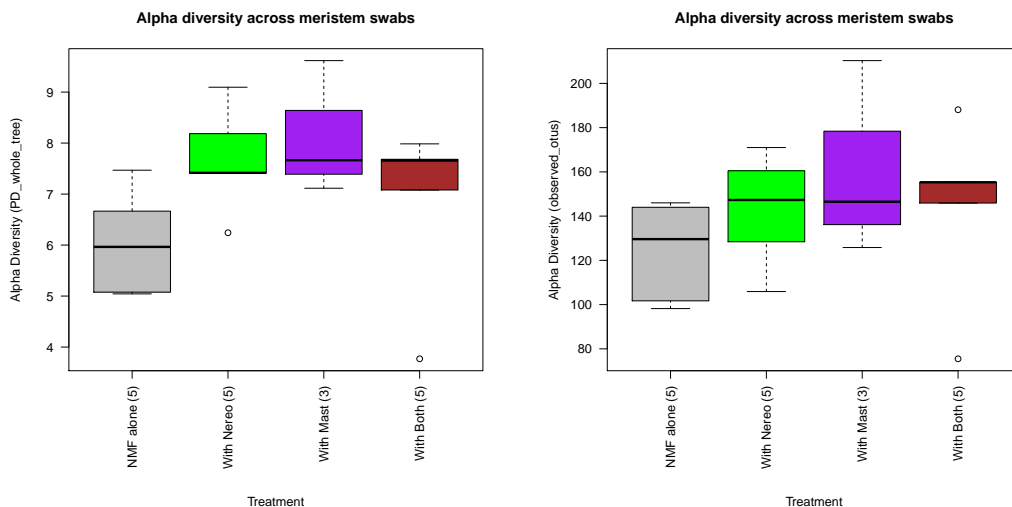


Figure 3.13: **S: Richness across NMF surface communities from M–W–NMF treatments.** Richness (PD_whole_tree metric on the left and observed_otus on the right) of NMF surface communities in the M–W–NMF experiment. There is no statistical difference between richness of any treatment. NMF Alone controls are less rich than NMF with (any) macroalgae treatments. For statistical results, refer to Table 3.9.

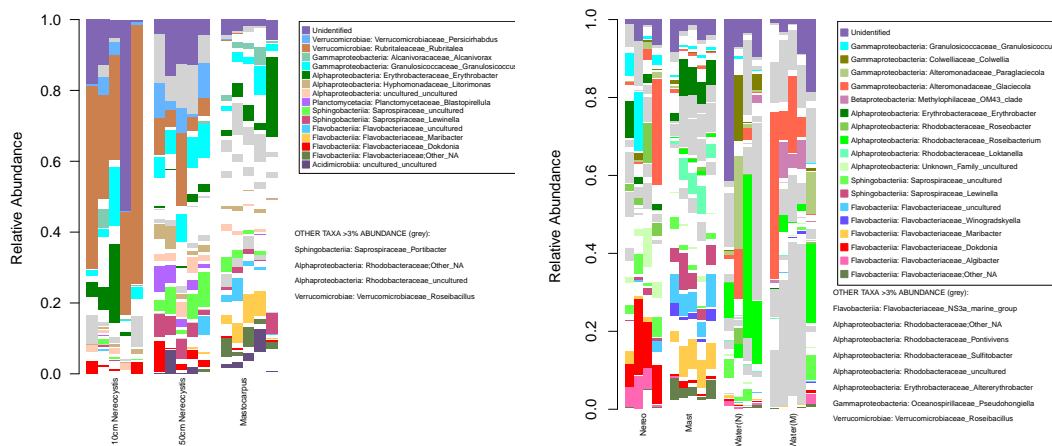


Figure 3.14: **S: Taxa summary of wild and lab-incubated seaweed samples.** Plots show taxa at the genus level for (A) wild and (B) lab-incubated seaweed samples.

| Group 1 | Group 2 | Bray-Curtis | | Un-weighted Unifrac | | Weighted Unifrac | |
|---------|---------|-------------|--------------------------|---------------------|--------------------------|------------------|--------------------------|
| | | p | FDR adj. p | p | FDR adj. p | p | FDR adj. p |
| Nereo | Mast | 0.001 | ($R^2=0.191, df=1,41$) | 0.001 | ($R^2=0.223, df=1,41$) | 0.001 | ($R^2=0.256, df=1,41$) |
| Nereo | Water | 0.001 | ($R^2=0.168, df=1,64$) | 0.001 | ($R^2=0.151, df=1,64$) | 0.001 | ($R^2=0.146, df=1,64$) |
| Mast | Water | 0.001 | ($R^2=0.242, df=1,42$) | 0.001 | ($R^2=0.224, df=1,42$) | 0.001 | ($R^2=0.235, df=1,42$) |

Table 3.3: **S: PERMANOVA results comparing *Nereocystis*, *Mastocarpus*, and water samples.** Pairwise PERMANOVA calculations were done separately.

| Group 1 | Group 2 | Bray-Curtis | | Un-weighted Unifrac | | Weighted Unifrac | |
|---------|-------------------------------|-------------|--------------------------|---------------------|------------|---------------------------|-------------------------|
| | | p | FDR adj. p | p | FDR adj. p | p | FDR adj. p |
| NMF | Water only | 0.094 | ($R^2=0.162, df=1,8$) | - | 0.083 | ($R^2=0.222, df=1,8$) | - |
| NMF | Nereo Mast Nereo + Mast | 0.001 | ($R^2=0.145, df=1,19$) | - | 0.003 | ($R^2=0.1662, df=1,19$) | - |
| Nereo | Mast | 0.005 | ($R^2=0.336, df=1,9$) | 0.012 | 0.012 | ($R^2=0.289, df=1,9$) | 0.021 |
| Nereo | Nereo + Mast | 0.087 | ($R^2=0.154, df=1,9$) | 0.087 | 0.764 | ($R^2=0.071, df=1,9$) | 0.764 |
| Mast | Nereo + Mast | 0.008 | ($R^2=0.250, df=1,9$) | 0.012 | 0.014 | ($R^2=0.265, df=1,9$) | 0.021 |
| | | | | | | 0.009 | ($R^2=0.323, df=1,9$) |
| | | | | | | 0.006 | ($R^2=0.219, df=1,9$) |
| | | | | | | 0.004 | ($R^2=0.199, df=1,9$) |

Table 3.4: **S: PERMANOVA results comparing water samples from M–W–NMF experiment.**

| Group 1 | Group 2 | Bray-Curtis | | Un-weighted Unifrac | | Weighted Unifrac | |
|---------|-------------------------------|-------------|--------------------------|---------------------|------------|--------------------------|-------------------------|
| | | p | FDR adj. p | p | FDR adj. p | p | FDR adj. p |
| NMF | Nereo Mast Nereo + Mast | 0.003 | ($R^2=0.125, df=1,17$) | - | 0.015 | ($R^2=0.198, df=1,17$) | - |
| Nereo | Mast | 0.03 | ($R^2=0.216, df=1,7$) | 0.048 | 0.385 | ($R^2=0.130, df=1,7$) | 0.385 |
| Nereo | Nereo + Mast | 0.271 | ($R^2=0.124, df=1,9$) | 0.271 | 0.284 | ($R^2=0.122, df=1,9$) | 0.385 |
| Mast | Nereo + Mast | 0.032 | ($R^2=0.206, df=1,7$) | 0.048 | 0.351 | ($R^2=0.144, df=1,7$) | 0.385 |
| | | | | | | 0.134 | ($R^2=0.175, df=1,7$) |
| | | | | | | 0.175 | ($R^2=0.137, df=1,9$) |
| | | | | | | 0.61 | ($R^2=0.138, df=1,7$) |

Table 3.5: **S: PERMANOVA results comparing NMF surface samples from M–W–NMF experiment.**

| PERMANOVA | | | Welch's t-Test | | |
|---------------------|---------|-------------------------|----------------|---------|-----------------------|
| Metric | p-value | | Metric | p-value | |
| Bray-Curtis | 0.039 | ($R^2=0.266, df=1,8$) | Chao1 | 0.188 | ($t=1.46, df=6.94$) |
| Un-weighted Unifrac | 0.023 | ($R^2=0.374, df=1,8$) | PD_whole_tree | 0.943 | ($t=0.07, df=5.8$) |
| Weighted Unifrac | 0.1 | ($R^2=0.179, df=1,8$) | Observed_otus | 0.17 | ($t=1.54, df=6.57$) |

Table 3.6: **S: PERMANOVA results comparing water samples from the M–W experiment.**

| Group 1 | Group 2 | Chao1 | | | PD_whole_tree | | | Observed_otus | | |
|---------|---------|----------|-------------------------|------------|---------------|-------------------------|------------|---------------|-------------------------|------------|
| | | p | | FDR adj. p | p | | FDR adj. p | p | | FDR adj. p |
| Nereo | Mast | 0.000641 | ($t=4.14, df=17.58$) | 0.00192 | 4.16e-07 | ($t=8.26, df=15.7$) | 1.25e-06 | 0.000104 | ($t=5.55, df=12.61$) | 0.000312 |
| Nereo | Water | 0.0375 | ($t=2.23, df=19.52$) | 0.0375 | 7.27e-06 | ($t=6.25, df=17.71$) | 1.09e-05 | 0.000525 | ($t=4.49, df=13.78$) | 0.000787 |
| Mast | Water | 0.0286 | ($t=-2.24, df=62.58$) | 0.0375 | 0.0224 | ($t=-2.34, df=62.27$) | 0.0224 | 0.122 | ($t=-1.57, df=62.15$) | 0.122 |

Table 3.7: **S: ANOVA results comparing richness of *Nereocystis*, *Mastocarpus*, and water.**

| Group 1 | Group 2 | Chao1 | | | PD_whole_tree | | | Observed_otus | | |
|---------|--------------|-----------|----------------------------|------------|---------------|----------------------------|------------|---------------|----------------------------|------------|
| | | p | | FDR adj. p | p | | FDR adj. p | p | | FDR adj. p |
| NMF | Water only | 2.605e-07 | ($t=-6.26, df=6.98$) | - | 0.00528 | ($t=-3.99, df=7$) | - | 0.00117 | ($t=-6.35, df=5.27$) | - |
| NMF | Nereo | 0.001 | ($t=-7.9526, df=18.061$) | - | 2.653e-09 | ($t=-9.8915, df=20.741$) | - | 9.913e-05 | ($t=-5.9102, df=11.068$) | - |
| | Mast | | | | | | | | | |
| | Nereo + Mast | | | | | | | | | |
| Nereo | Mast | 0.0121 | ($t=-3.76, df=5.23$) | 0.0363 | 0.000391 | ($t=-5.05, df=10.8$) | 0.00117 | 0.00634 | ($t=-3.63, df=8.25$) | 0.019 |
| Nereo | Nereo + Mast | 0.0269 | ($t=-3.15, df=4.78$) | 0.0404 | 0.0592 | ($t=-2.48, df=4.66$) | 0.0889 | 0.0442 | ($t=-2.4, df=7.72$) | 0.0663 |
| Mast | Nereo + Mast | 0.168 | ($t=1.46, df=12.53$) | 0.168 | 0.157 | ($t=1.53, df=9.8$) | 0.157 | 0.242 | ($t=1.24, df=9.88$) | 0.242 |

Table 3.8: **S: ANOVA and Welch's t-Test results comparing richness of water samples from M-W-NMF experiment.**

| Group 1 | Group 2 | Chao1 | | | PD_whole_tree | | | Observed_otus | | |
|---------|--------------|-------|--------------------------|------------|---------------|--------------------------|------------|---------------|---------------------------|------------|
| | | p | | FDR adj. p | p | | FDR adj. p | p | | FDR adj. p |
| NMF | Nereo | 0.271 | ($t=-1.167, df=9.857$) | - | 0.0621 | ($t=-2.127, df=9.044$) | - | 0.117 | ($t=-1.714, df=10.038$) | - |
| | Mast | | | | | | | | | |
| | Nereo + Mast | | | | | | | | | |
| Nereo | Mast | 0.286 | ($t=-1.13, df=10.06$) | 0.775 | 0.65 | ($t=0.47, df=10.94$) | 0.65 | 0.682 | ($t=-0.42, df=10.94$) | 0.951 |
| Nereo | Nereo + Mast | 0.517 | ($t=-0.69, df=5.3$) | 0.775 | 0.392 | ($t=0.92, df=6.59$) | 0.65 | 0.951 | ($t=-0.06, df=6.71$) | 0.951 |
| Mast | Nereo + Mast | 0.854 | ($t=0.19, df=8.51$) | 0.854 | 0.63 | ($t=0.5, df=8.2$) | 0.65 | 0.794 | ($t=0.27, df=8.41$) | 0.951 |

Table 3.9: **S: ANOVA and Welch's t-Test results comparing NMF surface samples from M-W-NMF experiment.**

Bibliography

- [Abelson and Denny, 1997] Abelson, A. and Denny, M. (1997). Settlement of Marine Organisms in Flow. *Ecology*, 28:317–339.
- [Anderson and Martone, 2014] Anderson, L. M. and Martone, P. T. (2014). Biomechanical consequences of epiphytism in intertidal macroalgae. *The Company of Biologists*, 217:1167–1174.
- [Armstrong et al., 2001] Armstrong, E., Yan, L., Boyd, K. G., Wright, P. C., and Burgess, J. G. (2001). The symbiotic role of marine microbes on living surfaces. *Hydrobiologia*, 461:37–40.
- [Bengtsson and Øvreås, 2010] Bengtsson, M. M. and Øvreås, L. (2010). Planctomycetes dominate biofilms on surfaces of the kelp *Laminaria hyperborea*. *BMC Microbiology*, 10(1):261.
- [Bengtsson et al., 2012] Bengtsson, M. M., Sjøtun, K., Lanzén, A., and Øvreås, L. (2012). Bacterial diversity in relation to secondary production and succession on surfaces of the kelp *Laminaria hyperborea*. *The ISME Journal*, 6:2188–2198.
- [Benjamini et al., 1995] Benjamini, Y., Hochberg, Y., Society, R. S., Benjamini, Y., Hochberg, Y., Society, R. S., Benjamini, y. Y., Hochberg, Y., Benjamini, Y., Hochberg, Y., Society, R. S., Benjamini, Y., Hochberg, Y., Society, R. S., Benjamini, y. Y., and Hochberg, Y. (1995). Controlling the False Discovery Rate : A Practical and Powerful Approach to Multiple Testing Author (s): Yoav Benjamini and Yosef Hochberg Source : Journal of the Royal Statistical Society . Series B (Methodological), Vol . 57 , No . 1 Published by :. *J R Statist Soc B*, 57(1):289–300.
- [Berland et al., 1972] Berland, B. R., Bonin, D. J., and Maestrini, S. Y. (1972). Are some bacteria toxic for marine algae? *Marine Biology*, 12(3):189–193.
- [Bhakuni and Rawat, 2006] Bhakuni, D. S. and Rawat, D. (2006). *Bioactive marine natural products*. Spring Science and Business Media.
- [Bloch, 1983] Bloch, K. E. (1983). Sterol, Structure and Membrane Function. *Critical Reviews in Biochemistry and Molecular Biology*, 14:47–92.
- [Bolinches et al., 1988] Bolinches, J., Lemos, M. L., and Barja, J. L. (1988). Population dynamics of heterotrophic bacterial communities associated with *Fucus vesiculosus* and *Ulva rigida* in an estuary. *Microbial Ecology*, 15(3):345–357.
- [Bondoso et al., 2014] Bondoso, J., Balague, V., Gasol, J. M., and Lage, O. M. (2014). Community composition of the Planctomycetes associated with different macroalgae. *FEMS Microbiology Ecology*, 88(3):445–456.
- [Bray and Curtis, 1957] Bray, J. R. and Curtis, J. (1957). An Ordination of the Upland Forest Communities of Southern Wisconsin. *Ecological Monographs*, 27(4):325–349.
- [Brock and Clyne, 1984] Brock, T. D. and Clyne, J. (1984). Significance of algal excretory products for growth of epilimnetic bacteria. *Applied and Environmental Microbiology*, 47(4):731–734.
- [Bulleri et al., 2002] Bulleri, F., Benedetti-Cecchi, L., Acunto, S., Cinelli, F., and Hawkins, S. J. (2002). The influence of canopy algae on vertical patterns of distribution of low-shore assemblages on rocky coasts in the northwest Mediterranean. *Journal of Experimental Marine Biology and Ecology*, 267(1):89–106.

- [Burke et al., 2011a] Burke, C., Steinberg, P., Rusch, D., Kjelleberg, S., and Thomas, T. (2011a). Bacterial community assembly based on functional genes rather than species. *Proceedings of the National Academy of Sciences of the United States of America*, 108(34):14288–14293.
- [Burke et al., 2011b] Burke, C., Thomas, T., Lewis, M., Steinberg, P., and Kjelleberg, S. (2011b). Composition, uniqueness and variability of the epiphytic bacterial community of the green alga *Ulva australis*. *The ISME Journal*, 5(4):590–600.
- [Caporaso et al., 2010] Caporaso, J. G., Kuczynski, J., Stombaugh, J., Bittinger, K., Bushman, F. D., Costello, E. K., Fierer, N., Peña, A. G., Goodrich, J. K., Gordon, J. I., Huttley, G. a., Kelley, S. T., Knights, D., Koenig, J. E., Ley, R. E., Lozupone, C. a., McDonald, D., Muegge, B. D., Pirrung, M., Reeder, J., Sevinsky, J. R., Turnbaugh, P. J., Walters, W. a., Widmann, J., Yatsunenکو, T., Zaneveld, J., and Knight, R. (2010). QIIME allows analysis of high-throughput community sequencing data. *Nature Publishing Group*, 7(5):335–336.
- [Carpenter and Cox, 1974] Carpenter, E. J. and Cox, J. L. (1974). Production of Pelagic Sargassum and a Blue-Green Epiphyte in the Western Sargasso Sea. *Limnology and Oceanography*, 19(3):429–436.
- [Case et al., 2011] Case, R. J., Longford, S. R., Campbell, A. H., Low, A., Tujula, N., Steinberg, P. D., and Kjelleberg, S. (2011). Temperature induced bacterial virulence and bleaching disease in a chemically defended marine macroalga. *Environmental Microbiology*, 13(2):529–537.
- [Chao, 1984] Chao, A. (1984). Nonparametric Estimation of the Number of Classes in a Population. *Scandinavian Journal of Statistics*, 11(4):265–270.
- [Characklis and Marshall, 1990] Characklis, W. G. and Marshall, K. C. (1990). *Biofilms*. Wiley, New York.
- [Chisholm et al., 1996] Chisholm, J., Douga, C., Ageron, E., Grimont, P., and Jaubert, J. (1996). ‘Roots’ in mixotrophic algae. *Nature*, 381:382.
- [Clasen and Shurin, 2014] Clasen, J. L. and Shurin, J. B. (2014). Kelp forest size alters microbial community structure and function on Vancouver Island, Canada. *Ecology*, 96(3):140815103525005.
- [Coveney and Wetzel, 1989] Coveney, M. F. and Wetzel, R. G. (1989). Bacterial metabolism of algal extracellular carbon. *Hydrobiologia*, 173(2):141–149.
- [Croft et al., 2005] Croft, M. T., Lawrence, A. D., Raux-Deery, E., Warren, M. J., and Smith, A. G. (2005). Algae acquire vitamin B12 through a symbiotic relationship with bacteria. *Nature*, 438:90–93.
- [Dahl, 2016] Dahl, D. B. (2016). *xtable: Export Tables to LaTeX or HTML*. R package version 1.8-2.
- [de Oliveira et al., 2012] de Oliveira, L. S., Gregoracci, G. B., Silva, G. G., Salgado, L. T., Filho, G. a., Alves-Ferreira, M. a., Pereira, R. C., and Thompson, F. L. (2012). Transcriptomic analysis of the red seaweed *Laurencia dendroidea* (Florideophyceae, Rhodophyta) and its microbiome. *BMC Genomics*, 13:487.
- [Dimitrieva et al., 2006] Dimitrieva, G. Y., Crawford, R. L., and Yüksel, G. Ü. (2006). The nature of plant growth-promoting effects of a pseudoalteromonad associated with the marine algae *Laminaria japonica* and linked to catalase excretion. *Journal of Applied Microbiology*, 100(5):1159–1169.

- [Dininno and McCandless, 1978] Dininno, V. and McCandless, E. (1978). Immunochemistry of lambda-type carrageenans from certain red algae. *Carbohydrate Research*, 67:235–241.
- [Dittami et al., 2015] Dittami, S. M., Duboscq-Bidot, L., Perennou, M., Gobet, A., Corre, E., Boyen, C., and Tonon, T. (2015). Host-microbe interactions as a driver of acclimation to salinity gradients in brown algal cultures. *The ISME journal*, 10(1):51–63.
- [Dobretsov and Qian, 2002] Dobretsov, S. V. and Qian, P.-Y. (2002). Effect of Bacteria Associated with the Green Alga *Ulva reticulata* on Marine Micro- and Macrofouling. *Biofouling*, 18(795099257):217–228.
- [Dring, 2006] Dring, M. (2006). Stress resistance and disease resistance in seaweeds: the role of reactive oxygen metabolism. In *Advances in Botanical Research*, pages 175–207. Academic Press LRD- Elsevier Science LTD, London.
- [Dromgoole and J, 1978] Dromgoole, F. I. S. W. B. and J, H. B. (1978). Nitrogenase activity associated with *Codium* species from New Zealand marine habitats. *N.Z. Journal of Marine and Freshwater Research*, 12(1):17–22.
- [Dubber and Harder, 2008] Dubber, D. and Harder, T. (2008). Extracts of *Ceramium rubrum*, *Mastocarpus stellatus* and *Laminaria digitata* inhibit growth of marine and fish pathogenic bacteria at ecologically realistic concentrations. *Aquaculture*, 274:196–200.
- [Edgar, 2010] Edgar, R. C. (2010). Search and clustering orders of magnitude faster than BLAST. *Bioinformatics*, 26(19):2460–2461.
- [Egan et al., 2013] Egan, S., Harder, T., Burke, C., Steinberg, P., Kjelleberg, S. S. S. S., and Thomas, T. (2013). The seaweed holobiont: Understanding seaweed-bacteria interactions. *FEMS Microbiology Reviews*, 37(3):462–476.
- [Egan et al., 2008] Egan, S., Thomas, T., and Kjelleberg, S. (2008). Unlocking the diversity and biotechnological potential of marine surface associated microbial communities. *Current Opinion in Microbiology*, 11(3):219–225.
- [Eren et al., 2014] Eren, A. M., Morrison, H. G., Lescault, P. J., Reveillaud, J., Vineis, J. H., and Sogin, M. L. (2014). Minimum entropy decomposition: Unsupervised oligotyping for sensitive partitioning of high-throughput marker gene sequences. *The ISME Journal*, 9(4):968–979.
- [Eveleigh et al., 1979] Eveleigh, M., Vollmer, C., and McCandless, E. (1979). Differentiation of the lambda carrageenans from Rhodophyta with immunological and spectroscopic techniques. *Journal of Phycology*, 14(1):89–91.
- [Faith and Baker, 2006] Faith, D. P. and Baker, A. M. (2006). Phylogenetic diversity (PD) and biodiversity conservation: some bioinformatics challenges. *Evolutionary bioinformatics online*, 2:121–128.
- [Falshaw et al., 2003] Falshaw, R., Bixler, H., and Johndro, K. (2003). Structure and performance of commercial kappa-2 carrageenan extracts. Part III. Structure analysis and performance in two dairy applications of extracts from the New Zealand red seaweed, *Gigartina atropurpurea*. *Food Hydrocolloids*, 17:129–139.
- [Fischer et al., 2014] Fischer, M., Friedrichs, G., and Lachnit, T. (2014). Fluorescence-Based Quasi-continuous and In Situ Monitoring of Biofilm Formation Dynamics in Natural Marine Environments. *Applied and Environmental Microbiology*, 80(12):3721–3728.
- [Fox and Weisberg, 2011] Fox, J. and Weisberg, S. (2011). *An R Companion to Applied Regression*. Sage, Thousand Oaks CA, second edition.

- [Fries, 1983] Fries, L. (1983). D-vitamins and Their Precursors as Growth Regulators in Axenically Cultivated Marine Macroalgae. *Journal of Phycology*, 20(1):62–66.
- [Goecke et al., 2010] Goecke, F., Labes, A., Wiese, J., and Imhoff, J. F. (2010). Chemical interactions between marine macroalgae and bacteria. *Marine Ecology Progress Series*, 409:267–299.
- [Hawley and Altizer, 2011] Hawley, D. M. and Altizer, S. M. (2011). Disease ecology meets ecological immunology: understanding the links between organismal immunity and infection dynamics in natural populations. *Functional Ecology*, 25(1):48–60.
- [Hoegh-Guldberg, 1988] Hoegh-Guldberg, O. (1988). A method for determining the surface area of corals. *Coral Reefs*, 7(3):113–116.
- [Hollants et al., 2011] Hollants, J., Leroux, O., Leliaert, F., Decleyre, H., De Clerck, O., and Willems, A. (2011). Who Is in There? Exploration of Endophytic Bacteria within the Siphonous Green Seaweed Bryopsis (Bryopsidales, Chlorophyta). *PLoS ONE*, 6(10):e26458.
- [Huggett et al., 2006] Huggett, M. J., Williamson, J. E., De Nys, R., Kjelleberg, S., and Steinberg, P. D. (2006). Larval settlement of the common Australian sea urchin *Heliocidaris erythrogramma* in response to bacteria from the surface of coralline algae. *Oecologia*, 149(4):604–619.
- [Huston, 1979] Huston, M. (1979). A General Hypothesis of Species. *The American Naturalist*, 113(1):81–101.
- [Ilead and Carpenter, 1975] Ilead, W. D. and Carpenter, E. J. (1975). Nitrogen fixation associated with the marine macroalga *Codium fragile*. *Limnology and Oceanography*, 20(5):815–823.
- [Johnson et al., 2001] Johnson, S., Thompson, M., and Hourigan, K. (2001). Flow past elliptical cylinders at low Reynolds numbers. *14th Australasian Fluid . . .*, pages 343–346.
- [Joint et al., 2002] Joint, I., Tait, K., Callow, M. E., Callow, J. A., Milton, D., Williams, P., and Cámara, M. (2002). Cell-to-Cell Communication across the Prokaryote-Eukaryote Boundary. *Science*, 298(5596):5–6.
- [Kain, 1987] Kain, J. (1987). Patterns of relative growth in *Nereocystis luetkeana* (Phaeophyta).
- [Kasai et al., 2007] Kasai, H., Katsuta, A., Sekiguchi, H., Matsuda, S., Adachi, K., Shindo, K., Yoon, J., Yokota, A., and Shizuri, Y. (2007). *Rubritalea squalenifaciens* sp. nov., a squalene-producing marine bacterium belonging to subdivision 1 of the phylum 'Verrucomicrobia'. *International Journal of Systematic and Evolutionary Microbiology*, 57(7):1630–1634.
- [Krumhansl and Scheibling, 2012] Krumhansl, K. A. and Scheibling, R. E. (2012). Production and fate of kelp detritus. *Marine Ecology Progress Series*, 467:281–302.
- [Küpper et al., 2002] Küpper, F. C., Müller, D. G., Peters, A. F., Kloareg, B., and Potin, P. (2002). Oligoalginat recognition and oxidative burst play a key role in natural and induced resistance of sporophytes of Laminariales. *Journal of Chemical Ecology*, 28(10):2057–2081.
- [Lachnit et al., 2009] Lachnit, T., Blümel, M., Imhoff, J. F., and Wahl, M. (2009). Specific epibacterial communities on macroalgae: Phylogeny matters more than habitat. *Aquatic Biology*, 5(2):181–186.
- [Lachnit et al., 2011] Lachnit, T., Meske, D., Wahl, M., Harder, T., and Schmitz, R. (2011). Epibacterial community patterns on marine macroalgae are host-specific but temporally variable. *Environmental Microbiology*, 13(3):655–665.
- [Lam and Harder, 2007] Lam, C. and Harder, T. (2007). Marine macroalgae affect abundance and community richness of bacterioplankton in close proximity. *Journal of Phycology*, 43(5):874–881.

- [Lam et al., 2008] Lam, C., Stang, A., and Harder, T. (2008). Planktonic bacteria and fungi are selectively eliminated by exposure to marine macroalgae in close proximity. *FEMS Microbiology Ecology*, 63(3):283–291.
- [Lehtola et al., 2006] Lehtola, M. J., Laxander, M., Miettinen, I. T., Hirvonen, A., Vartiainen, T., and Martikainen, P. J. (2006). The effects of changing water flow velocity on the formation of biofilms and water quality in pilot distribution system consisting of copper or polyethylene pipes. *Water Research*, 40:2151–2160.
- [Love et al., 2014] Love, M. I., Huber, W., and Anders, S. (2014). Moderated estimation of fold change and dispersion for rna-seq data with *deseq2*. *Genome Biology*, 15:550.
- [Lozupone and Knight, 2005] Lozupone, C. and Knight, R. (2005). UniFrac : a New Phylogenetic Method for Comparing Microbial Communities. *Applied and environmental microbiology*, 71(12):8228–8235.
- [Marshall et al., 2006] Marshall, K., Joint, I., Callow, M. E., and Callow, J. A. (2006). Effect of marine bacterial isolates on the growth and morphology of axenic plantlets of the green alga *Ulva linza*. *Microbial Ecology*, 52(2):302–310.
- [Mason et al., 2003] Mason, O., Hazen, T. C., Borglin, S., Chain, P. S., Dubinsky, E. A., Fortney, J. L., Han, J., Holman, H.-Y. N., and Hultman, J. (2003). Metagenome, metatranscriptome and single-cell sequencing reveal microbial response to Deepwater Horizon oil spill. *The ISME Journal*, 6(9):1715–1727.
- [Matsuo et al., 2005] Matsuo, Y., Imagawa, H., Nishizawa, M., and Shizuri, Y. (2005). Isolation of an Algal Morphogenesis Inducer from Marine Bacterium. *Science*, 307(5715):1596.
- [Matz et al., 2008] Matz, C., Webb, J. S., Schupp, P. J., Phang, S. Y., Penesyan, A., Egan, S., Steinberg, P., and Kjelleberg, S. (2008). Marine biofilm bacteria evade eukaryotic predation by targeted chemical defense. *PLoS ONE*, 3(7):1–7.
- [Maximilian et al., 1998] Maximilian, R., De Nys, R., Holmstrom, C., Gram, L., Givskov, M., Crass, K., Kjelleberg, S. A., and Steinberg, P. D. (1998). Chemical mediation of bacterial surface colonisation by secondary metabolites from the red alga *Delisea pulchra*. *Aquatic Microbial Ecology*, 15(3):233–246.
- [McHugh, 2003] McHugh, D. J. (2003). A guide to the seaweed industry. *FAO fisheries technical paper*, 441.
- [Meusnier et al., 2001] Meusnier, I., Olsen, J. L., Stam, W. T., Destombe, C., and Valero, M. (2001). Phylogenetic analyses of *Caulerpa taxifolia* (Chlorophyta) and of its associated bacterial microflora provide clues to the origin of the Mediterranean introduction. *Molecular Ecology*, 10(4):931–946.
- [Michelou et al., 2013] Michelou, V. K., Caporaso, J. G., Knight, R., and Palumbi, S. R. (2013). The Ecology of Microbial Communities Associated with *Macrocyctis pyrifera*. *PLoS ONE*, 8(6):1–9.
- [Miller and Page, 2012] Miller, R. J. and Page, H. M. (2012). Kelp as a trophic resource for marine suspension feeders: A review of isotope-based evidence. *Marine Biology*, 159(7):1391–1402.
- [Nakanishi et al., 1996] Nakanishi, K., Nishijima, M., Nishimura, M., Kuwano, K., and Saga, N. (1996). Bacteria that induce morphogenesis in *Ulva pertusa* (Chlorophyta) grown under axenic conditions. *Journal of Phycology*, 482(479):482–479.

- [Nedashkovskaya, 2004] Nedashkovskaya, O. (2004). *Algibacter lectus* gen. nov., sp. nov., a novel member of the family Flavobacteriaceae isolated from green algae. *International Journal of Systematic and Evolutionary Microbiology*, 54(4):1257–1261.
- [Newell et al., 1980] Newell, R. C., Lucas, M. I., Velimirov, B., and Seiderer, L. J. (1980). Quantitative Significance of Dissolved Organic Losses Following Fragmentation of Kelp (*Ecklonia maxima* and *Laminaria pallida*). *Marine Ecology Progress Series*, 2(1977):45–59.
- [Oksanen et al., 2017] Oksanen, J., Blanchet, F. G., Friendly, M., Kindt, R., Legendre, P., McGlenn, D., Minchin, P. R., O’Hara, R. B., Simpson, G. L., Solymos, P., Stevens, M. H. H., Szoecs, E., and Wagner, H. (2017). *vegan: Community Ecology Package*. R package version 2.4-3.
- [Ollos et al., 2003] Ollos, P. J., Huck, P. M., and Slawson, R. M. (2003). Factors Affecting Biofilm Accumulation in Model Distribution Systems. *American Water Works Association*, 95(1):87–97.
- [Persson et al., 2011] Persson, F., Svensson, R., Nylund, G. M., Fredriksson, N. J., Pavia, H., Hermansson, M., Persson, F., Svensson, R., Nylund, G. M., and Johan, N. (2011). Ecological role of a seaweed secondary metabolite for a colonizing bacterial community. *Biofouling*, 27(6):579–588.
- [Price et al., 2009] Price, M. N., Dehal, P. S., and Arkin, A. P. (2009). Fasttree: Computing large minimum evolution trees with profiles instead of a distance matrix. *Molecular Biology and Evolution*, 26(7):1641–1650.
- [Provasoli and Pintner, 1980] Provasoli, L. and Pintner, I. J. (1980). Bacteria induced polymorphism in an axenic laboratory strain of *Ulva lactuca* (Chlorophyceae). *Journal of Phycology*, 16:196–201.
- [R Core Team, 2016] R Core Team (2016). *R: A Language and Environment for Statistical Computing*. R Foundation for Statistical Computing, Vienna, Austria.
- [Rao et al., 2010] Rao, D., Skovhus, T., Tujula, N., Holmström, C., Dahllöf, I., Webb, J. S., and Kjelleberg, S. (2010). Ability for *Pseudoalteromonas tunicata* to colonize natural biofilms and its effect on microbial community structure. *FEMS Microbiol Ecol*, 73:450–457.
- [Riquelme et al., 1997] Riquelme, C., Rojas, A., Flores, V., and Correa, J. A. (1997). Epiphytic bacteria in a copper-enriched environment in northern Chile. *Marine Pollution Bulletin*, 34(10):816–820.
- [Rosenberg and Paerl, 1981] Rosenberg, G. and Paerl, H. W. (1981). Nitrogen fixation by blue-green algae associated with the siphonous green seaweed *Codium decortcatum*: effects on ammonium uptake. *Marine Biology*, 61(2-3):151–158.
- [Rusconi et al., 2014] Rusconi, R., Guasto, J. S., and Stocker, R. (2014). Bacterial transport suppressed by fluid shear. *Nature Physics*, 10(3):212–217.
- [Rusconi and Stocker, 2015] Rusconi, R. and Stocker, R. (2015). Microbes in flow. *Current Opinion in Microbiology*, 25:1–8.
- [Rutter and Vincent, 1988] Rutter, P. and Vincent, B. (1988). Attachment mechanisms in the surface growth of microorganisms. *Physiological models in microbiology*. CRC Press, Boca Raton, Fla, pages 87–107.
- [Scheuermayer et al., 2006] Scheuermayer, M., Gulder, T. A. M., Bringmann, G., and Hentschel, U. (2006). *Rubritalea marina* gen. nov., sp. nov., a marine representative of the phylum ‘Verrucomicrobia’, isolated from a sponge (Porifera). *International Journal of Systematic and Evolutionary Microbiology*, 56(9):2119–2124.

- [Schiel and Foster, 2006] Schiel, D. R. and Foster, M. S. (2006). The population biology of large brown seaweeds : Ecological consequences life histories of multiphase in dynamic coastal environments. *Annual Review of Ecology, Evolution and Systematics*, 37(2006):343–372.
- [Semenova et al., 2009] Semenova, E., Shlykova, D., Semenov, A., Ivanov, M., Shelyakov, O., and Netrusov, A. (2009). Bacteria-Epiphytes of Brown Macro Alga in Oil Utilization in North Sea Ecosystems. *Moscow University Biological Sciences Bulletin*, 64(3):107–110.
- [Seyedsayamdost et al., 2011] Seyedsayamdost, M. R., Case, R. J., Kolter, R., and Clardy, J. (2011). The Jekyll-and-Hyde chemistry of *Phaeobacter gallaeciensis*. *Nature Chemistry*, 3(4):331–335.
- [Shade and Handelsman, 2011] Shade, A. and Handelsman, J. (2011). Beyond the Venn diagram: the hunt for a core microbiome. *Environmental Microbiology*, 14(1):4–12.
- [Singer et al., 2010] Singer, G., Besemer, K., Schmitt-Kopplin, P., Hödl, I., and Battin, T. J. (2010). Physical Heterogeneity Increases Biofilm Resource Use and Its Molecular Diversity in Stream Mesocosms. *PLoS One*, 5(4):e9988.
- [Singh and Reddy, 2014] Singh, R. P. and Reddy, C. R. K. (2014). Seaweed-microbial interactions: Key functions of seaweed-associated bacteria. *FEMS Microbiology Ecology*, 88(2):213–230.
- [Staufenberger et al., 2008] Staufenberger, T., Thiel, V., Wiese, J., and Imhoff, J. F. (2008). Phylogenetic analysis of bacteria associated with *Laminaria saccharina*. *FEMS Microbiology Ecology*, 64:65–77.
- [Steinberg, 2002] Steinberg, P. D. (2002). Minireview: Chemical Mediation of Colonization of Seaweed Surfaces. *Journal of Phycology*, 629:621–629.
- [Steinberg et al., 1997] Steinberg, P. D., Schneider, R., and Kjelleberg, S. (1997). Chemical defenses of seaweeds against microbial colonization. *Biodegradation*, 8(3):211–220.
- [Stewart and Carpenter, 2003] Stewart, H. L. and Carpenter, R. C. (2003). The effects of morphology and water flow on photosynthesis of marine macroalgae. *Ecology*, 84(11):2999–3012.
- [Stratil et al., 2014] Stratil, S. B., Neulinger, S. C., Knecht, H., Friedrichs, A. K., and Wahl, M. (2014). Salinity affects compositional traits of epibacterial communities on the brown macroalga *Fucus vesiculosus*. *FEMS microbiology ecology*, 88(2):272–9.
- [Tait and Schiel, 2011] Tait, L. W. and Schiel, D. R. (2011). Dynamics of productivity in naturally structured macroalgal assemblages: Importance of canopy structure on light-use efficiency. *Marine Ecology Progress Series*, 421:97–107.
- [Thomas et al., 2008] Thomas, T., Evans, F. F., Schleheck, D., Mai-Prochnow, A., Burke, C., Penesyan, A., Dalisay, D. S., Stelzer-Braid, S., Saunders, N., Johnson, J., Ferriera, S., Kjelleberg, S., and Egan, S. (2008). Analysis of the *Pseudoalteromonas tunicata* genome reveals properties of a surface-associated life style in the marine environment. *PLoS ONE*, 3(9):1–11.
- [Tujula et al., 2010] Tujula, N. a., Crocetti, G. R., Burke, C., Thomas, T., Holmström, C., and Kjelleberg, S. (2010). Variability and abundance of the epiphytic bacterial community associated with a green marine Ulvacean alga. *The ISME journal*, 4(2):301–311.
- [Vega Thurber et al., 2012] Vega Thurber, R., Burkepile, D. E., Correa, A. M. S., Thurber, A. R., Shantz, A. A., Welsh, R., Pritchard, C., and Rosales, S. (2012). Macroalgae Decrease Growth and Alter Microbial Community Structure of the Reef-Building Coral, *Porites astreoides*. *PLoS ONE*, 7(9):1–10.

- [Venables and Ripley, 2002] Venables, W. N. and Ripley, B. D. (2002). *Modern Applied Statistics with S*. Springer, New York, fourth edition. ISBN 0-387-95457-0.
- [Wada and Hama, 2013] Wada, S. and Hama, T. (2013). The contribution of macroalgae to the coastal dissolved organic matter pool. *Estuarine, Coastal and Shelf Science*, 129:77–85.
- [Warnes et al., 2016] Warnes, G. R., Bolker, B., Bonebakker, L., Gentleman, R., Liaw, W. H. A., Lumley, T., Maechler, M., Magnusson, A., Moeller, S., Schwartz, M., and Venables, B. (2016). *gplots: Various R Programming Tools for Plotting Data*. R package version 3.0.1.
- [Weinberger, 2007] Weinberger, F. (2007). Pathogen-induced defense and innate immunity in macroalgae. *Biological Bulletin*, 213(3):290–302.
- [Weinberger et al., 1999] Weinberger, F., Friedlander, M., and Hoppe, H.-g. (1999). Oligoagars Elicit a Physiological Response in *Gracilaria Conferta* (Rhodophyta). *Biological Bulletin*, 35:747–755.
- [Wilson et al., 2010] Wilson, S. K., Depczynski, M., Fisher, R., Holmes, T. H., O’Leary, R. A., and Tinkler, P. (2010). Habitat associations of juvenile fish at Ningaloo Reef, Western Australia: The importance of coral and algae. *PLoS ONE*, 5(12):1–8.
- [Yakimov et al., 2003] Yakimov, M. M., Giuliano, L., Gentile, G., Crisafi, E., Chernikova, T. N., Abraham, W.-R., Lunsdorf, H., Timmis, K. N., and Golyshin, P. N. (2003). *Oleispira antarctica* gen. nov., sp. nov., a novel hydrocarbonoclastic marine bacterium isolated from Antarctic coastal sea water. *International Journal of Systematic and Evolutionary Microbiology*, 53:779–785.
- [Yoon et al., 2007] Yoon, J., Matsuo, Y., Matsuda, S., Adachi, K., Kasai, H., and Yokota, A. (2007). *Rubritalea spongiae* sp. nov. and *Rubritalea tangerina* sp. nov., two carotenoid- and squalene-producing marine bacteria of the family ‘*Verrucomicrobiaceae*’ within the phylum ‘*Verrucomicrobia*’, isolated from marine animals. *International Journal of Systematic and Evolutionary Microbiology*, 57:2337–2343.
- [Yoon et al., 2008] Yoon, J., Matsuo, Y., Matsuda, S., Adachi, K., Kasai, H., and Yokota, A. (2008). *Rubritalea sabuli* sp. nov., a carotenoid- and squalene-producing member of the family *Verrucomicrobiaceae*, isolated from marine sediment. *International Journal of Systematic and Evolutionary Microbiology*, 58:992–997.
- [Yurkov and Beatty, 1998] Yurkov, V. and Beatty, J. T. (1998). Aerobic Anoxygenic Phototrophic Bacteria. *Microbiology and Molecular Biology Reviews*, 62(3):695–724.
- [Zaneveld et al., 2016] Zaneveld, J. R., Burkepille, D. E., Shantz, A. A., Pritchard, C. E., McMinds, R., Payet, J. P., Welsh, R., Correa, A. M. S., Lemoine, N. P., Rosales, S., Fuchs, C., Maynard, J. A., and Thurber, R. V. (2016). Overfishing and nutrient pollution interact with temperature to disrupt coral reefs down to microbial scales. *Nature Communications*, 7(May):11833.
- [Zozaya-Valdes et al., 2015] Zozaya-Valdes, E., Egan, S., and Thomas, T. (2015). A comprehensive analysis of the microbial communities of healthy and diseased marine macroalgae and the detection of known and potential bacterial pathogens. *Frontiers in Microbiology*, 6(FEB):1–9.